Cannabinoid type 2 receptors mediate a cell type-specific plasticity in the hippocampus

DISSERTATION

To obtain the academic degree Doctor rerum naturalium (Dr. rer. nat.)
submitted to the Department of Biology, Chemistry and Pharmacy of the Free University, Berlin
by Anna Vanessa Stempel | from Siegburg, Germany | July, 2015

The experimental work of this thesis was completed from January 2012 to April 2015 under the supervision of
Prof. Dr. Dietmar Schmitz at the Neuroscience Research Centre (NWFZ) of the Charité – Universitätsmedizin Berlin, Germany.

1st reviewer: Prof. Dr. Ursula Koch

2nd reviewer: Prof. Dr. Dietmar Schmitz

Date of disputation: 14th October 2015

Acknowledgements

First and foremost, I would like to thank my supervisor *Dietmar Schmitz* for his unconditional support, generosity and advice. Thank you for having encouraged me always to explore independently, and for keeping me grounded while fighting it out with the cannabinoids. I have always felt appreciated and respected, and feel very lucky to have been your student.

Thanks to *Ursula Koch*, for agreeing to be my first reviewer, I really appreciate it.

Furthermore, I am indebted to and thank the following people that have supported and accompanied me in the last five years:

Jochen Winterer, for the science, the enthusiasm, the interneuron magic, the friendship, and his patience. Working with you has been perfect.

Jörg Geiger, for being a wonderful, fast-spiking mentor and sharing your vast knowledge so many a time. A PhD counts nothing in comparison to having obtained the 'advanced Stümper' award.

Tuğba Özdoğan, Ulrike Pannasch, Stephanie Wegener and Sarah Shoichet, for your invaluable scientific input, help and friendship.

Anne-Kathrin Theis and *Alexander Stumpf*, for your help with a very demanding project.

Friedrich Johenning, Christian Wozny, *Nikolaus Maier*, *Imre Vida* and *Henrik Alle*, from whom I have learned so much, for your help and guidance and enthusiasm.

Jörg Breustedt, for the discussions and the misanthropic/architectural banter and *Michael Kintscher*, for making lab life happy and (un)funny.

Anke Schönherr and *Susanne Rieckmann*, for being the base of the lab, your skilled assistance, guidance and patience, especially when I was fumbling around in the dark, scary depths of molecular biology.

Members of the *Schmitzlab*, past and present, for discussions, banter, food and an amazingly friendly and cooperative lab atmosphere.

The graduate college "Learning and Memory Consolidation in the Hippocampal Formation" (i.e. *Uwe Heinemann*, *Dietmar Schmitz* and the German Science Foundation) for its generous financial support.

My family, for their constant support and providing a perfect sanctuary and Dominic especially for proof-reading the thesis.

Synopsis

Endocannabinoids exert major control over neuronal activity by activating cannabinoid receptors (CBRs). The functionality of the endocannabinoid system (ECS) is primarily ascribed to the well-documented retrograde activation of presynaptically localised CB_1Rs (1) that are abundantly expressed in various brain regions and cell types (2, 3) and, upon retrograde activation by endocannabinoids, inhibit transmitter release. Depending on the receptors' location on either glutamatergic or GABAergic axon terminals, this phenomenon is referred to as depolarisation-induced suppression of inhibition (DSI) or excitation (DSE) (4–6). In stark contrast, very little is known about the relevance of CB_2Rs in neuronal signalling. Indeed, until recently the CB_2R was referred to as the 'peripheral' CBR reflecting its predominant expression in organs of the immune system (7) where it participates in the regulation of immune responses and is responsible for the anti-inflammatory effects of cannabis (8). A major problem of studying CB_2Rs has been their low expression levels in the central nervous system (CNS) and the lack of reliable antibodies, which has sparked controversy concerning their localisation in the brain (9, 10). Yet, the generation of CBR knockout (KO) mice (8, 11) and the production of a diverse array of synthetic cannabinoid agents (12) have advanced and facilitated research on CB_2Rs. Especially behavioural studies have suggested the presence of CB_2Rs in the CNS (13–15) with properties that extend their neuro-immunological function, and recent anatomical and electrophysiological studies support this notion (16–21). We find that action potential-driven release of the endocannabinoid 2-arachidonoylglycerol (2-AG) leads to a long-lasting membrane potential hyperpolarisation in hippocampal CA3 pyramidal cells (PCs) that is independent of CB_1R activation. A comparative study of hippocampal principal cells revealed that this mechanism is specific to CA3 and CA2. The hyperpolarisation is absent in CB_2R KO mice and can furthermore be blocked, mimicked and occluded by CB_2R-specific drugs. A detailed analysis of the phenomenon indicates that neuronally expressed, G Protein-coupled CB_2Rs are persistently activated in an agonist unbound state and signal via a calcium-sensitive cascade. Activation of CB_2Rs robustly affected the input/output function of CA3 PCs via a reduction in spike probability without depending on synaptic transmission. Their activation did not affect presynaptic transmitter release, and occurred in a purely self-regulatory manner, as suggested by dual recordings from neighbouring cells. To conclude, we describe a highly specific mechanism in the hippocampus that emphasises the importance of CB_2R function in basic neuronal transmission and challenges classic, CB_1R-focused views on hippocampal cannabinoid function. These findings are especially important as CB_2Rs are implicated in many complex neuropsychiatric diseases and may provide the basis for non-psychoactive treatments (22).

Zusammenfassung

Das endogene Cannabinoid-System (auch: Endocannabinoid-System, ECS), stellt einen zentralen neuromodulatorischen Bestandteil des Nervensystems dar und umfasst die G-Protein gekoppelten Cannabinoidrezeptoren CB_1 und CB_2 sowie deren natürliche Liganden, die Endocannabinoide (23). Das ECS beeinflusst diverse Lern- und Bewegungsprozesse, nimmt aber besonders in der hippokampalen Formation (HF) eine wichtige Rolle für die Vermittlung und Modulation physiologischer und pathophysiologischer Prozesse ein (24). Auch wenn das prominenteste Beispiel die Beeinträchtigung von Gedächtnis durch die Einnahme von Cannabis ist, so modulieren endogene Cannabinoide die Netzwerkaktivität der HF und die dessen zugrunde liegende neuronale Signalkaskaden auf vielfältige und beträchtliche Art und Weise (25). Klassischerweise wurden die Effekte des ECS auf neuronale Informationsverarbeitung allein dem CB_1-Rezeptor zugeschrieben, wohingegen der CB_2-Rezeptor als Teil des Immunsystems galt (8). Ein großes Problem in der Erforschung des CB_2-Rezeptors stellt dessen niedrige Expression im Zentralnervensystem (ZNS) und außerdem das Fehlen von spezifischen Antikörpern dar. Dies hat dazu geführt, dass die Lokalisierung des CB_2-Rezeptors im ZNS auch weiterhin kontrovers debattiert wird (9, 10). Dennoch hat die Herstellung sowohl von Cannabinoidrezeptor-Knockoutmäusen (8, 11) als auch von diversen synthetischen Cannabinoidpharmaka (12) die Forschung an CB_2-Rezeptoren wesentlich erleichtert und vorangetrieben. Vor allem Verhaltensstudien mit Mäusen weisen auf die Existenz von CB_2-Rezeptoren im ZNS hin (13–15), die nicht nur eine neuro-immunologische Funktion innehaben, sondern ebenfalls direkt neuronale Informationsverarbeitung beeinflussen und diese Ergebnisse werden von anatomischen und elektrophysiologischen Studien klar unterstützt (16–20). Wir beschreiben in dieser Arbeit nun eine weitere, vorher unbekannte Funktion des CB_2-Rezeptors anhand von elektrophysiologischen Messungen in akuten Hirnschnitten von Mäusen und Ratten. Wir finden, dass die Aktionspotentials-getriebene Freisetzung des Endocannabinoids 2-Arachidonoylglycerol zu einer langanhaltenden, hyperpolarisierenden Plastizität in hippokampalen Prinzipalzellen führt, die ausschließlich in CA3 und CA2 ausgelöst werden kann. Durch die kombinierte Verwendung von Knockout-Mäusen und Rezeptor-spezifischer Pharmakologie können wir zeigen, dass diese zelltyp-spezifische Hyperpolarisierung des Membranpotentials unabhängig von CB_1-Rezeptoren ist, sondern durch die Aktivierung von CB_2-Rezeptoren vermittelt wird. Die Aktivierung von CB_2-Rezeptoren hatte keinen Einfluss auf presynaptische Transmitterfreisetzung und anhand von zeitgleichen Ableitungen von benachbarten Pyramidenzellen können wir außerdem zeigen dass der Effekt, im Gegensatz zu presynaptischer CB_1-Rezeptoraktivierung, rein selbst-regulatorisch zu sein scheint. Zusammenfassend beschreiben wir eine zelltyp-spezifische Plastizität in der HF, der die Wichtigkeit der Funktion von CB_2-Rezeptoren im ZNS herausstellt. Dies ist besonders interessant, da der CB_2-Rezeptor in vielen komplexen neuropsychiatrischen Erkrankungen eine Rolle zu spielen scheint und hier die Grundlage für eine nicht-psychotrope Behandlungen bieten kann (13).

Table of contents

1 Introduction

The ability of an organism to adapt to environmental changes is the fundamental building block of evolutionary processes. For the most simple organisms, adaptation occurs on a purely physical or biochemical level (such as the mutation of a bacterial strain), but more complex organisms can also adapt to new environments by employing new behavioural strategies. In fact, all organisms with a nervous system display intelligent behaviour and have the ability to learn.

One of the most well studied behaviours, across many species, is associative learning: a new behaviour is learned based on the association of two previously unrelated events in the environment. For example, the vinegar worm *Caenorhabditis elegans*, with but 302 neurons, can learn to avoid pathogenic bacterial strains based on aversive olfactory stimuli (26). Similarly, the fruit fly *Drosophila melanogaster* and its larvae can be trained to avoid an odour by aversive conditioning (27, 28). The cricket *Pteronemobius Lineolatus* learns directional orientation while swimming ashore based on terrestrial or celestial cues (29). The domestic dog *Canis lupus familiaris* can be conditioned to associate an unconditioned stimulus (food) that triggers an unconditioned response (salivation) with a new, conditioned stimulus (tone) that will then elicit the same response. The latter experiment is of course part of a famous series of experiments performed by I. Pavlov who discovered and studied classical conditioning in dogs (30). In 1920, J.B. Watson and R. Rayner could show in another famous – but ethically questionable – experiment on a 9-month-old infant that behavioural conditioning applied to humans as well (31). To conclude, these examples illustrate well that the presence of a nervous system, however primitive or complex, enables animals to adapt to new environments by learning and changing their pattern of response to a given stimulus.

A common feature of all types of nervous systems is that they contain different levels of a strictly hierarchic organisation – ranging from genes and single molecules to neuronal circuits – upon which the behaviour of an organism is directly dependent. Thus, within any given neuronal circuit, the most fundamental functional unit is the neuron: its intrinsic biochemistry, anatomical composition and electrophysiology as well as the intricate, fine-tuned excitatory and inhibitory interactions of neuronal ensembles produce the functionally significant output underlying behavioural systems. Thus, to understand the mechanisms of information processing in the nervous system one must not only study the topology of its neural networks but also each cell type's unique intrinsic and neuromodulatory properties that control their in- and output (32, 33) and ultimately dictate the cells' function and integration into the network. Because the synaptic and molecular mechanisms underlying learning and memory storage are highly conserved between species (34), many seminal studies that have considerably advanced our knowledge of the molecular basis of learning were performed in 'simple' organisms, such as *Aplysia californica,* a marine mollusc with but 18,000 neurons. Amongst other things these studies demonstrated the participation of monosynaptic connections and neuromodulatory systems in both short- and long-term memory (35–37).

Nevertheless, even though a slug or a worm share basic learning rules with more complex organisms and simple model systems in general are well suited to the study of the biochemical cascades and single cell phenomenona underlying memory, they are unsuitable to investigate the complex cognitive functions of highly evolved mammalian brains that can contain up to a hundred billion neurons and an equal amount of non-neuronal glial cells in humans (38).

The hippocampal formation, that is crucial for the formation of declarative memories and representation of space (39, 40) and constitutes the focus of this thesis, is a major component of the mammalian brain. Like most parts of the brain, it is under control of neuromodulatory systems, including the dopaminergic, serotonergic, noradrenergic, cholinergic and endocannabinoid system, that act complementary to classical synaptic transmission and constitute a fundamentally important part of neurotransmission. They do not only influence but may in fact dictate neuronal network and behavioural states based on their modulation of single cell properties (41, 42). Specifically, we want to understand how endocannabinoid neuromodulation of single neurons, that itself is highly conserved across species (43), affects hippocampal information processes with a focus on CB_2Rs.

In this introduction I will firstly discuss the hippocampal formation in a top-down approach: its importance in learning and memory formation, the anatomical design of the circuitry and the cell-physiological mechanisms that bestow the hippocampus with its characteristic properties with a focus on CA3. In a second part I will then introduce the ECS and discuss its neuromodulatory effects, both on a cellular and behavioural level before closing the loop by pointing out the most important features of its role in hippocampal memory processes.

1.1 The hippocampal formation

1.1.1 A historical account

The hippocampal region (dentate gyrus, CA1-3 and subiculum), together with its adjacent perirhinal, entorhinal, and parahippocampal cortices forms the medial temporal lobe (44, 45) that is essential for declarative memory (referring to factual memories that can be consciously recalled). Declarative memory can further be subdivided into episodic memory (of autobiographical events) and semantic memory (of factual information). The hippocampus has since long been thought to play a pivotal role in episodic memory formation and spatial navigation, and many theories suggest a two-stage model of information processing where information is learned and initially processed in the hippocampus before being transferred to neocortical areas for long-term storage in a process referred to as consolidation (46, 47). But how was the involvement of the hippocampus in memory formation discovered in the first place?

Neurosurgical treatment of psychiatric diseases, often referred to as psychosurgery, has a complex and controversial history. Its origins can be traced back to antiquity but it was especially popular in the treatment of mental disorders in the 1930-1950s. The use of psychosurgery declined rapidly thereafter due to an increased awareness of its ethical problems, potentially devastating side effects and the development of new drugs to treat neuropsychiatric diseases. However, in their 'golden ages', the results of lobotomies and temporal pole resections (especially amygdalohippocampectomies) have revolutionised our understanding of information and memory processing (48).

"The removals [...] probably destroyed the anterior two-thirds of the hippocampus and hippocampal gyrus bilaterally, as well as the uncus and amygdala. The unexpected and persistent memory deficit which resulted seemed to us to merit further investigation (39)."

The above quote is from a seminal paper by W. Scoville, a neurosurgeon and B. Milner, a psychologist who pioneered the analysis of memory deficits in patients after bilateral medial temporal-lobe resection (39). Later of course, Henry Molaison (before his death known as H.M.), who lost the capacity to form new long-term, declarative memories after the bilateral removal of his hippocampi and amygdala in an attempt to cure his intractable epilepsy, became their most famous patient (and subject). By studying him, B. Milner together with S. Corkin and others contributed substantially to the understanding of declarative memory formation (49, 50). What was so remarkable about H.M. was that he exhibited profound, global anterograde amnesia but did not display a loss of general intellectual ability. For example, even though he lost the ability to retain semantic and episodic memory, he retained the capacity to acquire new motor skills and showed evidence of perceptual learning (51). These findings established that declarative memory is a discrete cerebral function and that the medial temporal lobe is important for its acquisition but did not provide evidence for the singular role the hippocampus plays in the latter. Studies on monkeys which displayed amnesia after localised hippocampal lesioning however indicated a crucial role for the hippocampus in memory formation (52). The first unequivocal evidence for the importance of the hippocampus in memory acquisition in humans was then provided by the case of patient R.B. who development an anterograde amnesia with no signs of additional cognitive impairments after an ischemic episode. A post-mortem histological analysis of his brain revealed a bilateral lesion confined to area CA1 of the hippocampus (53). Together with the case of H.M., these findings showed that damage to the hippocampus is sufficient to produce memory impairments but that additional damage to adjacent parts of the medial lobe aggravates those impairments (54), indicating that the parahippocampal cortices themselves contribute to memory function (55). They furthermore strengthened the idea that multiple forms of memory exist with declarative and non-declarative (procedural memory such as habits) representing separate systems (55).

1.1.2 Current view of hippocampal function

A very detailed picture of the role of the hippocampus in memory formation has emerged since then. In addition to neuropsychological studies on humans, especially a combination of behavioural, lesioning, electrophysiological and anatomical studies in rodents, guinea pigs, cats and monkeys have advanced our knowledge on the hippocampal function in memory that entails mainly the acquisition of long-term episodic and spatial memory but not short-term cognitive functions such as perception (52, 55–57). A very important aspect of memory is the ability to recall information and adapt behaviour based on contextual schemas or patterns. The ability to recall a memory from a partial cue is called pattern completion, whereas the ability to separate similar patterns or memories is called pattern separation. Both are important features of (hippocampal) information processing in humans and rodents and occur to varying degrees along the CA3-CA1 axis (58).

The hippocampus as a spatial map

As mentioned above, the hippocampus is necessary for spatial navigation and to provide the spatial context of an event. Early studies by J. O'Keefe and others lay the foundation of the idea that the hippocampus represents "a spatial map" of the environment (40)[1]. Together with J. Dovstrovsky, he discovered that certain hippocampal principal cells, called place cells, can code for the current location of the animal and display place-specific firing patterns (place fields) (59)[2]. R.M. Morris developed a water navigation task (known as the Morris water maze) (60) to investigate their functional significance and, together with J. O'Keefe, showed that place navigation is heavily impaired in rats with hippocampal lesions (61). Similar to place cells, head direction cells were later identified to spike as a function of the animal's head direction independent of its location in space (like an internal compass) (62). The necessary cellular features to encode space are provided by the hippocampus in ensemble with the entorhinal cortex (EC), that constitutes the main input to the hippocampus and in which cells exhibit a similar degree of spatial modulation (63). Notably, place and head direction cells have been shown to be able to perform both pattern separation and completion, thus displaying features characteristic for contextual hippocampal learning. For example, place field firing is robustly maintained even in the absence of most initial cues, suggesting that a stored pattern can be retrieved based on only a fraction of the initial input (64). On the other hand, head direction cells have been shown to dynamically adapt to direction errors (as tested by a navigational task requiring path integration to find the nest in the dark in absence of any cues) by 'resetting' the firing according to the right direction (65).

Network oscillations

Depending on the behavioural state, different types of network oscillations can be observed in the hippocampus that can be recorded as extracellular local field potentials (LFPs). They arise from the spatiotemporally coordinated, synchronous spiking of cell ensembles and are being been heavily investigated because of their potential computational capacity to store information. During exploratory behaviour, theta (5-10Hz) and gamma (30-120Hz) oscillations are most prominent. In both humans and rodents, gamma oscillations are nested within theta oscillations and exhibit a theta-dependent modulation of their frequency with their power varying within the theta cycle (66, 67). It is thought that the coupling and interaction of hippocampal theta and gamma rhythms as observed during exploratory behaviours may serve as a coding scheme for working memory and to provide the basis for the simultaneous encoding of multiple layers of information (68). The hippocampus exhibits several types of gamma oscillations including locally generated, slow oscillations (30-65Hz) and intermediate/fast oscillations (60-120Hz) that propagate to CA3 from EC that projects to the hippocampus (69–72). Accordingly, by means of wire array recordings in freely moving rats, it has been shown that hippocampal theta/gamma is coupled to theta/gamma oscillations in the EC (73). In humans, a depth-electroencephalogram (EEG) study came to similar conclusions: patients (with unilateral temporal lobe epilepsy) were implanted with depth-EEG electrodes in the EC and hippocampus and field EEG activity in the gamma frequency range was recorded while they were performing a word memorisation task. Successful memorisation was accompanied by a transient and fast-onset (<200ms) increase in EC–hippocampal gamma synchronisation that was absent in unsuccessful memorisation (74). The authors concluded that "effective declarative memory formation is accompanied by a direct and temporarily limited cooperation" between EC and hippocampus (74).

Another prominent type of hippocampal oscillation are sharp wave ripple complexes (SWR) that are thought to be crucial for the consolidation of spatial memory and occur during feeding, awake immobility, and slow-wave sleep (75). The occurrence of theta/gamma and SWR is mutually exclusive which suggests that they perform separate tasks in hippocampal information processing. For example place cells fire sequentially earlier in theta phase as the animal approaches/passes its place field (theta phase precession) (59, 76). Conversely, when the animal is resting/sleeping and SWR are the prominent oscillatory pattern, a reactivation of the place cells (temporally compressed and in reverse order) can be observed, a process also called replay (77). One hypothesis regarding its physiological role is that, by temporally compressing spikes to match the time constant of N-Methyl-D-aspartate receptors (NMDARs), it may provide a basis for Hebbian learning and spike-timing-dependent plasticity (STDP) which will be discussed in more detail in Chapter 1.1.4.3 (77).

1 | It was not until 1996 that M. Bunsey and H. Eichenbaum showed that the hippocampal processing of non-spatial declarative memory function is conserved between humans and rats, too. By behavioural testing (that depended on non-spatial memory recall) in combination with hippocampal lesioning, they could show that rodent non-spatial declarative memory is processed in the hippocampus (57).

2 | Interestingly, the location of a place field is not correlated to the anatomical position of the corresponding place cell in the hippocampus (373).

1.1.3 Hippocampal anatomy

In 1893, S. Ramón y Cajal described the architecture of the hippocampus; his drawings are not only famous but describe in miniscule detail the different types of neurons and the circuitry of the hippocampal formation. The basis of his drawings is the Golgi stain, a reaction discovered by C. Golgi in 1873, in which silver nitrate reacts with potassium dichromate to form silver chromate particles that stain neuronal membranes black. The beauty of this technique is that it stains a limited number of neurons at random, and even if the random nature of the process is still not understood, it yields analysable representations of neuronal tissue that would otherwise appear black (Figure 1.1.1). The anatomical studies of the hippocampus (and cerebral cortex) by S. Ramón y Cajal and his student L. de Nó have advanced the field of neuroscience research substantially. Besides the typical laminar structure of the hippocampus and the different classes of cell types divided topologically along its axis, they noted that fibres from extrinsic and intrinsic sources terminated on distinct domains of the dendritic tree, they described spines and L. de Nó even proposed the existence of dendritic summation of sub-threshold inputs based on his observations as early as 1934 (83).

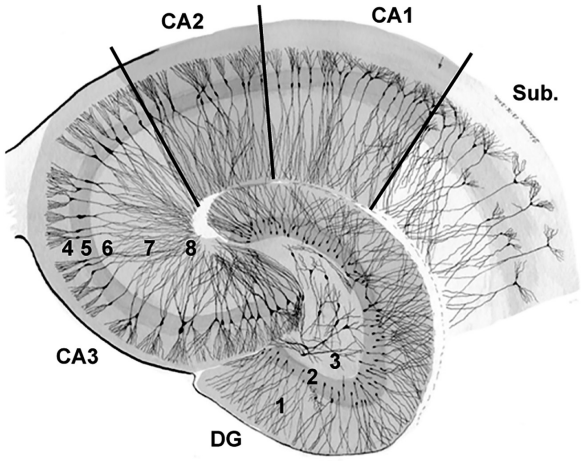

Figure 1.1.1 Drawing of a horizontal section of the hippocampus by L. de Nó. The different grey shades indicate the width of the principal cell layer and subfields. The numbers mark the different layers of the dentate gyrus (1-3) and the hippocampus proper (4-8). Molecular layer - 1, stratum granulosum - 2, hilus (polymorphic layer) - 3, stratum oriens - 4, stratum pyramidale - 5, stratum lucidum (only in CA3) - 6, stratum radiatum - 7, stratum lacunosum-moleculare - 8. Adapted and modified from (83).

As mentioned above, the anatomical organisation of the hippocampus has a unique laminar structure and connectivity pattern, the latter being predominantly unidirectional. It is divided into several subfields: the dentate gyrus that contains the fascia dentate and the hilus, and the Cornu ammonis (CA) areas CA3, CA2 and CA1 (Figure 1.1.1). Transcriptional profiling of DNA expression has confirmed the anatomical division between the hippo-campal subregions by revealing subfield-specific gene expression (84). Classically, the hippocampus is depicted as a trisynaptic circuit with feed-forward excitatory connections onto the three main principal glutamatergic cell types – namely granule cells (GCs), CA3 PCs and CA1 PCs – not taking into account CA2 and hilar mossy cells (see Figure 1.1.2 for a simplified wiring diagram). The dentate gyrus constitutes the main input to the hippocampus and receives information from layer 2 cells of the medial EC (mEC) and lateral EC (lEC) via two distinct pathways, the medial and lateral perforant path (mPP and lPP) (85). The main principle cells of the dentate gyrus are the small, elliptical GCs that are tightly packed in the stratum granulosum in one of two blades of the dentate gyrus. Their spiny, apical dendrites branch in a characteristic cone-shaped manner and are located in the molecular layer (ML) constituting the outer part of the dentate gyrus (86). They receive input from the lPP that terminates in the outer third of the ML and the mPP that terminates in the middle third of the ML. Their unmyelinated axons, called mossy fibres (Mf), have unusually large boutons and form en passant synapses with mossy cells and interneurons (INs) in the hilus, and CA3 PCs (86, 87). Downstream of the dentate gyrus, CA3 PCs provide ipsilateral input to CA1 PCs via the Schaffer collaterals (SC), and project to contralateral CA1 and CA3 via commissural fibres. Additionally, they form a dense, recurrent ipsilateral network with axons called associative fibres. Together, these two fibre-tracts form the associational-commissural (AC) fibres (88). Both CA3 and CA1 PCs receive additional, direct input from EC layer 3 cells by the temporo-ammonic (TA) pathway to their distal, apical dendrites. Finally, CA1 PCs project to the subiculum and back to the deep layers of the EC which in turn feed information back to layer 2/3 cells of the EC (89).

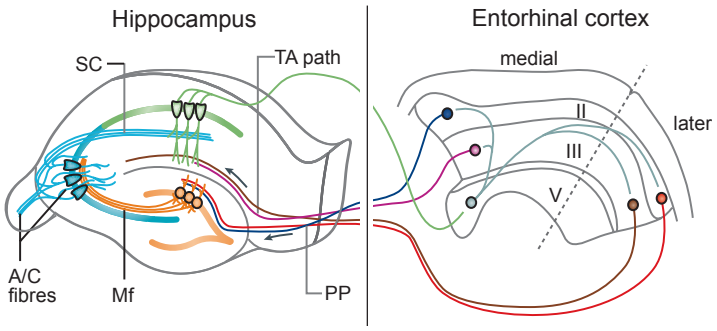

Figure 1.1.2 Schematic wiring diagram of the hippocampal formation. GCs in the dentate gyrus receive input from the superficial layers of the EC which is then routed via CA3 to CA1 and the subiculum, before being sent back to the deep layers of the EC. CA3 and CA1 additionally receive direct EC input. Adapted and modified from (88).

Of course, the complexity of hippocampal circuitry goes far beyond the connections here described and defies the simplicity implied by most wiring schemes. In the following I list some examples: CA3 PCs densely innervate the hilus and the ML of the dentate gyrus (90) and project to CA2 (91); displaced GCs have been found to be located in CA3 (92); CA2 PCs receive direct input from CA3, the DG and EC (93, 94); all hippocampal principal cell types can be differentiated into subclasses according to their morphological, electrophysiological and connective properties (90, 95–98) and can be electrically coupled to each other via gap junctions (99). Furthermore, GABAergic[3] INs, a class with over 20 subtypes in the hippocampus alone, represent about 10% of the neuronal population and regulate both principal cells and other IN types by local feed-forward and feed-back modulation (78). The latter is mostly localised – but not limited – to a given subfield. For example, a fraction of feedback INs in CA1 has been shown to project back to CA3 (90). Last but not least, the hippocampus is under control of many distinct local or long-range neuromodulatory systems. An example of intrinsic neuromodulation, in which local neurons themselves produce the neuromodulator, is the ECS that will be discussed in detail in chapter 1.2. Extrinsic modulation originates mostly from subcortical areas such as the septum, raphe nuclei or thalamus that innervate the hippocampus via long-range fibres (100–102).

Despite its complexity, as a unifying rule it can be stated that 1) the majority of neocortical information to the hippocampus is routed via the EC through the DG and that 2) nearly all outputs from the hippocampus originate in CA1 and the subiculum and target cells in the deep layers of the EC, which projects to neocortical regions as well as back to the EC.

Most data on hippocampal anatomy/connectivity stems from studies in rodents, but the basic intrinsic circuitry is very similar between human and rodent brain (103). Differences include the orientation of the hippocampus within the brain (see Figure 1.1.3) that is based on developmental differences between the species and the presence of a CA4 subfield in humans (44). Concerning the latter, some have argued that mossy cells may be analogous to CA4 PCs. Similar to CA3 PCs, they have thorny excrescences with large spines as contact sites for Mf boutons and a pyramid-like shape as already noted by L. de Nó who referred to them as 'modified pyramids' (86). Also, in humans, CA4 is located in the 'the concavity of the gyrus' – which corresponds to the hilus (44). To conclude, the rodent hippocampus is well suited for detailed analyses and allows for comparative conclusions.

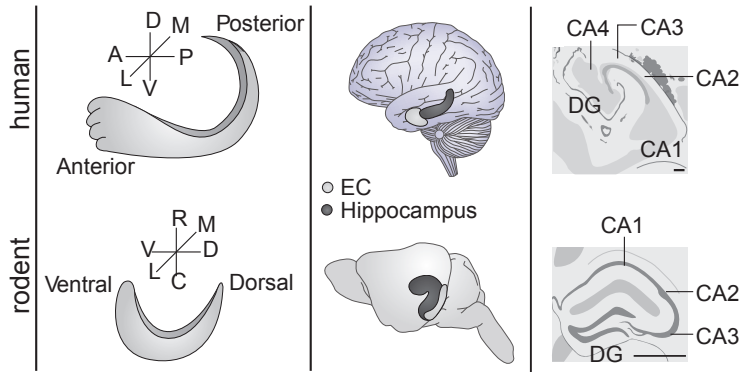

Figure 1.1.3 Cross-species comparison of hippocampal anatomy. Left panel: illustra-tion of the longitudinal axis of the hippocampus with is described as ventrodorsal for rodent and anteroposterior for human hippocampus. Note the 90° offset in the orientation of the rodent hippocampus to match the orientation of the human hippocampus. Middle panel: location of the hippo-campus (dark) and EC (light grey) in the brain. Right panel: Drawings of mouse and human hippocampi based on Nissl-stain cross sections. A: anterior, C: caudal, D: dorsal, L: lateral, M: medial, P: posterior, R: rostral, V: ventral. Adapted and modified from (103).

The gargantuan amount of information available on the hippocampus and its cell types makes it impossible to summarise it adequately. In the following, I will thus focus on area CA3 and its main principal neuron, the CA3 PC, and will also limit the description of neuromodulation and (intrinsic) plasticity types accordingly.

1.1.4 Properties of CA3 pyramidal cells

Ultimately, the properties of a network depend directly on the properties of its neurons, both active and passive. CA3 PCs receive many different streams of information along their dendritic tree, and their cellular, both morphological as well as electrophysiological, properties dictate subsequent processing and routeing.

1.1.4.1 Morphology

The importance of morphological characteristics of CA3 PCs is well illustrated through their alterations in pathophysiological brain states that are accompanied by neurite atrophy such as during depression and anxiety (104), schizophrenia (105), epilepsy (106), Alzheimer's disease (107) and hyperthyroidism (108).

Reconstructions of biocytin-labelled CA3 PCs have provided us with a very detailed picture of the diverse morphological features of CA3 PCs. The length and arborisation of the dendritic tree of CA3 PCs varies according to their location within the CA3 subfield (109). CA3a/b PCs (more proximal to CA1) have larger dendritic trees with a length of 19-26mm whereas CA3c PCs (located closer to the dentate gyrus) have significantly shorter dendritic trees (10.4-11.6mm). This morphological comparison suggests that at least two distinct subgroups of CA3 PCs can be distinguished: 1) CA3a/b PCs with much more complex dendritic branching and an increased dendritic length and 2) comparatively smaller CA3c cells with a reduced surface area and shorter dendrites (Figure 1.1.4).

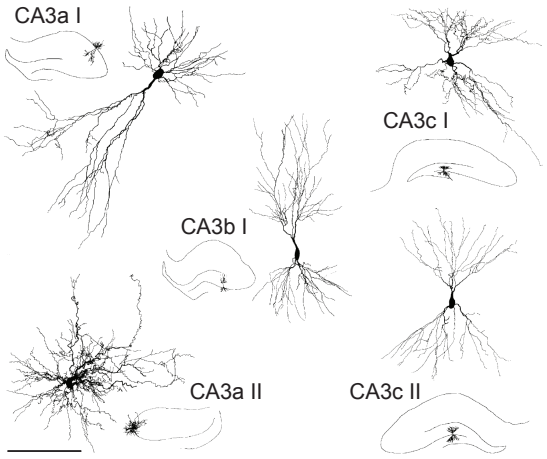

Figure 1.1.4 Dendritic arborisation of CA3 PCs. The location of each cell is indicated in the insets. Scale bar: 255, 258, 274, 260 and 254µm (clockwise). Adapted from (109).

In spite of this, CA3 PCs share a general similarity in their structure and are especially alike in their inputs. The apical dendrites of CA3 PCs branch close to the soma (in contrast to CA1 PCs that have a more distinct main apical dendrite). The most proximal part of the apical dendrite (≥100µm) in stratum lucidum contains clusters of large spines (the thorny excrescences) that receive input from GC Mfs (110). The recurrent AC connections are located on the basal dendrites in stratum oriens (and mid-apical dendrites in stratum radiatum) (111). Direct EC connection via the TA path impinges on the most distal apical dendrites in stratum lacunosum-moleculare. In addition, a CA3 PC is under the tight control of many different classes of inhibitory INs with distinct projection patterns that control its input (on distal and/or proximal dendritic segments) and output (on somatic and axo-axonic segments) (112–116).

CA3 pyramidal neurons have extensive axonal arborisations (150-300mm total length) with an average density of approximately 20 boutons per 100 µm. Thus, a single neuron may communicate with 30,000 to 60,000 other neurons (117). Both AC and SC axons are unmyelinated and can conduct at velocities of 0.2–0.4mm/ms. Action potentials are initiated ~30–40µm away from the soma, where the density of voltage-gated sodium channel is highest (118). Their primary axon has up to eight axon collaterals that usually ramify further and innervate stratum oriens and stratum radiatum of CA3, CA2 and CA1, and the dentate gyrus (see p10) but only rarely extend into the subiculum and not at all to the EC (119). In contrast to CA1, CA3 and CA2 PCs have a bilateral recurrent innervation pattern (via the A/C fibres) (120). The SC projections of CA3 to CA1 follow a topographical gradient: proximal CA3 PCs, located closer to the dentate gyrus, project more heavily to septally located CA1. Vice versa, CA3 PCs located closer to the CA1 subfield project preferentially to more temporally located CA1 PCs (119). CA3a PCs preferentially innervate the basal dendrites, whereas CA3c PCs predominantly impinge on apical dendrites of CA1 and CA3 PCs (117). The majority of recurrent CA3 fibres stay within the subfield of the 'parent cell' (117).

Genetic analysis of the principal cells of the main hippocampal subfields has furthermore shown that they divide into distinct subpopulations with discrete temporal developmental profiles. These subpopulations preferentially connect to each other within a subfield and interconnect selectively across subdivisions as well (121). Even though the functional significance

of this remains to be tested, these "parallel connectivity channels" (121) could facilitate the simultaneous processing of separate streams of information.

1.1.4.2 Intrinsic properties

The recurrent connectivity of CA3 PCs renders the CA3 network prone to hyperactivity and the hippocampus one of the brain areas with the lowest seizure threshold (122). Because of the potentially devastating outcome of epileptic, excitotoxic activity through severe tissue damage and cell death, a tight network control is of utmost necessity. Mostly, this is thought to depend on the control of principal cell firing by inhibitory INs that maintain a balanced excitation-inhibition ratio (123). However, cell-intrinsic mechanisms are also in place to balance excitatory and inhibitory processes.

Resting membrane potential and spike generation

First and foremost, the excitability of a neuron depends on its resting membrane potential, input resistance, and (receptor-) channel composition. Concomitantly, the transmembrane electrical potential difference of *any* cell depends on the concentrations of ions present across that membrane (mostly potassium, sodium and chloride) and the membrane's permeability to those ions (the latter being dictated by the presence of respective pumps and channels)[4]. Because the permeability of potassium is highest ($K^+ \rightarrow Cl^- \rightarrow Na^+$ with a ratio of 100:10:1), it contributes most to the resting membrane potential which is thus usually close to the K^+ reversal potential (124)[5]. The resting membrane potential is actively maintained by the activity of the sodium-potassium pump (Na^+/K^+-pump, an ATPase) that moves two potassium ions into the cell while moving three sodium ions out per one molecule ATP. This leads to a net hyperpolarisation of the cell and maintains, in concert with the different ion permeabilities, the unequal distribution of ions across the membrane that constitute the negative resting membrane potential (124). Conversely, acute block of the Na^+/K^+-pump with 10µM ouabain leads to a depolarisation of 5-30mV of CA3 PCs in acute slices and often to epileptic activity and/or depolarisation block due to sustained firing (own unpublished observation and (125)). It is estimated that the activity of the Na^+/K^+-pump consumes about twenty percent of a cell's total energy demand (126).

Voltage-gated sodium (Na_v), potassium (K_v) and calcium (Ca_v) channels underlie the action potential of CA3 PCs. The highest density of Na_v and K_v channels is at the axon initial segment (AIS), where sufficient depolarisation leads to their voltage-dependent activation and action potential generation. Na_v and K_v channels are additionally expressed along the entire dendritic tree and have been shown to facilitate the backpropagation of action potentials generated in the axon into the proximal dendrite. Ca_v are expressed at highest densities along the proximal dendrites of CA3 PCs and cause the characteristic burst firing that some CA3 PCs display, for example during exploratory behaviour in vivo (127, 128). In distal CA3 PC dendrites, not only Ca_v, but also Na_v channels are able to generate dendritic spikes with a low initiation-threshold due to their high expression (129). This feature of distal CA3 PC dendrites has been postulated to be important to accurately transfer input from distal PP synapses to the soma that are carry spatiotemporal information from grid cells in the EC (129). Generally, the refractory period after an action potential that depends on the inactivation of Na_V channels, is the main determinant for the unidirectional propagation of action potentials and reduces excitability. In addition to the fast-inactivating current, Na_V channels give rise to a non-inactivating, persistent sodium current (comprising up to 5% of the current) with important physiological consequences: in a subthreshold range it depolarises the membrane potential, thereby regulating dendritic excitability, repetitive firing and enhancing synaptic transmission (130). In immature hippocampal neurons, where depolarising GABA promotes network oscillations called giant depolarising potentials (GDPs), the persistent sodium current promotes the slow regenerative depolarisation that generate the intrinsic bursts which in turn trigger the GDPs (131). Whether the persistency is caused by different Na_V subunits or gating states of the same subunits is not clear.

Afterhyperpolarisation

Similar to K_v channels that are activated at depolarised potentials and, together with the inactivation of Na_v channels, lead to the repolarisation of the membrane potential after its Na_v-mediated rising phase, additional potassium channels are activated by the membrane potential depolarisation and corresponding calcium influx. Thus following neuronal activity – single spikes, repetitive or burst firing – several of these voltage- and calcium-activated potassium conductances mediate a transient hyperpolarisation of the membrane potential of CA3 PCs referred to as afterhyperpolarisation (AHP). The AHP provides a direct, non-delayed and cell-intrinsic graded negative feedback response to spiking. Its amplitude and duration depend on the number of spikes and calcium-influx. It is separated into three components, the fast, medium and slow AHP (fAHP, mAHP and sAHP respectively) of which each is mediated by distinct conductances (132). The fAHP is activated immediately

4 | Ion movement that underlies synaptic transmission of course contributes to both the resting membrane potential and excitability of a neuron as well but will not be discussed here.

5 | The resting membrane potential of CA3 PCs is approximately -84mV in a hippocampal slice of P25-30 mice (own observations, see table 3.2.1; but corrected for liquid junction potential, see methods).

during an action potential and lasts several tens of milliseconds and thus contributes to action potential repolarisation. Its current (I_c) is mediated by BK-type potassium channels (called 'big potassium' due to their large conductance of 200-400pS) that open in a calcium- and voltage-dependent manner with their calcium-dependence depending on the membrane potential (133). The mAHP is activated within 5ms after the action potential and lasts for several hundreds of milliseconds. The predominant underlying current (I_{AHP}) is mediated by calcium-activated SK channels (called SK because of their small conductance of ~10pS), but voltage-gated M-channels (I_M) contribute to the mAHP as well (133, 134). It affects instantaneous firing rate, sets the tonic firing frequency of neurons and regulates burst firing and oscillatory activity of neurons (134). The slow AHP is usually activated by repetitive firing (such as burst firing), rises to a peak over many hundred milliseconds and its slow decay can last up to 5-20s[6]. It is mediated by a slow, calcium-dependent potassium current but the molecular identity of the underlying channel is not known (133, 134). Similar to the mAHP, the sAHP has been postulated to modulate spike frequency (135). During trains of action potentials it additionally acts as an activity-dependent gain control through shunting of inputs, and modulates the threshold for induction of long-term potentiation (LTP) and long-term depression (LTD) (136, 137). In pathophysiological network states such as epilepsy, the AHP that follows epileptiform burst discharges is of critical importance to prevent seizure development (138). Similarly, in a rat model of epilepsy ('genetically epilepsy-prone rat', GEPR), the sAHP of CA3 PCs was shown to be significantly reduced (139). The AHP is under control of a variety of neuromodulators including dopamine and serotonin that usually lead to its suppression (140, 141).

Hyperpolarisation-activated cyclic nucleotide-gated channels

Hyperpolarisation-activated cyclic nucleotide-gated (HCN) channels are non-selective cation ion channels that belong to the superfamily of K_V channels. The predominant isoforms in the adult hippocampus are HCN1 and HCN2[7]. Whereas HCN2 expression is very uniform between the hippocampal subfields, HCN1 is expressed at higher levels in CA1 than in CA3. All HCN isoforms are predominantly, but not exclusively, expressed on PC dendrites. HCN channels are curious in that they are activated by hyperpolarising potentials and are permeable to cations. That means that at a hyperpolarised membrane potential they will open and, *being permeable* to potassium and sodium, depolarise the membrane potential. These features lead to the very characteristic 'sag' potential (and rebound depolarisation) that can be seen in response to hyperpolarising current pulses especially in CA1 PCs: upon hyperpolarisation of the membrane, HCN channels will open and introduce a depolarising membrane potential shift in the initial voltage response (the 'sag') before reaching steady-state (see figure 3.1.1B, upper panel for an example trace). To conclude, (somato-)dendritic HCN channels influence the membrane resistance, contribute to the resting membrane potential and modulate action potential firing and integration of synaptic inputs (142) in most cortical cells, including hippocampal principal neurons (142). When presynaptically expressed, they suppress transmitter release (143). In CA3 in particular, HCN channels have been shown to be pivotal for network synchronisation during hippocampal development and their block leads to increased burst firing of CA3 PCs (144). Furthermore, HCN1 KO mice display improved hippocampus-dependent learning, their theta oscillations power is augmented (145) and their place fields in both CA3 and CA1 are larger and more stable in comparison to wildtype (WT) mice (146).

Additional channels influencing the excitability of CA3 PCs

ATP-sensitive potassium (K_{ATP}) channels have been shown to be expressed at high densities in CA3 PCs and their activity-dependent opening hyperpolarises the membrane potential, thereby reducing excitability (147). Like the AHP, they are thus likely to play an important role during pathophysiological network states when ATP will be released through neuronal activity and thus counterbalance the hyperexcitability by activating K_{ATP} channels (147, 148). Different subtypes of K_V channels, expressed along the dendritic tree of most hippocampal principal cells, affect spiking as well as dendritic integration and summation of excitatory postsynaptic potentials (EPSPs). For example, the slowly inactivating D-type K_V (K_D) channels causes delayed spiking due to its sub-threshold activation, reduces action potential precision, and positively affects the temporal integration of excitatory inputs due to its long subsequent inactivation period (149). K_D channels have also been shown to inhibit the spike afterdepolarisation and, as a consequence, action potential bursting (150, 151). A-type K_V (K_A) channels limit both the backpropagation and dendritic initiation of action potentials upon their activation (152).

1.1.4.3 Intrinsic and synaptic plasticity mechanisms

Synaptic long-term plasticity

Synaptic plasticity processes such as LTP and LTD are widely considered to underlie the encoding of new memories (153). To summarise many decades of discoveries, 'classic' NMDAR-dependent LTP as found at the SC-CA1 synapse leads to an insertion of α-amino-3-hydroxy-5-methyl-4-isoxazolepropionic acid receptors (AMPARs) into previously silent synapses,

6 | See figure 3.1.1 and table 3.1.1 for a comparison of the AHP in CA3 PCs, CA1 PCs and dentate gyrus GCs. A very large amplitude and long-lasting AHP with a prominent sAHP component is characteristic for CA3 PCs, whereas CA1 PCs have a pronounced fAHP and mAHP component but the AHP decays very quickly due a less pronounced sAHP component.

7 | Allen Brain Atlas, mRNA expression for HCN1 (gene ID: 15165) and HCN2 (gene ID: 15166)

thus increasing synaptic strength, and its long-term manifestation depends on protein synthesis (154). LTD on the other is either mediated by postsynaptic NMDAR- or metabotropic glutamate receptor (mGluR)-dependent endocytosis of AMPARs, or may also exhibit a presynaptic expression mechanism (155), depending on the synapse. STDP, a form of Hebbian learning that depends on the correlated activity of a pre- and postsynaptic cell (156), is assumed to be implemented by a specific form of pairing-induced plasticity which for most synapses depends on the activation of NMDARs: a short temporal delay of pre- versus postsynaptic spiking leads to either potentiation (pre before post) or depression (post before pre) of synaptic inputs (157, 158). For CA3 PCs, it has been hypothesised that the efficient backpropagation of action potentials into their dendrites, that provides a large and temporally precise feedback, is ideally suited to facilitate the induction of STDP (129, 159). Interestingly, while spike timing-dependent LTP (tLTP) requires postsynaptic NMDARs, different forms of spike timing-dependent LTD (tLTD) have been shown to require either postsynaptic NMDARs or co-activation of presynaptic NMDARs and presynaptic (or astrocytic) CB_1Rs (see p33 and (158, 160)).

However, other NMDAR-independent forms of LTP that solely depend on the activity of the presynaptic neurons or postsynaptic calcium-permeable AMPARs, have been discovered at various synapses (161, 162). Another important type of synaptic plasticity occurs in response to chronic block or activation of neuronal activity which leads to a homeostatic adaptation of synaptic strength. This mechanism, called synaptic scaling, was first described by G.G. Turrigiano and S.B. Nelson in 1998 (163) using chronic pharmacological activation and inhibition of cortical neurons in culture. They observed that neurons responded to low network activity by upregulating the strength of their excitatory synapses and to increased firing rates by downregulating them. This mechanism was later shown to depend on a change in the number of postsynaptic glutamate receptors (164). [8]

Plasticity of intrinsic excitability

Many forms of cell-intrinsic plasticity, including homeostatic scaling, have been described in which activity-dependent signalling will lead to the up- or downregulation of (receptor-) channels or other proteins by endocytosis, reorganisation, or (persistent) activation (165–167). Particularly, both physiological and pathophysiological repetitive network activity has been shown to induce homeostatic plasticity of intrinsic excitability in pyramidal neurons that regulates, mostly voltage-gated, ion channels (168). It has thus been postulated that this form of plasticity acts to "adjust the output firing level of the postsynaptic neuron to stabilise network activity within physiological bounds" (169). In the following I will discuss principles that have emerged for CA3 PCs, while for a general review of cell-intrinsic plasticity mechanisms, the reader is referred to (164, 168, 170–172).

Repetitive somatic firing at physiological frequencies (10Hz for 2s) can induce a long-term potentiation of the intrinsic excitability (LTP-IE) of CA3 PCs by a calcium- and tyrosine kinase dependent internalisation of K_D channels (150) in adult hippocampal slices. Similarly, glutamate-evoked burst firing in hippocampal cultures leads to changes in the localisation and phosphorylation state of $K_V2.1$ channels. Their typical organisation in discrete clusters is lost after glutamate stimulation and their current-voltage relationship is shifted towards more hyperpolarised potentials. Both effects were reported to be mediated by the calcium-dependent activation of calcineurin, that in turn causes a rapid, but reversible dephosphorylation of the channel (165). Conversely though, two studies using homeostatic plasticity paradigms in cultured hippocampal cells reported that 1) activity deprivation by the application of dendrotoxin, a K_V channel blocker, reduces the K_D channel current and thereby increases action potential precision and network synchrony (169) and 2) enhanced activity (through block of inhibitory synaptic transmission) for 48h lead to an increase in the K_V1-mediated current (173), which passes through low-voltage activated K_V1 channels (174). Slice cultures have a higher neuronal connectivity and consequentially an increased excitability (175), thus homeostatic forms of K_V plasticity might occur under control/baseline conditions already and confound subsequent analysis. Furthermore, slice cultures are usually obtained from early postnatal (P0-P7) tissue. A study by I. Soltesz and colleagues, who investigated the mechanisms of homeostatic plasticity in vivo, found that synaptic scaling only occurs in juvenile, but not adult animals (176). Thus, whether these opposing plasticity mechanisms on K_V function would co-exist in the same cell (with or without a developmentally regulated temporal separation) and whether they would occur under physiological conditions, remains to be experimentally tested.

Both physiological and pathophysiological neuronal activity induces changes in HCN channel expression, arguing for the channel's important role in determining hippocampal principal cell excitability. HCN1 and HCN2 mRNA levels (of all hippocampal subfields) have been shown to be reduced after kindling and kainate-induced epilepsy in rats (177) In CA1 PCs, induction of NMDAR-dependent LTP at the SC-CA1 PC synapse using a theta-burst protocol enhances HCN channel expression in a calcium/calmodulin-dependent protein kinase II (CaMKII) dependent manner (178). AMPAR-mediated

8 | For a more complete and detailed overview of synaptic plasticity research, which is beyond the scope of this thesis, the reader is referred to excellent reviews that discuss the mechanisms underlying LTP and LTD as well as their role in memory formation (153, 155, 374–377).

synaptic transmission induced by glutamate application or direct depolarisation was found to increase the HCN-mediated current (I_h) in CA1 PCs as well, in a calcium but cyclic adenosine monophosphate (cAMP)-independent manner (179). Conversely, high frequency stimulation (HFS)-induced LTP of SC-CA1 PC synapses was shown to lead to a downregulation of I_h (180). It follows that Hebbian forms of plasticity and direct activation of glutamate receptors cause persistent changes of HCN channel expression and function. But whether these manifest as an up- or downregulation of HCN channels is likely to depend on the subcellular location of LTP expression and the downstream signalling molecules (142).

Mutations in certain Na_V channel subunits cause epilepsy, and correspondingly, kindling-induced seizures lead to an upregulation of $Na_V1.6$ subunit mRNA and protein levels in CA3 PCs that is paralleled by an increase in persistent sodium current (181).

As a last example, the activity of the Na^+/K^+-pump itself has been shown to be modulated by high frequency stimulation where repetitive spiking of a CA3 principalneuron leads to a long-lasting hyperpolarisation of the same neuron in a conductance-independent manner. Experiments with the Na^+/K^+-pump blocker ouabain suggest that this is mediated by an increased activity of the Na^+/K^+-pump that follows an activity-dependent intracellular rise in calcium release (125), yet the downstream signalling cascade that links an increase in calcium to the activity of the pump is unknown.

In vitro, long-term changes in intrinsic excitability can be induced with the same parameters that elicit synaptic plasticity (150, 169, 172). This indicates that the same stimuli and activity patterns will induce complementary, isochronic forms of plasticity, as has been confirmed experimentally (178). Certainly, persistent changes of the intrinsic excitability of neurons will have substantial implications for neuronal information processing through adaptive dynamics. Nevertheless, it will be important to analyse the function of intrinsic plasticity in vivo and to experimentally assess its necessity for learning and memory formation.

In addition to the above examples, a wide variety of neuromodulators affect excitability by through their action on ion channel properties. For example, dopamine, serotonin, acetylcholine, endocannabinoids and neuropeptides (such as somatostatin, VIP or cholecystokinin) all modulate the function of various ion channels either directly or indirectly through calcium-dependent cascades and (de-)phosphorylation (167). In the second part of this introduction (chapter 1.2) I will discuss the ECS and its neuromodulatory functionality.

1.2 The endocannabinoid system

Although the medical and spiritual use of the Cannabis plant (Figure 1.2.1) can be traced back to ~2000 BC, the physiology and molecular composition of the cannabinoid system was completely unknown until 25 years ago. This obvious discrepancy can be explained historically, because it was not until the 19th century that cannabis as a psychostimulant spread from China and the Middle East to Europe and America (182, 183) and thus also spurred research on its underlying mechanism of action. Furthermore, even after the successful isolation of the delta-9-tetrahydrocannabinol (THC), the main psychoactive compound of Marijuana, in 1964 (184), it took nearly 25 years to identify its main binding site in the brain: the CB_1R (185, 186). The CB_2R was identified soon after in the periphery, in cells and organs of the immune system (7). The identification of cannabinoid receptors of course suggested the presence of endogenous ligands and the first of many endocannabinoids, N-arachidonoylethanolamide (anandamide) and 2-AG, were discovered in 1992 and 1995 (187, 188). Since then, we have witnessed an immense surge of research into the ECS, and it is now well appreciated to be an integral part of the immune, digestive, reproductive, cardiovascular and central nervous systems in the healthy, unstimulated state as well as in disease (189). Given the topic of this thesis, I will limit the introductory information on the endocannabinoid system – comprising ligands, synthesising and degrading enzymes, receptors, ion channel targets and down-stream signalling cascades – to the neuromodulatory function of anandamide and 2-AG in CNS signalling. For further information, the reader is referred to a review by A. Howlett et al. (12).

Figure 1.2.1 Cannabis sativa. Drawing with (A) flowering male and (B) seed-bearing female plant. From: Köhler's medicinal plants (384).

1.2.1 Endogenous cannabinoids

Endocannabinoids are, similar to phytocannabinoids of herbal origin, small membrane-derived lipid molecules. In the brain, they are produced by various cell types including neurons, astrocytes and macrophage lineage cells such as microglia. The two most abundant endocannabinoids in the CNS, namely 2-AG and anandamide, are both metabolites of the polyunsaturated fatty acid arachidonic acid that is a non-essential fatty acid predominantly derived from dietary essential fatty acids (187, 188). Besides being a major constituent of membrane phospholipids and regulating membrane fluidity (190), arachidonic acid, upon its stimulated release from phospholipids, can directly act on ion channels or protein kinases in the cell, or be transformed into one of its many metabolites, called eicosanoids (191, 192).

1.2.1.1 Pathways involved in endocannabinoid synthesis

Anandamide is produced from N-arachidonoylphosphatidylethanolamines (N-arachidonoyl-PE), a family of membrane phospholipids. The latter are synthesised from phosphatidyl-ethanolamines by the enzyme N-acyltransferase that is activated via adenylyl cyclase and protein kinase A (PKA). N-arachidonoyl-PEs are further processed to yield anandamide via several pathways, the most well-studied involving N-acylphosphatidylethanolamine-specific phospholipase D (NAPE-

PLD) that directly converts N-arachidonoyl-PE to anandamide (193, 194) (Figure 1.2.2, left panel). Many complementary (and compensatory) synthesis pathways have been suggested to exist, especially since NAPE-PLD KO mice appear to not have reduced anandamide levels (194). An alternative pathway of anandamide production via the conjugation of arachidonic acid with ethanolamine that has been shown to occur in the liver, could explain this discrepancy (195). However, further studies are needed to show that the same pathway occurs in other tissues as well.

2-AG is the most abundant endocannabinoid in the brain with concentrations about 200fold higher than anandamide. It can be produced via two complementary pathways: firstly, via the metabolism of phosphatidylinositol to 2-arachidonyl-lysophospholipid by the enzyme phospholipase A1 (PLA1) and its subsequent conversion into 2-AG by lysophospholipase C (lyso-PLC). Secondly, via the phospholipase C β (PLCβ)-mediated cleavage of phosphoinositides (PI) into inositol 1,4,5-trisphosphate (IP_3) and diacylglycerol (DAG); the latter of which is then converted to 2-AG by 1,2,-diacylglycerol lipases (DAGL) (193, 196) (Figure 1.2.2, right panel). DAGL has two different isoforms, DAGLα and DAGLβ, with DAGLα being exclusively responsible for the production of 2-AG in the CNS as shown by comparative KO studies with deletion of either isoform (197, 198) and confirmed in this thesis (see results 3.5).

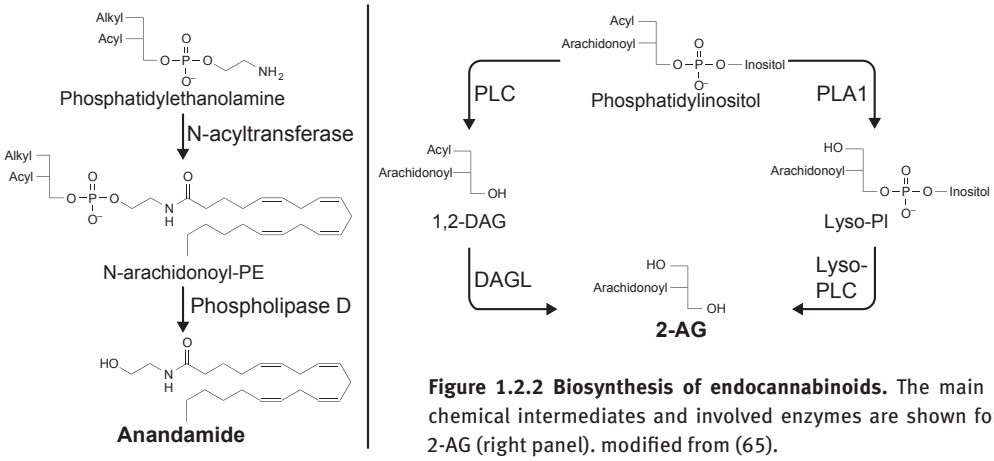

Figure 1.2.2 Biosynthesis of endocannabinoids. The main synthesis pathways including chemical intermediates and involved enzymes are shown for anandamide (left panel) and 2-AG (right panel). modified from (65).

Synthesis of 2-AG and anandamide can be triggered by a rise in intracellular calcium concentrations to micromolar levels (199), for example following neuronal activity and membrane depolarisation, which will activate PLC and N-acetyltransferase respectively (196, 200). Additionally both enzymes can be activated in a G Protein-mediated way that enhances endocannabinoid production without being dependent on the elevation of calcium. For anandamide, adenylyl cyclase stimulation via $G\alpha_s$ has been shown for vasointestinal peptide (VIP) receptors via VIP (196), whereas dopamine receptor activation was reported to increase anandamide levels 8fold by activating PLCß via Gßy (193). For 2-AG, a multitude of possible G Protein-coupled receptor (GPCR)-dependent pathways exist that activate adenylyl cyclase via $G\alpha_{q/11}$, including mGluRs (199) and muscarinic acetycholine receptors (mAChR) (201, 202). A third, synergistic mode of activation has been described to occur during synaptic activity, when subtle rises in calcium to sub-micromolar concentrations coincide with weak mGluR activation via glutamate release. Under these conditions, a calcium-assisted mGluR1 to PLC cascade, in which PLC acts as a coincidence detector, can induce cannabinoid release. In fact, this activation mode has been suggested to underlie physiological cannabinoid release during synaptic transmission (199) (also see p19).

1.2.1.2 Mode of endocannabinoid synthesis

It is still a matter of debate whether endocannabinoids are only produced 'on demand', or whether additional preformed stores exist. For anandamide, it has been shown that calcium acutely stimulates anandamide synthesis and that this is accompanied by de novo production of its precursor N-arachidonoyl-PE (193). These findings support the 'on demand' synthesis of anandamide and would also explain its low baseline levels (203). Conversely, it has been argued that the high concentrations of 2-AG in the brain indicate that they may fulfil important housekeeping functions rather than only being produced on demand. Indeed, only a small percentage of the total 2-AG is thought to activate CBRs, other important purposes being to terminate DAG/PKC-mediated signalling and providing a substrate for arachidonic acid and eicosanoid synthesis respectively (203). In acute hippocampal slices as well as neuronal cultures, acute pharmacological block of DAGLα was shown to abolish synaptic, retrograde 2-AG signalling (204). These results would strengthen the hypothesis of an on-demand, activity-dependent synthesis at the level of synaptic transmission. However the same study showed that the 2-AG content in hippocampal slices after preincubation of slices with the DAGLα blocker was reduced by only 30%, thus not depleting basal 2-AG levels substantially (204). Since all these results are based on pharmacological blockage of (or genetic interference) with complex signalling pathways, caution should be exerted when interpreting them. Furthermore, tonic 2-AG

release[9] could still a) be based on ongoing, spontaneous synaptic activity, when low calcium increase coincide with metabotropic glutamate receptor activation or intracellular microdomains see a sufficient local increase in calcium concentrations and b) be DAGLα independent. To conclude, many open questions remain that need to be answered to disentangle this immensely complex issue: do different pools of 2-AG exist and if yes, are they produced and stored independently? Does the PLA1/Lyso-PLC pathway compensate for the DAGLα-dependent 2-AG synthesis when the latter is blocked and could this account for a spatial segregation of signalling pathways? If different pools exist, could a spatial segregation also explain the functional discrepancy between the observed loss of DSI and 30% reduction in total 2-AG level? Do different cell types employ different storage and release modes?

1.2.1.3 Endocannabinoid release and storage

Despite a very detailed biochemical knowledge on endocannabinoid synthesis, very little is known about the processes involved in their storage and release. The storage mechanisms of endocannabinoids and whether they exist at all, is not known. If only on-demand synthesis existed, storage of eiconoseids would not be necessary and it is certain that they are not stored in vesicles like classic neurotransmitters. It has been postulated based on observations in dorsal root ganglion cell lines that both DAGLα and 2-AG may localise to lipid rafts in the plasma membrane (205). Lipid rafts are enriched in cholesterol and sphingolipids, able to compartmentalise neurotransmitters and involved in endocytosis and trafficking of signalling molecules. Further experiments are necessary to strengthen this hypothesis and to elucidate anandamide storage mechanisms. Furthermore, in contrast to hydrophilic neurotransmitters such as glutamate and GABA, lipophilic substances do not easily diffuse in the extracellular space. It seems more likely that endocannabinoids diffuse laterally within the cell membrane and experimental results support this notion. First, it has been shown that agonists can approach CBRs by lateral diffusion and second, a study by Z.H. Song and T.I. Bonner showed that an intramembranous lysine residue in the third transmembrane domain of the CB_1R is responsible for binding to several agonists (193, 206). However, the fact that endocannabinoids do not only act trans-synaptically between neurons but mediate communication between neurons and astrocytes as well (207), suggests that interstitial mobility must occur. Based on electrophysiological studies it has been postulated that endocannabinoids can diffuse by approximately 20µm (4). The mechanisms that underlie their activity-triggered extrusion from the membrane and diffusion through water-filled space, again, remain an open question.

1.2.1.4 Neuronal and glial origin of endocannabinoids

Anandamide has been shown to be produced by both neurons and astrocytes (208), but whether glial cells, in particular astrocytes, also produce 2-AG has been a matter of debate. Immunofluorescence and immunoelectron microscopy studies have reported the lack of detectable DAGLα in astrocytes (195) whereas its presence in neurons is certain. In CA1 PCs and cerebellar Purkinje cells, it is highly compartmentalised and predominantly localised to postsynaptic spines that oppose CB_1R positive terminals, with no or weak expression on somatodendritic domains (209, 210). These results have been confirmed in human tissue and with DAGLα KO controls respectively (211). Interestingly, a study analysing the dynamics in DAGLα protein amount before and after inflammation, reported that both microglial cells and astrocytes were immunoreactive for DAGLα after stimulation with inflammatory lipopolysaccharides, whereas only a specific subtype of astrocytes was weakly immunoreactive under control conditions (212). Additionally, DAGLα and DAGLß expression was shown in oligodendrocytes and their progenitor cells (213). These findings could a) explain the discrepancy in the literature based on cell type and activity state and b) strongly point towards an involvement of glial cells in 2-AG signalling since they express the necessary molecular machinery.

1.2.1.5 Deactivation of endocannabinoid signalling activation

As mentioned above, endocannabinoids can passively diffuse through the membrane, but their reuptake into the cell is thought to be accelerated by a carrier-mediated transport via an energy-independent process called facilitated diffusion. Despite accumulating evidence for the existence of these transporter molecules in both neuronal and glial cell types, they have so far not been characterised molecularly which will be necessary for a complete understanding of endocannabinoid signalling (192, 193). Once 2-AG and anandamide are internalised, they will be hydrolysed by their respective degradation enzymes. According to the expression of the transporter molecule, the machinery needed for the degradation of endocannabinoids is found in both neurons and glial cells (193).

Anandamide is broken down to arachidonic acid and ethanolamine by the enzyme fatty acid amide hydrolase (FAAH) that is located postsynaptically (Figure 1.2.3, right panel). In hippocampal neurons, FAAH is present in the somata and dendrites of principal cells but not in INs. More precisely, electron microscopy analysis of its subcellular distribution revealed that FAAH is mostly localised to membranes of smooth endoplasmic reticulum (ER) and mitochondria (214). Additionally, many

9 | Tonic cannabinoid release has been reported at some synapses (266, 378), but it remains an open question whether this is due to spontaneously occurring neuronal activity or whether release can happen spontaneously without de novo synthesis of 2-AG in a calcium-triggered manner.

more enzymes that metabolise anandamide, such as cyclo-oxygenase-2 (COX-2), have been identified and further research is needed to clarify their roles in anandamide metabolic pathways (192). After its transporter-mediated reuptake, 2-AG is enzymatically degraded by monoacylglycerol lipase (MAGL) (Figure 1.2.3, left panel) that accounts for 85% of brain 2-AG hydrolase activity (215). MAGL is enriched in neuronal axon terminals opposing postsynaptic DAGLα (211) and thus exhibits an ultrastructural localisation complementary to postsynaptic FAAH. Interestingly, it has been shown that at cerebellar synapses, 2-AG degradation after DSI is synapse independent and also involves MAGL activity in Bergman glia (216). This finding argues against a synapse-specific degradation where postsynaptically released 2-AG only reaches the opposing presynapse, but supports a scenario in which termination of 2-AG signalling by MAGL occurs within certain spatial restriction. At least two other additional serine hydrolases are involved in 2-AG degradation, namely ABHD6 and ABHD12. Both are located postsynaptically which suggests that they have non-overlapping functions (217). Furthermore, some crosstalk appears to exist between the degradation of 2-AG and anandamide, because both FAAH and COX-2 have also been shown to degrade 2-AG and modulate DSI (192) (but see (217)). To conclude, even though the majority of each endocannabinoid is produced and degraded by one primary enzyme with a discrete spatial expression pattern, alternative degradation routes do exist. It remains to be elucidated whether these pathways are brain region specific or whether they all interact globally. For 2-AG, it seems settled that even though its main synthesis and degradation enzymes have a seemingly perfect spatial overlap that supports local, synapse-specific degradation, experimental evidence points towards a less spatially restricted re-uptake pattern at least in some cases. Whether the presence of spatially segregated degradation hydrolases also supports the hypothesis of separate endocannabinoid pools, needs to be tested.

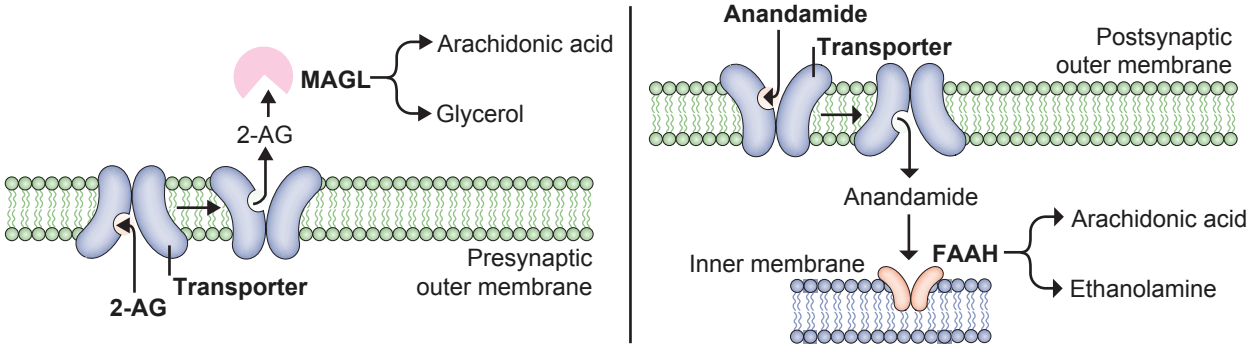

Figure 1.2.3 Main degradation pathways for 2-AG and anandamide. Modified from (193).

1.2.2 Cannabinoid receptors

In 1988, W. Devane and colleagues could show the specific binding of a radiolabelled cannabinoid analogue in rat brain. Their findings provided "the strongest argument currently available for a cannabinoid receptor. The binding site described here is entirely consistent with a receptor that would be associated with a second messenger system via a G protein" (185). Two year later, in March 1990, Herkenham et al. took a similar approach to analyse the distribution of this ligand binding site in human, monkey, dog, guinea pig and rat brain (218). Their study confirmed its G Protein-coupled nature (as shown by inhibition of binding by guanine nucleotides) and noted its very high abundance in most brain areas. Of course, this cannabinoid binding site was the CB_1R. Its gene structure, identified by molecular cloning, was published in August 1990 (186), and its mRNA expression pattern was shown by ISH in 1993 (219) which matched the earlier binding studies perfectly. In the same year, a second CBR was cloned – the CB_2R. In contrast to the CB_1R that is expressed in the brain but not in the periphery (except for in testes albeit at very low levels (220)), the CB_2R was reported to be a "peripheral receptor for cannabinoids [...] that is not expressed in the brain but rather [...] in the spleen" (7). Today, CB_1 and CB_2 are well established members of the family of CBRs. So far, no other receptors have been classified as CBRs, although experimental evidence strongly supports the existence of additional CBRs. For example, anandamide acts as a full agonist at the orphan G Protein-coupled receptor 55 (GPR55) that, based on the sequence homology of its binding site, was suggested to be a novel CBR (221, 222). Similarly, GPR35, -118 and- 119 have been shown to be activated by cannabinoids or eiconoseids (223). Of these, GPR55 has so far been strongly implicated to be a CBR.

1.2.2.1 The cannabinoid type 1 receptor

The CB_1R is encoded by the gene CNR1; its protein product is 473 amino acids long and considered one of the most widely expressed GPCRs in the brain. It has been cloned from rat, mouse, monkey and human tissue with its amino acid sequence being ›97% identical between species (12). A meta-analysis of a total of 119 CB_1R distribution studies reported very similar distribution densities for human and rat brain (from highest to lowest) (224):

Human	Substantia nigra›globus pallidus›dentate gyrus›hippocampus›cerebral cortex›striatum›cerebellum›amygdala›thalamus=hypothalamus
Rat	Substantia nigra›globus pallidus›cerebellum›hippocampus=striatum›dentate gyrus›cerebral cortex›amygdala›hypothalamus›thalamus

In addition to its strikingly high abundance, the CB_1R has a unique distribution pattern: it is predominantly located in certain types of GABAergic INs (especially cholecystokinin-positive basket cells (CCK^+ BCs), and at lower levels also in glutamatergic neurons, including hippocampal pyramidal cells and astrocytes (160, 207, 209) (Figure 1.2.4). It has been estimated that about 10% of total CB_1R amount is present in glutamatergic cells (225). On a subcellular level, CB_1R are mainly expressed in the presynaptic element of GABA- and glutamatergic synapses respectively (1), as detailed in Figure 1.2.4. However, in striatal medium spiny neurons for example they are additionally localised to the somatodendritic domain and postsynaptic density of spines (226). Furthermore, a significant amount of CB_1R protein (approximately 15%) has been shown to be located on mitochondrial membranes ($mtCB_1Rs$) with 30% of neuronal mitochondria containing CB_1Rs, suggesting a considerable impact of cannabinoid signalling on mitochondrial function (see also chapter 1.2.3.1).

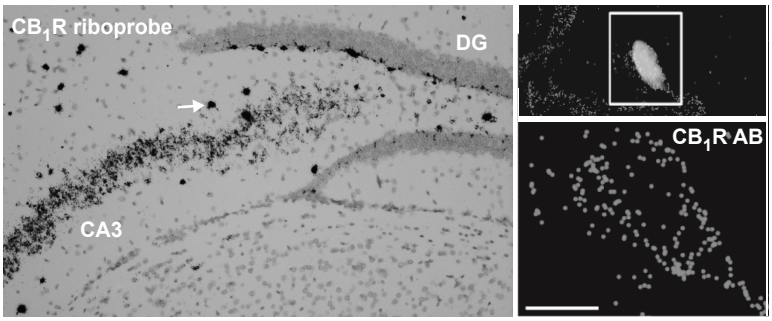

Figure 1.2.4 CB_1R distribution in the hippocampus. Left: ISH with riboprobes against CB_1R mRNA (performed by author using RNAscope technology) showing densely labelled INs (white arrow) and much lower, diffuse labelling in the pyramidal cell layer. Upper right: biocytin-filled axon terminal of a hippocampal, CCK+ BC. Lower right: super-resolution imaging of CB_1R immunolabelling on the identified bouton depicting CB_1R localisation points. The latter reveals localised and high expression of CB_1Rs at presynaptic terminals. Scale bar: 1µm, AB: antibody. Modified from (227).

Constitutive CB_1R KO animals were first generated in 1999 and display an increased mortality rate, memory deficits, hypoactivity and a decreased sensitivity to pain (hypo- or analgesia). Most THC-induced behaviours that are absent in these KOs include ring-catalepsy (complete immobility), hypomobility and hypothermia (11). However not all THC-mediated behaviours were abolished in the KO, then hinting towards the presence of other CBRs (see also below). An important tool to dissect the function of CB_1Rs better was the design of conditional KO mice lacking CB_1R in glutamatergic (VGlut-Cre) and GABAergic (VGAT-Cre) neurons respectively. In regard to THC, they shed light on both the different types of neurons and brain areas involved in its function. Surprisingly and in contrast to what had been predicted, VGAT-CB_1R KO mice exhibited unaltered behavioural responses to THC (228). Conversely, the lack of CB_1 in glutamatergic neurons abolished most behavioural effects observed after THC treatment (including locomotor, cataleptic and hypothermic effects that dependent on cortical neurons). The protective effects of the ECS against epileptic seizures in the hippocampal formation were also shown to depend on glutamatergic CB_1Rs only (229), thus underlining their importance despite much lower abundance. One explanation might be the finding that CB_1Rs seem to have much more efficient signal amplification at the receptor-G Protein interface in glutamatergic than GABAergic neurons, accounting for 50% of CB_1R-activated G Protein-signalling (230). Of course, CB_1Rs on GABAergic neurons do affect other behaviours, such as analgesia and anxiety (193).

1.2.2.2 The cannabinoid type 2 receptor

The CB_2R exhibits only 48% structure homology with the CB_1R, and a 82% identical amino acid sequence across species (human vs. mouse) (12). The mouse CB_2R is 13 amino acids shorter than the human CB_2R (360 amino acids long) at the COOH terminal. The rat CNR2 gene may be polymorphic encoding a protein of either 360 or 450 amino acids (231). CB_2Rs are most abundant in tissue of the immune system, and are highly expressed in T cells and macrophages (including microglia) (8). In fact, they were identified because scientists actively sought a second CBR that could explain the immunosuppressive, anti-inflammatory effects of THC that were not mediated by CB_1Rs (7). When A. Zimmer and colleagues generated and analysed a constitutive CB_2R KO mouse to test this hypothesis, they found that immunomodulation of cannabinoids was indeed absent in these mice (8). More precisely, they could show that the THC-mediated inhibition of T-cell activation through macrophages was abolished by the lack of CB_2R. Conversely, they concluded that CB_2Rs are absent from brain tissue based on two additional findings. First, they reported the absence of radioligand binding in the brain of WT animals that was in contrast to the very high labelling observed in the spleen. Second, they used hypothermia and catalepsy as behavioural readouts to test whether CNS-mediated effects of THC administration were altered in CB_2R KO mice. Both behaviours appeared unaltered in the KO (as would be expected due to the results in the CB_1R KO), thus leading the authors to the conclusion that CB_2Rs were absent from the CNS. Similar to ligand binding studies, initial ISH studies also reported no detectable CB_2Rs mRNA in the brain (12)

thus supporting the conceptual divide of 'peripheral CB_2Rs' and 'CNS CB_1Rs'. In the following years however, behavioural and physiological studies repeatedly suggested the presence CB_2Rs in the CNS (13) with a functionality that goes far beyond a purely neuro-immunological one (15, 232, 233). Today, CB_2R mRNA expression has been reported for most brain areas, including cortex, striatum, midbrain and hippocampus, albeit at much lower levels than in spleen (approximately 60-fold less) which could explain the difficulty in detecting it (19). ISH assays with co-staining for neuronal markers suggest a neuronal expression of CB_2R (234) but their subcellular distribution remains mostly unknown due to the lack of specific antibodies (10). One study employed subcellular membrane fractionation to look at radioligand binding in intracellular versus plasma membrane fractions (confirmed by antibody probing against intracellular nucleoporin and plasma membrane-bound Na^+/K^+-ATPase as markers) from prefrontal cortex. The results confirm the subcellular pattern of distribution of CB_1Rs and suggest an equal expression of CB_2R on both types of membranes (17).

In the following sections I will describe the characteristics of CBRs and their role in neuronal transmission without separating CB_1R and CB_2R. Firstly, they exhibit very similar biochemical and pharmacological properties (235) and secondly, KO studies have shown that they are able to functionally compensate for the lack of the respective other receptor (236). It follows that their possible downstream targets will largely overlap and that other factors such as their expression pattern and G Protein-coupling will determine their function (this is true for the functional diversity of each subunit, too).

1.2.2.3 Cannabinoid receptors are classic G Protein-coupled receptors

Like all GPCRs, CBRs have seven transmembrane domains that are connected by three extracellular and intracellular loops and possess an extracellular N-terminal tail, and an intracellular C-terminal tail. As indicated by their name, GPCR signal via G Proteins – guanine nucleotide-binding proteins that are composed of three subunits (α, β and γ). In its inactive, unbound state, the G Protein is only loosely associated to the GPCR and is bound to guanosine diphosphate (GDP) via its α subunit (step 1, see Figure 1.2.5 for an illustration of all involved steps). Upon ligand binding, the GPCR undergoes a conformational change that tightly couples the G Protein to the third intracellular loop and C-terminus of the GPCR. This causes the release of GDP and uptake of guanosine triphosphate (GTP) by the G Protein (step 2); in the GTP-bound state the G Protein dissociates from the receptor and separates into the Gα subunit and a Gβγ dimer (step 3). In this state, the G Protein subunits will initiate downstream signalling (step 4) (237–239).

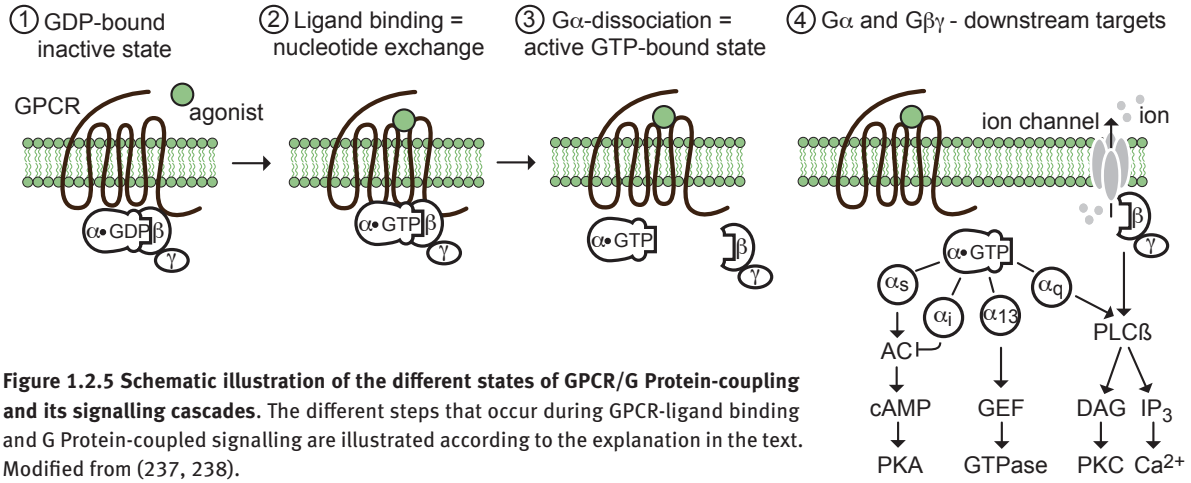

Figure 1.2.5 Schematic illustration of the different states of GPCR/G Protein-coupling and its signalling cascades. The different steps that occur during GPCR-ligand binding and G Protein-coupled signalling are illustrated according to the explanation in the text. Modified from (237, 238).

Depending on the G Protein (G_s, G_i, $G_{12/13}$ and G_q), its α subunit operates via complementary signalling pathways: G_s stimulates adenylyl cyclase activity and leads to an increase in intracellular cAMP concentrations and enhanced PKA activity. G_i on the other hand inhibits adenylyl cyclase, thereby reducing cAMP levels. $G_{12/13}$ acts via guanine nucleotide exchange factors (GEF) and, besides many other things, mediates activation of small GTPases (221). The Gβγ subunit can either directly modulate the activity of ion channels or activate PLCß, a pathway that is shared with the G_q subunit (237–239). Even though GPCRs can signal as monomers, they mostly form homo- or heterodimers. Both CB_1- and CB_2Rs have been shown to dimerise. Interestingly, they can also form functional CB_1/CB_2 heterodimers and their co-expression has been reported for many brain areas including the globus pallidus, nucleus accumbens and pineal gland (240). Even though its functionality is not clear, CB_1/CB_2 dimerisation could help explain discrepancies reported in the effects of ligand-receptor binding (241) that may result from altered and novel receptor pharmacology.

1.2.2.4 Downstream targets of cannabinoid receptors

In respect to the Gα subunit, CB_1- and CB_2Rs are most often coupled to $G_{i/o}$ thus inhibiting adenylyl cyclase activity. Both CBRs have additionally been shown to affect cell migration by activating mitogen-activated protein kinase (MAPK)-signalling via G_i (242, 243). In some rare cases, CB_1- but not CB_2Rs can also couple to G_s and stimulate adenylyl cyclase (240, 244). GPR55 couples to G_{13} and is thought to affect cell migration (222). The reported effects of CBR coupling to the Gβγ subunit are mostly based on a direct modulation of ion channel activity. In the following, I will give examples of the downstream targets of CBR-activated $G\alpha_i$ and Gβγ with a focus on ion channel modulation.

Voltage-gated calcium channels

In cultured hippocampal neurons (as well as in neuroglioblastoma cells), cannabinoids inhibit both N- and P/Q-type voltage-activated calcium channels (VGCC). This effect has been suggested to result from a direct interaction of Gβγ with the VGCCs. Experiments with pertussis toxin, that blocks the interaction between $G_{i/o}$ and the associated GPCR, suggests that the involved G Protein is $G_{i/o}$ (245, 246). A prominent example is the inhibition of presynaptic VGCC by CB_1Rs that leads to a reduced transmitter release (see chapter 1.4.3).

Calcium-activated chloride channels

In pyramidal cells of prefrontal cortex, the activation of intracellularly located CB_2R by 2-AG has been reported to lead to a membrane potential depolarisation by opening of calcium-activated chloride channels (CaCCs) (17, 247). The exact mechanism is not clear, but it is thought that a PLC-dependent increase in IP_3 will lead to an increased activation of IP_3 receptors. IP_3 receptors are calcium channels located on the ER and their activation will increase intracellular calcium concentrations, thereby also activating CaCCs.

Voltage-gated potassium channels

Activation of CBRs in cultured neurons has been shown to modulate K_A and K_D potassium currents. For both ion channels, it decreases their voltage-dependent deactivation and thereby increases the net amount of current flowing. The change in voltage-dependency is thought to be caused by a reduced cAMP-mediated phosphorylation of the channels that is the result of an inhibition of AC activity via the G Protein-coupled CBR (248–250). Furthermore, activation of CB_1Rs in acute hippocampal slices decreases both I_h (251) and I_M (252) in CA1 PCs, yet the mechanisms underlying their modulation are not clear.

G-Protein coupled inwardly rectifying potassium channels

CBRs can activate G Protein-coupled inwardly rectifying potassium channels (GIRK) via their βγ subunit thus leading to a hyperpolarisation. Both CB_1- and CB_2Rs have been shown to interact with GIRK1 when co-expressed recombinantly (253, 254); physiological data has underlined these initial findings (255) and will be discussed in more detail in chapter 1.2.4.

1.2.2.5 Direct modulation of ion channels of endocannabinoids

There is accumulating evidence that cannabinoids can also directly modulate ion channels such as non-selective cation and presynaptic potassium channels (256, 257). For example, anandamide has been shown to activate the non-selective cation channel TRPV1 (transient receptor potential vanilloid subfamily, member 1). Activation of TRPV1 (and subsequent calcium influx) leads to reduced synaptic transmission based on clathrin-dependent internalisation of AMPARs and mediates a form of LTD at hippocampal mPP-GC synapses (257). Another very recent study showed that arachidonic acid, upon activity-dependent postsynaptic release, can itself act as a retrograde messenger at the Mf-CA3 synapse. It directly binds to and inhibits presynaptic K_V channels independent of CBR activation, which leads to a broadening of the presynaptic action potential and subsequently to an increase in glutamate release. This in turn robustly *potentiates* synaptic transmission over several minutes and reduced the threshold for the induction of presynaptic LTP at this synapse (256). Given that most cannabinoid-mediated modulation that has been reported so far is inhibitory in nature, this is a rather surprising and exciting finding. Last but not least, anandamide was reported to suppress TTX-sensitive (hence Na_V channel-dependent) firing in cultured cortical neurons. Because this effect was not inhibited by the mixed CB_1-/CB_2R antagonist AM-251, a direct and CBR-independent activation was suggested. Conversely, a follow-up study in mouse brain synaptic preparations found that AM-251 could abolish the depolarisation of synaptoneurosomes by a sodium channel-specific neurotoxin. Additionally, it displaced the binding of a sodium channel radioligand. Taken together, these two studies suggest a direct interaction of CBR (inverse) agonists with Na_V channels (258).

1.2.3 The endocannabinoid system in synaptic transmission

Despite their discovery in the early 1990s, the role of endocannabinoids and their receptors in neurotransmission remained mostly unclear; exceptions being early studies on the modulation of potassium currents by cannabinoids (250) and the observation that CB_1R agonists decreased synaptic transmission by a presynaptic mechanism (259). Concurrent with the cloning of CBRs, research on inhibitory synaptic transmission had exposed a phenomenon in which postsynaptic depolarisation of a neuron would lead to a transient inhibition of presynaptic inputs – *DSI* (260–262) (Figure 1.2.6). It was shown that this mechanism was triggered by postsynaptic calcium influx and involved a retrograde activation of a presynaptic G Protein-linked second messenger, yet the retrograde messenger molecule and target receptor remained unidentified (263, 264). Ten years later, on 29 March 2001, two independent research groups (led by R. Nicoll and M. Kano) provided unequivocal experimental evidence regarding the nature of the ominous retrograde messenger involved in the suppression of inhibitory synaptic transmission: endocannabinoids (4, 6). Another paper, published on the same day, furthermore extended these findings to the suppression of excitatory inputs (5). In summary, these papers did not only bring together two previously unrelated strings of research, cellular neurophysiology and endocannabinoid function, but they introduced a new paradigm of how diffusible, 'retrograde' messengers could modulate synaptic transmission and, through DSI and DSE, brought endocannabinoids to the attention of a broader neuroscience community (2).

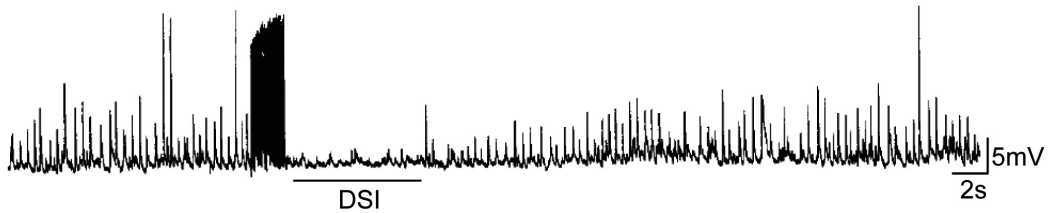

Figure 1.2.6 Transient inhibition of spontaneous IPSPs by high frequency action potential trains. IPSPs were recorded in current-clamp with KCl-filled electrodes and thus appear as positive voltage deflections. Addition of 10µM Carbachol increases the frequency and amplitude of IPSPs. The transient inhibition was named *DSI*. Modified from Pitler & Alger (262).

1.2.3.1 Endocannabinoid-mediated short-term depression (eCB-STD)

In their seminal paper on DSE (5), A. Kreitzer and W. Regehr directly demonstrated the retrograde nature of the phenomenon by monitoring presynaptic calcium responses while eliciting DSE through postsynaptic depolarisation. With this approach, they could show the suppression of calcium influx into the presynaptic terminals during DSE. Importantly, they were able to prevent this suppression by including a calcium chelator in the postsynaptic neuron to block cannabinoid release (5). Today, it is well established that both DSI and DSE crucially depend on a postsynaptic rise in calcium (265) which will stimulate 2-AG production. Upon its release, 2-AG binds to and activates presynaptic CB_1Rs on inhibitory or excitatory terminals which in turn leads to a reduction in presynaptic transmitter release via inhibition of calcium channels (see Figure 1.2.7. for a schematic illustration of DSI/DSE). Paired recordings of evoked inhibitory postsynaptic currents (IPSCs) from CCK+ BCs onto CA1 PCs showed that DSI could be completely abolished by application of conotoxin, a blocker of N-type calcium channels (266). The latter will block presynaptic calcium entry and thereby explain the reduction/failure in transmitter release observed during this phenomenon. Recent data has provided evidence that in addition to CB_1Rs in the outer cell membrane, $mtCB_1Rs$ are involved in DSI, possibly by "decreasing mitochondrial respiration and altering the energy supply in the form of ATP needed for the ongoing release of neurotransmitters" (267). The transient nature of the presynaptic inhibition is thought to be caused by a rapid degradation of 2-AG. As detailed above, the degradation enzyme MAGL has been shown to be located pre-synaptically, thus close to the site of 2-AG action, and its pharmacological block leads to a prolongation of DSI (211, 268). A prominent feature of DSI is that it "spreads" between synapses and cells, thus providing further evidence that 2-AG does not only act in a synapse-specific manner (see also p14). By means of dual recordings from neighbouring cells, R. Wilson and R. Nicoll showed that DSI, when elicited in one cell, can elicit a presynaptic inhibition of transmitter release in cells up to 20µm away in distance (measured at the soma) as well (4).

In addition to DSI/DSE, other forms of eCB-STD exist as well: NMDAR-dependent influx of calcium (269), and short-term activation of metabotropic receptors, including mGluRs, mAChRs and CCK receptors (201, 270, 271), can induce eCB-STD of transmitter release. Generally, the various forms of eCB-STD have been found at both excitatory and inhibitory synapses in most brain areas, including the hippocampus, cerebral cortex, cerebellum, amygdala, striatum, NAc, hypothalamus and brain stem (see (231) for a detailed review).

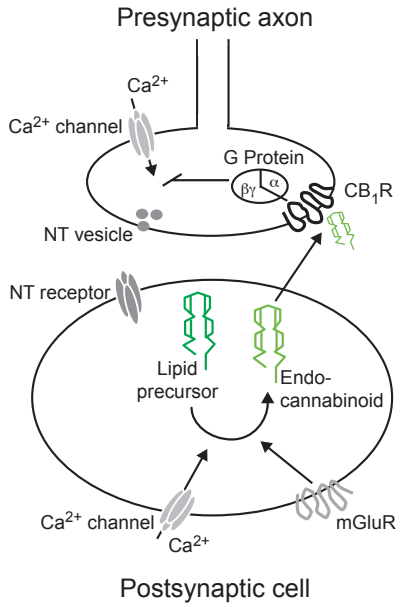

Figure 1.2.7 Endocannabinoid- mediated retrograde signalling. Postsynaptic Ca^{2+}-influx or mGluR activation lead to synthesis and release of endocannabinoids that bind to presynaptic CB_1Rs and inhibit neurotransmitter (NT) release. Modified from (385).

On a critical note, questions have been raised about the physiological relevance of DSI, because various patterns of stimulation that mimic hippocampal PC firing were insufficient to elicit it in CA1 PCs (recorded in acute hippocampal slices) (272). Even depolarising pulses of the postsynaptic cell to 0mV that are commonly used to elicit DSI did not reduce the sIPSC frequency when their duration was below 75ms – in terms of synaptic transmission a rather long, 'unphysiological' time window. On the other hand, Maejima et al. could show that mGluR-driven eCB-STD in the cerebellum can be elicited under "physiological conditions" – meaning with synaptic activity rather than postsynaptic, depolarising step pulses (273). In their study, they repetitively stimulated excitatory parallel fibres (PFs) and observed a CB_1R-dependent decrease in synaptic transmission at climbing fibres (CFs) on the same Purkinje cell. Similarly, synaptic stimulation of cortico-striatal synapses and co-activation of dopamine D_2 receptors was also shown to reduce transmitter release in a CB_1R-manner (274). These results support the hypothesis discussed earlier (p12), suggesting that a synergistic mode of activation (rise in calcium occurring simultaneously with postsynaptic metabotropic receptor activation through neurotransmitter release) is more likely to occur under physiological conditions. Ultimately, in vivo recordings will have to show which forms of eCB-STD, including DSI/DSE, do indeed occur in the intact brain.

1.2.3.2 Endocannabinoid-mediated long-term depression (eCB-LTD)

In line with the ubiquitous expression pattern of presynaptic CB_1Rs, the short-term depression of transmitter release by endocannabinoids has been shown to occur in most brain areas. But can endocannabinoids additionally mediate presynaptic forms of long-term plasticity? In spring 2002, two papers were published in short succession reporting two different forms of eCB-LTD. First, G.L. Gerdeman et al. found that stimulation of cortico-striatal excitatory synapses with high frequency stimulation (100Hz for 1s, repeated 4x with 10s intervals), paired with depolarisation of the postsynaptic neuron, induced LTD of synaptic inputs that depended on postsynaptic release of anandamide and activation of presynaptic CB_1Rs (275). Second, D. Robbe et al. showed that they could induce LTD at cortex-nucleus accumbens excitatory synapses with low-frequency synaptic stimulation (13Hz for 10min). This form of LTD was described to be mediated by postsynaptic mGluR5 activation and subsequent activation of presynaptic CB_1Rs by endocannabinoids (released through mGluR-triggered calcium release from intracellular stores) (276). The observation that simultaneous pre- and postsynaptic activation seems a necessary requirement for its induction, suggests that eCB-LTD may be input-specific, in contrast to eCB-STD. Another form of LTD, namely tLTD (see p17), has been shown to depend on CB_1R activation. In cortical L5 PCs, the co-activation of presynaptic NMDARs (by presynaptic glutamate release) and CB_1Rs (by postsynaptic endocannabinoid release) was shown to induce tLTD (158)[10]. Subsequent studies could show that pharmacological inhibition of this form of eCB-LTD may even unmask coincident tLTP which is induced by the same pre- versus post-pairing protocol via postsynaptic calcium-influx and postsynaptic NMDAR activation, but is masked by the concurrent induction of eCB-tLTD (277).

It is of note that, although endocannabinoid-mediated long-term plasticity requires activation of CB_1Rs for many minutes, this in itself is not sufficient to induce LTD. Neither the pharmacological activation of CB_1Rs nor the repeated induction of DSI for 10min can elicit LTD. This suggests that other factors, such as synaptic stimulation and/or co-activation of other receptors, may be necessary for the transition of short-term endocannabinoid effects into long-term plasticity mechanisms, but the

10 | Whether presynaptic or astrocytic CB_1R mediate this form of tLTD is controversial and will be discussed in section III.

nature of these factors however is not known and they may well differ between brain areas (2). Furthermore, in the majority of cases, CBRs are necessary for the induction but not maintenance of eCB-LTD. The mechanisms underlying the presynaptic changes are not well understood either, but the involvement of cAMP/PKA signalling and RIM1α, a protein of the presynaptic release machinery, and of presynaptic potassium channels respectively, has been suggested (278, 279).

1.2.3.3 Modulation of synaptic transmission by astrocytic cannabinoid receptors

As mentioned earlier, CB_1Rs are expressed on astrocytes and their activation with CBR agonists leads to increased astrocytic calcium signalling. This effect is completely abolished in CB_1R KO mice. Their functional role is not well researched, but at least two studies hint towards their involvement in astrocyte-neuron communication (160, 207). A first study showed that endocannabinoids – released from hippocampal principal cells during spiking – diffuse through the extracellular matrix and activate CB_1Rs on close-by astrocytes. This in turn leads to a PLC-dependent release of calcium from intracellular stores. The rise in calcium triggers the release of glutamate from the astrocyte that then activates NMDARs on pyramidal neurons, closing the signalling loop (207). A second study showed that, based on the same mechanism of glutamate diffusion, presynaptically expressed tLTD of cortical synapses may depend on astrocyte-signalling as well. In this case, the spiking-induced activation of astrocytes via cannabinoids and the subsequent release of astrocytic glutamate will activate presynaptic NDMARs and induce tLTD (160). This study, with elaborate control experiments, questions the results obtained by Sjöström et al. (158) who argued that presynaptic CB_1R mediate tLTD, but have no direct proof. However, their experiments were performed at a different cortical synapse and neither study provides authoritative evidence. Experiments with cell-type specific CB_1R KOs at both synapses would give an answer to the question whether both forms of tLTD exist.[11]

1.2.4 Regulation of neuronal excitability by endocannabinoids

In addition to regulating synaptic transmitter release, the ECS also alters the intrinsic properties of neurons and their excitability on both a short- and long-term time scale.

In somatosensory cortex, the activity-dependent release of 2-AG was shown to persistently hyperpolarise a subset of layer 2/3 PCs and low-threshold firing INs by ~5mV. This phenomenon, called slow self-inhibition (SSI), was reported to be mediated by a CB_1R-dependent activation and opening of postsynaptic GIRK channels where the increased GIRK conductance leads to a hyperpolarisation of the cell membrane potential through potassium extrusion. Because the endogenously released 2-AG, activated CB_1R and GIRK channel are presumably all localised one the same neuron, this effect is considered a type of autocrine self-modulation.

In medial prefrontal cortex, layer 2/3 PCs were reported to depolarise by ~30mV after CB_2R activation. The studies on this phenomenon were the first to report the presence of functional CB_2R in the medial prefrontal cortex and their physiological activation by endogenous 2-AG (247). The depolarisation is mediated by the activation of CaCCs and extrusion of chloride from the cell (as described on p29). Because the depolarisation response had a latency of >5 min after CBR agonist application, the authors hypothesised that the CB_2Rs were located intracellularly. Indeed, membrane fractionation experiments (see p15), and additional experiments with intracellular application of agonists which dramatically reduced the latency, supported their hypothesis (17, 247).

A recent study in hippocampal slice cultures showed that chronic CB_2R activation increases excitatory synaptic transmission and the number of dendritic spines in CA1 PCs. The effects were gone in slices from CB_2R KOs and when WT slices were preincubated with a CB_2R antagonist (21). However, the effects only occurred after 7-10days incubation with the agonist, which certainly raises potential issues regarding its physiological relevance. It will be interesting to see whether physiologically relevant activation patterns can induce this plasticity, and whether this phenomenon is exclusive to CA1.

Chronic inhibition experiments in hippocampal slice cultures also indicated that endocannabinoid levels are subject to homeostatic scaling. The generalised downscaling of inhibitory synapses after blockage of neuronal firing for 3-5days was shown to be accompanied by an enhanced uptake and degradation of anandamide. The reduced presynaptic inhibition by cannabinoids thus led to the strengthening of a specific subset of CB_1R-expressing INs (mostly CCK+ and VIP+ INs) that exhibited an increased GABA release probability (280). This mechanism could potentially provide a means to selective tune inhibitory synapses and to stabilise network activity in a cell type-specific way.

11 | The idea of an astrocytically-mediated tLTD is intriguing, because it would allow for associative, heterosynaptic plasticity to occur. Each astrocyte contacts 300–600 neuronal dendrites and activates 3-12 pyramidal cells (379, 380). They are thus well suited to signal to populations of synapses.

Last but not least, similar to the morphological changes in CA3 PCs, the expression of both CB_1- and CB_2Rs has been shown to be modulated in response to stress and epilepsy. A study that used maternal deprivation as a stress paradigm found that CB_1R mRNA levels were downregulated in a sex-specific manner after stress, with only males showing this reduction. Conversely, CB_2R mRNA levels were upregulated after stress in both sexes (281). In epilepsy, CB_1R expression has been shown to be drastically reduced (282).

1.2.5 The endocannabinoid system and its role in behaviour

Common effects associated with the recreational use of marijuana include an intensification of sensation, proprioception and clarity of perception and awareness, increased internal physical needs such as hunger and long-term memory impairments. Furthermore, medicinal cannabis has been used to treat pain and anxiety conditions for millennia. Yet, what is the physiological basis of these observations/applications and what do we know about them? Behavioural and electrophysiological analyses of the effects of THC and endogenous cannabinoids have confirmed the involvement of the ECS in hunger, pain, anxiety, reward and many other behaviours. The breadth of affected behaviours is most likely due to the dense, ubiquitous expression of all components of the ECS in the CNS and also explains its association to psychiatric mood disorders and drug abuse.

1.2.5.1 Working and declarative memory

The effects of cannabis use on memory function can be divided into two phases: an acute phase of intoxication with verbal and working memory impairments induced by a single dose of THC and a chronic phase, in which the long-term use leads to impairments that persist following abstinence (283). A longitudinal study with 1037 subjects that were followed from their birth to age 38 found that persistent, adolescent-onset cannabis use was associated with significant neuropsychological and cognitive decline such as attention and memory problems. Neuropsychological functions were assessed through working memory, rapid visual information processing, learning recall, associative learning, processing speed and perceptual reasoning; cognitive function was given as a measure of IQ test results (corrected for education). Importantly, cessation of cannabis use did not fully restore neuropsychological functions (284). Taken together, this study thus suggests that early-onset cannabis use may result in altered brain development and enduring neuropsychological changes and establishes the onset of cannabis use as a critical determinant of its harmful effects. In contrast, most studies report that lasting deficits in executive functioning or IQ do not occur in adult-onset chronic, short-term or occasional cannabis users, even though they do also exhibit working and declarative memory impairments that however tend to normalise with abstinence (285), but see (286). 'Innate' behavioural effects of endogenous cannabinoids are of course more difficult to assess, but the disruption of any major part of the cannabinoid system (ligands, receptors, degradation enzymes) negatively influences declarative memory as shown by behavioural experiments in constitutive CB_2R (287), CB_1R (288) and DAGLα KO mice (289). To assess the specific functional role of each component of the ECS, receptor subtype- and endocannabinoid-specific KO models need to be generated in an area- and cell type-specific manner and compared behaviourally.

1.2.5.2 Feeding

Cannabinoid agonists, including THC, anandamide and 2-AG, stimulate food intake via the activation of CBRs in the hypothalamus. Conversely, inhibition of CB_1Rs via i.p. injection of antagonists cause a reduction in food intake and bodyweight in mice (193). Given to pups within the first 24h after birth even led to their death within 4-8days due to reduced milk intake and growth rate (290). In line with this, CB_1R KO mice eat less than their WT littermates after temporary food restriction (291). The hypothalamus sends and receives information via dopaminergic, opioid and GABAergic pathways (and others). All of the involved cells and their respective target areas, such as ventral tegmental area (VTA) and nucleus accumbens, influence feeding behaviour *and* express CBRs. Also, feeding-regulating hormones such as leptin can affect the synthesis of endocannabinoids in the hypothalamus and are thought to mediate at least some of the cannabinoid-related phenotype (291, 292). Taken together, due to the complexity of the circuits involved and the multitude of possible sites of concomitant endocannabinoid modulation, the exact modes of action are not clear and will certainly differ according to the behavioural state/task. Despite this, endocannabinoids are of great therapeutic potential. For example, THC has been approved by the American Food and Drug Administration for the treatment of anorexia and a CB_1R antagonist is being clinically evaluated for the treatment of obesity (193).

1.2.5.3 Complex neuropsychiatric diseases and drug abuse

The correlation of genetic variances in the CNR2 gene suggest that the CB_2R may play a role in the etiology of schizophrenia (293), anxiety (294, 295) and depression (296). For example, genetic population studies found mutations in the CNR2 gene to correlate with the occurrence of schizophrenia and affected patients were shown to have reduced CB_2R mRNA and protein levels. (293). In line with this, the CB_2R KO, when challenged behaviourally, displays 'schizophrenia-like' behaviours such as reduced motor activity, increased anxiety or decreased prepulse inhibition of an acoustic startle response (297). Conversely, studies in mice have shown that overexpression of CB_2Rs ameliorates symptoms of schizophrenia, depression and anxiety

(294, 296, 298). However, the cause for CB_2R dysfunction in those illnesses remains elusive. It has been postulated that because many other neuromodulatory systems are coupled to the ECS, a downregulation of CB_2Rs may lead to dysfunctions in connected modulatory systems (similar to the effects on feeding). Physiological studies have highlighted the role of CB_2Rs in reward and drug abuse. More specifically, two studies by E. Gardner, Z.X. Xi and colleagues suggested that brain CB_2Rs modulate the neuronal circuit underlying the cocaine reward system (299). In the first study, they administered selective CB_2R agonists into the nucleus accumbens (which plays an important role in motivation, pleasure, and reward and hence in addiction) and subsequent CB_2R activation inhibited cocaine self-administration in mice (299). In the second study, the systemic administration of a CB_2R agonist reduced the mean firing rate of VTA dopamine neurons as assessed by extracellular single unit recordings in vivo[12]. This effect could be reversed by injection of a CB_2R antagonist and were absent in CB_2R KO mice. On a behavioural level, CB_2R activation by bilateral microinjections of CB_2R agonists decreased dopamine-dependent cocaine self-administration that could be blocked by co-administration of the antagonist (19). Interestingly, the antagonist itself had no effect on cocaine self-administration indicating that in neuronal circuits for reward, CB_2Rs might not be tonically active. The effects of CB_1R in cocaine-administration are less well understood, but in contrast to CB_2R KO mice, which had unaltered baseline dopamine levels, CB_1R KO mice display significantly reduced dopamine levels (299) arguing for a significant function in dopaminergic signalling.

Association studies have also found evidence for polymorphisms in the CNR1 gene to correlate to a variety of diseases, including attention deficit hyperactivity disorder (ADHD), Parkinson's disease and schizophrenia, to name but a few. However, none of these studies provide a functional basis for their observations and contrasting reports of the associations are not seldom, rendering the results controversial (see for example discrepancies in regards to mutations in CNR1 affecting intravenous drug abuse (300, 301)).

1.2.6 Endocannabinoid signalling in the hippocampal formation

In the hippocampus, research is mostly limited to the CB_1Rs (and other orphan receptors) and until now, to the best of my knowledge, no study has been published on the physiological role of native CB_2Rs in hippocampal information processing[13] even though evidence points towards a role of CB_2Rs in hippocampus-dependent learning (287)[14]. CB_1Rs are expressed on SC and AC, but not Mf, fibres and on IN terminals[15] where they mediate short- and long-term plasticity changes of synaptic transmitter release. Their effects on synaptic transmission are not different from the generalised synaptic function of CB_1Rs and the reader is referred to chapter 1.2.3. Importantly, CB_1Rs are implicated in the modulation of hippocampal network activity and CB_1R agonists have been shown reduce SWR, theta and gamma power (302–304). They do not appear to be crucial for their generation, because baseline gamma power is not altered in CB_1R KO animals (302). Depending on the type of oscillation, these network effects can be explained by CBRs expressed on inhibitory INs – that are thought to underlie the initiation and timing of oscillations – and/or on the inhibition of glutamate release from pyramidal cells that (305–307). For example, the inhibition of SWRs has been shown to be primarily dependent on the inhibition of glutamatergic feed-forward excitation without altering inhibitory input. This can be explained by the expression of CB_1Rs within the neuronal microcircuit underlying SWR generation: a subtype of inhibitory INs, namely fast spiking parvalbumin-positive basket cells (PV+ BCs) that spike reliably during SWR, do not express CB_1Rs on their axon terminals and are not modulated by cannabinoid-dependent inhibition of their inputs because CB_1Rs-expressing glutamatergic fibres do not target INs. They are thus 'cannabinoid-independent'. The main population of INs expressing CB_1Rs (CCK+ BCs), is not involved in the entrainment and only spikes unreliably during SWR. Finally, glutamatergic neurons express CB_1Rs and their activity-dependent transmitter release is 'cannabinoid-dependent' thus leading to a reduction of their synaptic currents (303, 308). On the other hand, the modulation of gamma oscillations by CB_1R agonists has been shown to depend on the suppression of excitatory inputs onto both PCs and PV+ BCs (302) with a temporal delay between the reduction in IN and PC spiking (IN›PC). The differences in the involvement of cell types between the two types of oscillations can possibly be explained by differences in their generation/entrainment (308, 309). Generally, because EC and dentate gyrus Mf inputs are not subject to strong cannabinoid-modulation, it seems likely that the changes observed in SWR and gamma oscillations reflect mostly intrahippocampal changes[16].

12 | Complementary electrophysiological experiments in slices showed that the acute bath application of a CB_2R antagonist led to a hyperpolarisation of dopamine neurons and an increase in both their AP duration and AHP.

13 | Taking into account two studies looking at artificially expressed CB_2Rs in cultures of autaptic neurons (236) and the effects of chronic pharmacological CB_2R activation in CA1 PCs in slices cultures (21).

14 | This behavioural/anatomical study reports fewer synapses and memory deficits in hippocampus-dependent aversive memory consolidation in CB_2R KO mice.

15 | DSI is present at GABAergic-glutamatergic and GABAergic-GABAergic synapses whereas DSE is only present at glutamatergic-glutamatergic but not glutamatergic- GABAergic synapses (381).

16 | For theta oscillations that are primarily driven by septal inputs, this will of course be different.

As expected from the effects of cannabinoids on hippocampal network oscillations, THC consumption has been shown to interfere with hippocampal memory formation in humans (285) and in mice where THC administration negatively affected short-term memory and altered task-specific firing of hippocampal cells (310). On a cellular level, high resolution microscopy has shown that chronic THC administration in mice leads to a significant (74%) and long-lasting loss of presynaptic CB_1Rs that only slowly but fully recovered within six weeks (227). Thus it can be hypothesised that the effects of THC are at least partially due to an altered IN function and excitation/inhibition balance.

To conclude, while the role of CB_1Rs is well established in hippocampal information processing, knowledge on the physiological function of CB_2R is miniscule – despite the mounting evidence of their importance in brain function.

1.3 Aim of this study

In this study, we intend to characterise CB_2R function in the hippocampus which had been unknown when we started this project and discovered a plasticity mechanism dependent on (non-CB_1R) CBRs: while recording from hippocampal CA3 PCs to examine their intrinsic physiological properties, we observed that trains of action-potentials elicited a long-lasting hyperpolarisation of the membrane potential in these cells. To our knowledge, this type of neuronal plasticity has not been described before and our aim was thus to characterise this phenomenon. In a step by step analysis, we sought to identify the receptor (CB_2) and its ligand (2-AG), the receptor's location (neuronal versus glial), the underlying mechanism and downstream effector, important influencing factors (such as synaptic transmission or crosstalk between active neurons), and its main characteristics. Furthermore, we probed for the differences between CB_2- and CB_1R-mediated neuromodulation and asked whether their effect on neurotransmission is complementary or compensatory. Finally, we examined the functional significance of CB_2Rs on a cellular (in vitro) and network (in vivo) level.

2 Methods

2.1 Technical equipment

Vibratome	VT1200S (Leica, Germany)
Interface storage chamber	Haas-type, custom-made (Charité Berlin, Germany)
Water baths	WBT series (Carl Roth, Germany)
Recording chamber	submerged (Luigs and Neumann, Germany)
Heatable perfusion cannula	with temperature sensor PH01 and temperature controller TC02 (Multichannel Systems, Germany)
Oscilloscope	HM1507-3 (Hameg Instruments, Germany)
Amplifier	Axoclamp 700A (Molecular Devices, Canada)
Digitiser	BNC 2090 (National Instruments, USA)
A/D Board	PCI 6035E (National Instruments, USA)
Micromanipulators	Mini 25, 3 axes (Luigs and Neuman, Germany)
Stimulus generator	Master 8 (A.M.P.I, Israel)
Extracellular stimulation unit	Iso Flex (A.M.P.I, Israel)
Glass electrode puller	DMZ Universal Puller (Zeitz Instrumente, Germany)
Borosilicate glass capillaries	GC150F-10 or GC150TF-10 (Harvard Apparatus, UK)
Recording and bath electrodes	chlorided AG-8W silver wire (Science products, Germany)
Upright microscope	BX-51 WI with differential interference contrast (DIC) optics and video microscopy (Olympus, Japan)
Water immersion objective	LumPlan FL/IR 60x 0.9NA (Olympus, Japan)
Phase objective	UPlanFL N 4X×0.13 PhP (Olympus, Japan)
Fluorescence microscope	DMI4000 B (Leica, Germany)
Plastic syringes	(B. Braun, Germany)
Perfusion tubing	(Carl Roth, Germany)

Software
IGOR Pro 6.12 (WaveMetrics Inc., USA) with custom-written plug-ins
NeuroMatic (http://www.neuromatic.thinkrandom.com)
Prism 5 (GraphPad Software, USA)
Illustrator (Adobe Systems Inc., USA)
Image J (Research Services Branch, National Institue of Health, USA)
Matlab (Mathworks, MA) with custom-written scripts

2.2 Experimental preparations

2.2.1 Ethics statement and animal handling

Animal husbandry and experimental procedures were performed in accordance with the guidelines of local authorities (Berlin, Germany), the German Animal Welfare Act and the European Council Directive 86/609/EEC. Animals were housed on a 12:12h reversed day-night cycle with food and water available ad libitum.

2.2.2 Genetically modified animals

All knockout mice used in this study were kindly provided by Prof. Andreas Zimmer (Bonn, Germany) (8, 11, 289). Constitutive CB_1R-, CB_2R-, and DAGLα KO mice with a C57BL/6J background were bred using a homozygous breeding protocol. Additionally, a subset of constitutive CB_2R KO mice was bred from heterozygous parents and their WT littermates were used as controls. Neuron-specific, conditional knockout mice for CB_2R were generated using the *Cre/loxP* technology (311). To this purpose, transgenic mice expressing Cre recombinase under the Synapsin I promoter (312, 313) were bred with floxed CB_2R animals. In this case, Cre-negative offspring was used as a control. DNA isolation from mouse tissue (from tail cuts or ear marks) and

subsequent genotyping were performed according to standard protocols (see for example (314)). Tissue samples were taken after sacrificing the animal in case of homozygous breedings and additionally taken from pups at P10-P16 for heterozygous or Cre-based breedings.

2.2.3 Slice preparation

Hippocampal slices were prepared from male and female P21-P35 C57BL/6 and KO mice, and Wistar rats (where indicated). Animals were anesthetised with isoflurane and decapitated. Their brains were quickly removed and transferred to sucrose-based ice-cold artificial cerebrospinal fluid (aCSF) containing (in mM): 87 NaCl, 26 $NaHCO_3$, 50 Sucrose, 10 Glucose, 2.5 KCl, 1.25 NaH_2PO_4, 3 $MgCl_2$, 0.5 $CaCl_2$ for mice and 87 NaCl, 26 $NaHCO_3$, 75 Sucrose, 25 Glucose, 2.5 KCl, 1.25 NaH_2PO_4, 7 $MgCl_2$, 0.5 $CaCl_2$ for rat brain, respectively. Tissue blocks containing the hippocampus were mounted on a VT1200S Vibratome and horizontal slices of 300-400µm thickness were cut. Slices were subsequently stored for 1-5h in an Haas-type interface chamber (315) at near-physiological temperature (~35°C) and superfused with aCSF containing (in mM): 119 NaCl, 26 $NaHCO_3$, 10 Glucose, 2.5 KCl, 1 NaH_2PO_4, 1.3 $MgCl_2$, 2.5 $CaCl_2$ (pH 7.4; 285-300mOsm; ~1ml/ min). ACSF was equilibrated with 95% O_2 and 5% CO_2.

2.3 Electrophysiology

2.3.1 General setup

For recordings, individual hippocampal slices were transferred to a submerged chamber, perfused with aCSF (~5ml/ min, pre-heated to 33-34°C in a water bath and re-heated during perfusion into the recording chamber with a PH01 heatable perfusion cannula via a TC02 temperature controller) and visualised with infrared differential interference contrast optics on an Olympus BX-51 WI microscope. Extracellular field and patch-clamp recordings were performed with a MultiClamp 700A amplifier and monitored using an HM1507-3 oscilloscope. Signals were filtered at 2-4 kHz, digitised at 5-10 kHz with 16-bit resolution using a BNC-2090 interface board (PCI 6035E A/D board) and recorded in IGOR Pro 5.0 with custom-made plug-ins. Putative hippocampal principal cells were identified based on their location, morphology and electrophysiological properties. CA2 PCs were additionally filled with 30µM Alexa and post-hoc identified under a fluorescence microscope according to their dendritic arborisation.

2.3.2 Pharmacological agents

All drugs were purchased from Sigma Aldrich, Tocris (both Germany) or Cayman Chemical (via Biomol, Germany). If not stated otherwise, experiments were performed in the continuous presence of $GABA_A$- and $GABA_BR$ blockers (1µM gabazine/ SR95531 hydrobromide and CGP55845 respectively) to isolate excitatory transmission, and 100nM NBQX to prevent epileptiform activity. For recording $GABA_AR$-mediated evoked inhibitory postsynaptic currents (IPSCs), the aCSF was supplemented with 25µM D-AP5, 10µM NBQX and 1µM CGP55845 to block AMPAR-, NMDAR- and $GABA_BR$-mediated transmission respectively. Field recordings were performed in aCSF only. Additional drugs were bath applied to the whole slice. Cannabinoid receptor (inverse) agonists used are listed in the table on following page and were the following (concentration in µM): AM-251 (inverse CB_1R agonist, 2-5); SR144528 (inverse CB_2R agonist, 1); 2-AG (endogenous agonist, 10); WIN55,212-2 (WIN, synthetic agonist, 1) and HU-308 (CB_2R-specific synthetic agonist, 1). We found that 2-5µM AM-251, a concentration that is typically used in electrophysiological experiments to block CB_1Rs, also blocked CB_2Rs. We thus tested the specificity of AM-251, SR144528 and HU-308 for CB_1- and CB_2Rs respectively at the concentrations used in this study in the appropriate CBR KO mice (see chapters 3.4 and 3.7 respectively). These controls were additionally necessary because the K_i values reported in the literature vary over orders of magnitude depending on the expression system (native tissue vs. cell culture) and whether human or rodent cloned cannabinoid receptors were used.

Table 2.4.1. Cannabinoid receptor (inverse) agonists and their binding affinities.

	concentration (in µM)	CB_1R Ki value (nM)	CB_2R Ki value (nM)	Relative affinity	Reference
Agonists					
WIN 55,212-2	1	62.3 $_{h*}$	3.3 $_{h*}$	$CB_1R<CB_2R$	(235)
		9.87 $_{h*}$	0.29 $_{h*}$		(316)
		0.41 $_{m*}$	0.56 $_{m*}$		(316)
		0.14 $_{r, brain}$	1.3 $_{r, spleen}$		(316)
2-AG	10	472 $_{h*}$	1400 $_{h*}$	$CB_1R>CB_2R$	(188)
HU-308	1	>10,000 $_{h*}$	22.7 $_{h}$	$C_{B1}R<CB_2R$	(317)
Inverse agonists					
SR144528	10	437 $_{h*}$	0.60 $_{h*}$	$CB_1R<CB_2R$	(318)
		50.3 $_{h*}$	1.99 $_{h*}$		(316)
		0.41 $_{m*}$	0.56 $_{m*}$		(316)
		27.6 $_{r, brain}$	0.24 $_{r,spleen}$		(316)
		305 $_{r,brain}$	0.30 $_{r,spleen}$		(318)
AM-251	2-5	7.49 $_{r, brain}$	2290 $_{m, spleen}$	$CB_1R>CB_2R$	(319)

* expressed in recombinant expression system (cell culture)
h: cloned human cannabinoid receptor
m: mouse cannabinoid receptor, either native (when tissue indicated) or cloned
r: rat cannabinoid receptor, either native (when tissue indicated) or cloned

2.3.3 Whole-cell and perforated patch recordings

Patch pipettes were pulled from borosilicate filamented glass capillaries (outer diameter 1.5mm, inner diameter 0.86 or 1.17mm) with a DMZ Universal Puller and fire-polished to a final resistance of 2-3 MΩ for whole-cell recordings (denoted as wc in figures). Pipettes were backfilled with filtered intracellular solution containing (in mM): 130 $KMeSO_3$ (or, in some experiments, 140 $KMeSO_4$), 10 KCl, 10 HEPES, 4 NaCl, 4 Mg-ATP, 0.5 Na-GTP, 5 phosphocreatine, 285–290 mOsm, pH was adjusted to 7.3 with KOH. For perforated patch recordings (denoted as pp in figures) (320), pipettes with a final resistance of 3-5 MΩ were tip-filled with the same intracellular solution. They were then backfilled with intracellular solution additionally supplemented with gramicidin (80µg/ ml) which was freshly prepared as a stock solution (20mg/ ml, diluted in dimethyl sulfoxide, DMSO) on the day of use. For experiments with intracellular application of the non-hydrolysable GDP analogue GDP-β-S, Na-GTP in the intracellular solution was replaced with GDP-β-S, which was added freshly on the day of use.

All recordings, unless indicated differently, were performed in current-clamp mode. The resting membrane potential and input resistance (denoted as R_{in} in figures) were determined directly after establishing the whole-cell configuration or, for perforated patch recordings, when the access resistance (denoted as R_a in figures) had stabilised (Figure 2.3.1). More precisely, only cells with a stable access resistance below 60MΩ were used, with the exception of the dual perforated patch experiments, where the control cell was used if an access resistance below 100MΩ was achieved.

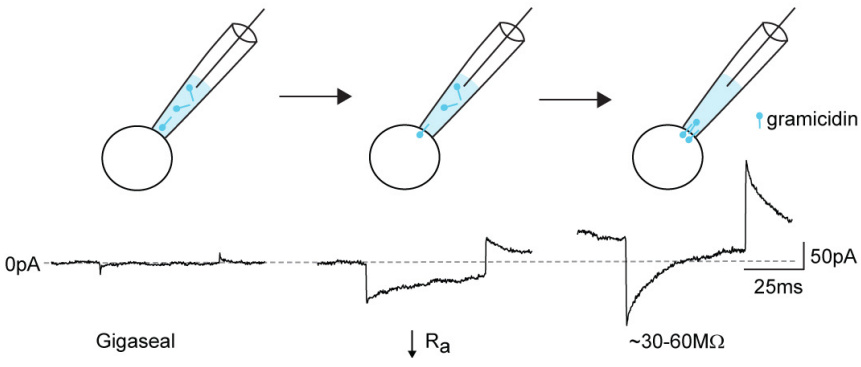

Figure 2.3.1 Perforated patch recordings allow stable electrical access without interfering with the cell's intracellular composition. This is achieved by supplementing the intracellular solution with a pore-forming antibiotic (here: Gramicidin D, indicated by blue symbols) that leaves the membrane intact and is permeable only to small cations. After the formation of a gigaseal (cell-attached configuration, left panel), the antibiotic will slowly start integrating into the neuronal membrane which can be seen as a reduction in R_a (middle panel) that is continuously monitored by applying short voltage test pulses (-4mV, 50ms) in voltage clamp configuration every 15s. The recording is started when the R_a has stabilised at a sufficiently low level to ensure proper electrical access/ control over the recorded neuron (right panel). In this example, the R_a stabilised at 48MΩ; on average across cells included in Chapter 3.1 the R_a was 34.3±1.3 MΩ. Note that the increase in holding current upon successful perforation (right panel) is due to the resting membrane potential of the cell that is more negative than its holding potential in voltage clamp (here: -60mV) indicating that the recorded cell is healthy.

Experiments were only continued if cells had a resting membrane potential more hyperpolarised than -55mV. The cells were further characterised by recording their membrane response / firing pattern to current injections of increasing strengths (-20 to +800pA, increment: 20-50pA, 1s). Afterwards, the membrane potential was adjusted to -60mV with continuous, direct current injection if not stated otherwise. Input and access resistance and pipette capacitance were monitored continuously throughout the experiment and the latter two were compensated for using bridge balance and capacitance neutralisation. Experiments were stopped if cells depolarised by more than 5mV or the access resistance changed ›15% over the course of the recording.

2.3.4 Action potential protocols

The standard action potential protocol used consisted of 15 trains with 50 action potentials each (750 action potentials, 10ms inter-stimulus interval, 20s inter-train interval). Individual action potentials were elicited by 2ms, somatic current injections (1-2nA) (Figure 2.3.2A). The theta-burst protocol used to test the induction threshold of CA1 PCs consisted of 10 bursts of five stimuli (applied at 100Hz) with a 200ms interburst interval, repeated every 5s 60x (3000 action potentials). For the physiological spike train, the unit activity of a putative CA3 place cell recorded in a rat traversing a linear track rat was used (76, 321). More specifically, an action potential protocol was implemented using a five minute stretch of inter-spike intervals of this cell's place field firing pattern (Figure 2.3.2B). Because the physiological spike train stemmed from rat data, this dataset was acquired in rat accordingly.

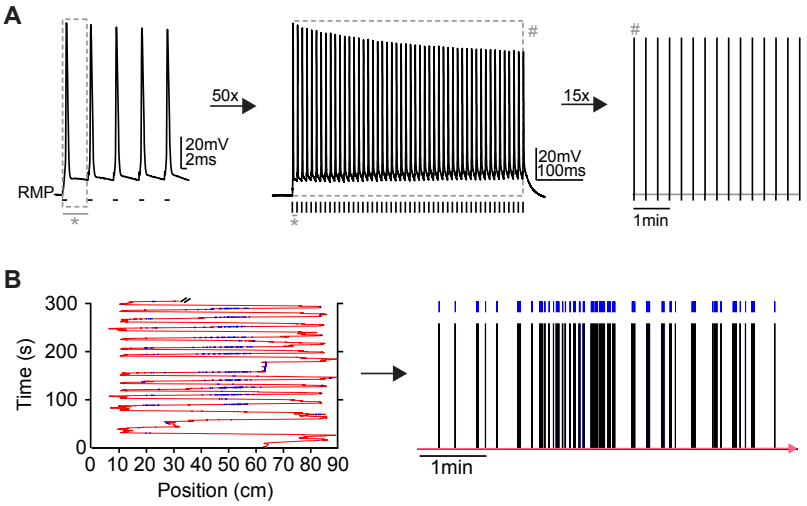

Figure 2.3.2 Current injection protocols used to trigger action potentials. (A) Single action potentials were induced by 2ms long, suprathreshold current injections (indicated by horizontal black lines) that were delivered via the patch pipette with a 10ms inter-stimulus interval between single action potentials (grey line, left panel). Trains of fifty action potentials each were elicited (middle panel). The induction protocol consisted of 15 such action potential trains that were delivered with 20s intervals between trains (right panel). (B) The physiological spike train was constructed from the place field firing of a single neuron that preferentially fired at positions 40-60cm while traversing a linear track as illustrated in the left panel (red line – trajectory of animal on linear track, blue dots – action potentials). The points in time at which action potentials occurred were implemented in a 5min long current injection protocol that mimicked the irregular spike activity observed in vivo (right panel, colour-code same as in left panel).

2.3.5 Recordings of IPSCs

Pharmacologically isolated (25µM AP5 and 10µM NBQX), evoked IPSCs (denoted as eIPSCs in figures) were recorded in voltage-clamp configuration at a holding potential of -50 or -70mV (resulting in either out- or inward currents). The stimulation electrode (borosilicate glass, as above) was positioned in stratum radiatum of CA3 ~150µm away from the recorded cell (towards the hilar region of the dentate gyrus) and the experiment were only started when the evoked IPSCs displayed monosynaptic rise and decay kinetics. DSI was elicited by depolarising the cell to 0mV (3x 1s, 5s interval or 1x 5s). Cells that showed a ›15% reduction in the amplitude of the evoked IPSCs after the depolarising step were considered DSI-positive.

Pharmacologically isolated (25µM AP5 and 10µM NBQX), spontaneous IPSCs for the analysis of DSI were recorded with a intracellular solution containing 140mM KCl to reverse and increase the driving force for chloride and in the presence of 20µM Carbachol to boost their frequency.

2.3.6 Recordings of synaptically evoked EPSPs and action potentials

To test for the change in spike probability of CA3 PCs before and after pharmacological CB_2R activation, a stimulation electrode was placed in stratum radiatum of CA3 and synaptic, glutamatergic responses (EPSPs) were evoked and recorded in current clamp in the continuous block of GABAergic transmission. The stimulation strength was adjusted to an initial spike probability of ~80%.

2.3.7 Extracellular field recordings

For field recordings, both the stimulation and recording pipette (borosilicate glass, as above; tip diameter: ~20µm) were filled with aCSF and placed in stratum radiatum of area CA3. Field EPSPs were evoked by stimulating presumptive A/C fibres (duration: 100µs, frequency: 0.05Hz) using a stimulus isolator (Isoflex, A.M.P.I) and adjusted to 60% of the maximal amplitude. The fEPSP slopes were determined as dV/dt (in mV/ms) of 10 to 90% of the amplitude in each individual trace.

2.3.8 In vivo wire array recordings*

After one week of handling and habituation to the recording room, 10 male WT mice were implanted under isoflurane anesthesia with arrays of single tungsten wires (40µm, California Fine Wire Company) in the hippocampus (coordinates relative to bregma, at anteroposterior: -1.94mm, lateral: 2.3mm, ventral: 2.15mm). Reference and ground electrodes were miniature stainless-steel screws in the skull. Implanted electrodes were secured on the skull with dental acrylic. After one day of recovery, animals were placed in a 1x1m open arena and were allowed to explore freely during recordings. Electrodes were connected to operational amplifiers (Neuralynx, USA) to eliminate cable movement artefacts. Electrophysiological signals were differentially amplified, bandpass filtered (1-9000Hz) and acquired continuously at 30303Hz. After 1h of baseline recordings animals were injected with either vehicle (10mg/kg DMSO) or with HU-308 (10mg/kg, dissolved in DMSO) and were recorded in the arena for one more hour. After completion of the experiments, mice were deeply anesthetised and electrolytic lesions at selected recording sites were performed. Subsequently the animals were perfused intracardially with 4% PFA solution and decapitated. Brains were fixed, cut in 50µm slices and stained with cresyl violet for confirmation of recording sites .

* | See page 29 for contributions.

2.4 Data analysis

2.4.1 In vitro electrophysiological data

Data analysis was performed in IGOR Pro 6.12 using the IGOR analysis software package Neuromatic. Statistical comparisons between groups were performed in Prism 5. Sample sizes are given as the number of experiments (n) and the number of animals (N). Individual membrane potential values (denoted as V_m in figures) were determined from a 10ms average around the detected minimum within a 100ms time window every 20s. The minimum average was taken to circumvent distortions due to the high spontaneous activity in CA3 PCs. The input resistance was calculated from a 50ms average of the steady-state membrane potential response to a hyperpolarising test pulse (400ms, -20 to -80pA). Given membrane potential values were normalised to a 1min baseline (3 values) before the action potential induction protocol or, for drug application, to a 2min baseline. For summary time plots of the global membrane potential average, the individual values of all experiments were averaged per point in time; alternatively, the median (including 25^{th} and 75^{th} percentile) at a certain time point is calculated as the average of 1min (3 values/ experiment). Exemplary membrane potential recordings are unfiltered raw traces if not indicated otherwise. Properties of the AHP were analysed from the average response to the first 2-3 action potential trains elicited during the induction protocol. Its maximal amplitude was calculated from a 10ms minimum average within the first 500ms, and its area from a 10s window after the action potential train.

Given membrane potential values are not corrected for liquid junction potential (LJP), which was calculated to be 10mV (PCalcW, Molecular Devices; USA) (322) for the $KMeSO_3$-based intracellular solution. A LJP develops whenever two solutions with different compositions (and ionic mobilities) come into contact (323); in whole-cell patch clamp recordings these are the intracellular fluid of the cell and the solution in the recording pipette. An estimate of the potential difference arising between them can be calculated according to the generalised Henderson LJP Equation where for N polyvalent ions, the potential (V) of solution (S) with respect to the pipette (P) is given by the following equation (also see (323) for a detailed review and derivation of the mathematical formula):

$$V^s - V^p = (RT/F)S_F ln\left\{\sum_{i=1}^{N} z_i^2\, u_i a_i^P / \sum_{i=1}^{N} z_i^2\, u_i a_i^S\right\} \quad (1)$$

where

$$S_F = \sum_{i=1}^{N}\left[(z_i u_i)(a_i^S - a_i^P)\right] / \sum_{i=1}^{N}\left[z_i^2 u_i (a_i^S - a_i^P)\right] \quad (2)$$

where V^S-V^P represents the potential of the solution with respect to the pipette and *u*, *a* and *z* represent the mobility, activity and valence (including sign) of each respective ion species (i). *R* is the gas constant, *T* is the temperature in Kelvin and *F* is the Faraday constant. With a LJP of 10mV (V^S-V^P), the corrected membrane potential would thus be $V_m = V_p$ -10mV. For perforated patch experiments using Gramicidin D, which is not permeable to chloride but only to small cations, the LJP between the cell and the perforating pipette is negligible (320).

This is because no permeant anions are present on either side of the seal, and the concentrations of the main permeant cations, namely potassium and sodium, that thus dictate the LJP, will be approximately equal.

For the analysis of spontaneous EPSPs and IPSCs (denoted as spEPSPs and spIPSCs in figures), individual events were detected with a threshold-based algorithm in Neuromatic and a total of 5-10s were analysed for each time point. The amplitude of each event was defined as the 10ms average maximum within a 100ms time window after the stimulation. Examples show individual traces.

The distribution of data was assessed with the D'Agostino and Pearson omnibus normality test. Normally distributed data sets were compared with a two-tailed Student's t-test and values are expressed as mean±SEM. Nonparametric tests were used as indicated and data presented as median (including the 25thand 75th percentile). The averages of the change in membrane potential (denoted as ΔV_m in figures) across cells were assessed with the appropriate paired tests (Student's t-test or, if indicated, Wilcoxon signed-rank test). Correlation analyses were carried out using either the Pearson (for data sampled from Gaussian distribution, indicated by r) or Spearman (nonparametric, indicated by r_s) correlation coefficient. Results were considered significant at $p<0.05$.

The percentage of reactive cells in each experiment was calculated from a -2.1mV cut-off to facilitate the comparison between different (recording-) conditions/manipulations. This cut-off was based on the mean of the whole-cell hyperpolarisation (-1.8mV) plus its standard error (-0.3mV). To give a 'biologically relevant' estimate of the average ΔV_m, only the values of reactive cells are averaged for data sets in which washout in the whole-cell configuration led to a skewed data distribution (see Results 3.2 and Figure 3.2.2).

2.4.2 In vivo electrophysiological data*

Signal processing was carried out off-line by custom-written MATLAB algorithms. The LFP was processed by low-pass filtering and down-sampling of the wideband signal to 1250Hz. Phase-amplitude coupling of theta and gamma oscillations was assessed for epochs of theta oscillations with a theta/delta power ratio of at least five. The theta phase was obtained by Hilbert transformation of the 5-10Hz filtered signal. Gamma oscillation peaks were detected in the 30-85Hz and 65-120Hz band-pass filtered signal (70), and their amplitudes and theta phases were subsequently calculated. The gamma amplitude – theta phase modulation coefficient (M_{gt}, see (67)) was computed for each theta/delta ratio-standardised theta amplitude bin. Power spectral density was computed using the multitaper method ([NW] = 3, window size 1024) and standardised to the power in the 30-45Hz band during baseline recordings.

Correlation coefficients (Pearson's or Spearman's, depending on the data distribution) of M_{gt} and the theta amplitude were computed and Fisher z-transformed. The statistical significance of single comparisons was determined by a repeated measures two-way ANOVA (treatment x drug) followed by Bonferroni post-hoc tests. Distributions' normality and variances were estimated by the Lillieforce and built-in MATLAB variance test, respectively.

* | These experiments were performed and analysed by Tuğba Özdoğan. For further information please see the *Statement of contributions*.

3 Results

3.1 Characterisation of hippocampal principal cells

Hippocampal principal cells can be distinguished based not only on their location in the hippocampus and their apparent morphology, but also on their distinct electrophysiological properties (95, 127, 324). To ascertain that we recorded from the right cell type (most importantly to distinguish glutamatergic principal cells from inhibitory INs), each neuron was electrophysiologically characterised before the start of the experiment and an 'online' analysis of its properties including firing pattern, input resistance, resting membrane potential was performed. Differences in resting membrane potential, input resistance and AHP are shown and listed below (Figure 3.1.1 and Table 3.1.1) and present a summary of all WT cells recorded in perforated patch configuration in the initial part of this study. An additional list with the membrane properties of the CA3 PCs cells recorded in whole-cell configuration can be found in the next chapter for comparison (Table 3.2.1). Especially in regards to the initial membrane potential and input resistance, these are likely to be more appropriate given the better and quicker access to the recorded cell.

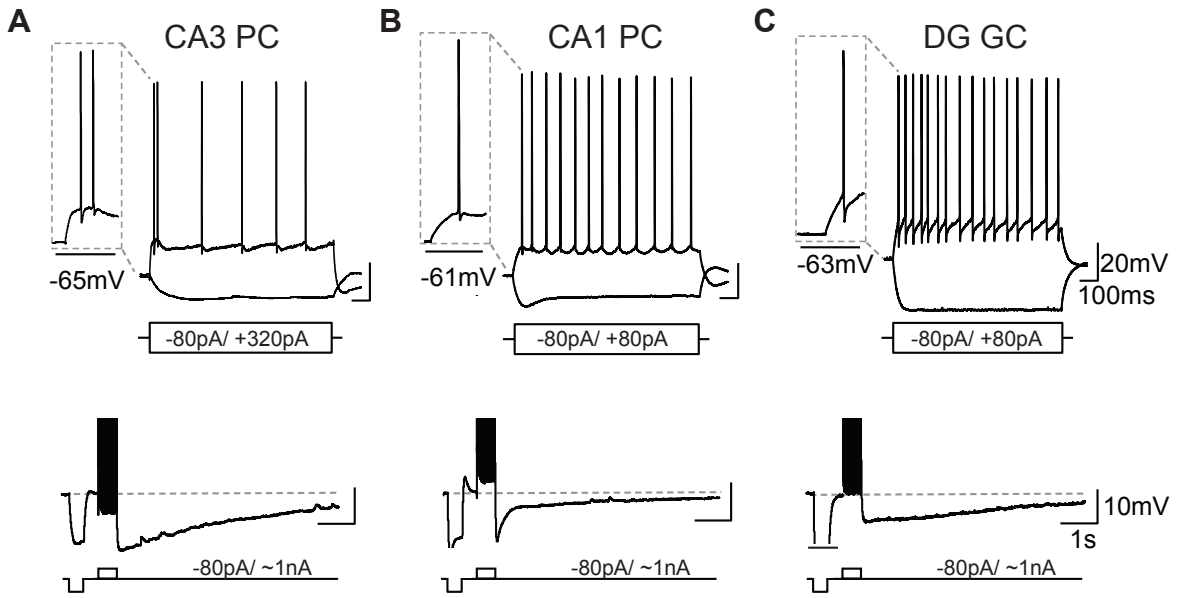

Figure 3.1.1 Electrophysiological characterisation of hippocampal principal cells recorded in perforated patch configuration. (**A-C**) Upper panels: Current injections of different amplitudes (indicated below the traces: -80; +320 or +80pA) were used to characterise the cells' R_{in} and spike pattern in current-clamp mode. Note the differences in the spike shape (insets), the pronounced I_h current in CA1 PCs and the high R_{in} of dentate gyrus GCs (as deduced from the membrane potential change). Lower panels: The AHP (induced by 50 action potentials, black rectangle) is characteristically different between the cell populations. While CA3 PCs have a large maximal amplitude and long-lasting AHP, CA1 PCs exhibit a large, initial (fast) AHP that decays very quickly. Dentate gyrus GCs have smaller maximal amplitudes but a slower decay than CA1 PCs. Reasons for these differences are (besides others) the expression of different calcium-activated potassium and hyperpolarisation-activated non-selective cation (HCN) channels. The latter also constitutes the current underlying the characteristic membrane potential deflection observed in CA1 PCs upon negative current injection. The membrane deflection in (C) in response to a -80pA test pulse before the action potential train was cut off for display purposes (indicated by black line).

Table 3.1.1 Passive and active membrane properties of hippocampal principal cells recorded in perforated patch configuration.

	CA3 PCs (n=17)	**CA1 PCs** (n=8)	**DG GCs** (n=8)
Resting V_m (mV)	-67.9±1.5	-60.6±1.02	-76.4±2.8
R_{in} at rest (MΩ)	194.4±16.3	133.0±10.3	227.7±27.8
AHP, max (mV)	-13.3±0.6	-12.3±0.45	-6.245±0.6
AHP, area (mV/s)	-54±4.1	-22.1±1.7	-14.91±3.7
R_a (MΩ)	34.05±1.5	36.2±3.1	32.7±1.9

3.2 Backpropagating action potentials induce a long-lasting hyperpolarisation in hippocampal CA3 PCs

Transient, repetitive stimulation of neurons activates a post-spike AHP that, depending on the cell type, can last for many (tens of) seconds and limits prolonged depolarisation of the membrane potential (325). We observed that trains of action potentials additionally elicit a long-lasting membrane potential hyperpolarisation in CA3 PCs that was complementary to and continued even after the AHP subsided (Figure 3.2.1). In perforated-patch configuration, the hyperpolarisation was present in all cells tested, persisted for the duration of the recording (up to 20 minutes after the induction, see chapter 3.6) and was as large as up to 10mV.

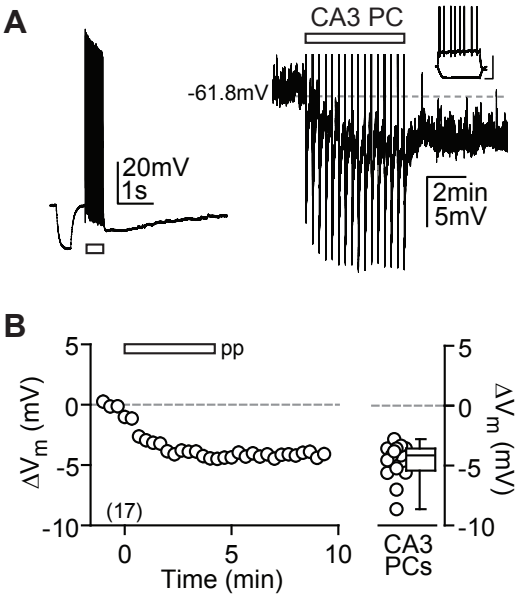

Figure 3.2.1 Action potential firing induces a V_m hyperpolarisation of CA3 hippocampal principal cells. (**A**) Perforated patch recording of a CA3 PC in which current injection-triggered action potential trains (black rectangle) are followed by an AHP (left panel, example of first AP train) but additionally induce a long-lasting V_m hyperpolarisation (right panel). The baseline V_m value is shown and indicated by the dashed grey line. Action potentials have been truncated and test pulses cut for display purposes in this and all later figures displaying time plots of raw traces. Right inset: firing pattern of the same CA3 PC (scale bar: 40mV, 0.2s). (**B**) Summary time course of the ΔV_m average of all CA3 PCs recorded in perforated patch (n(N)=17(13), left panel) and the median ΔV_m (including 25th and 75th percentile) calculated from min5-6 (-4.1, -5.4 and -3.6mV, right). The V_m after the induction protocol is significantly different from baseline (paired t-test: $p<0.0001$). Note that the high frequency and amplitude of spontaneous EPSPs in CA3 PCs render the baseline V_m seemingly noisy at there here displayed time resolution in the range of minutes.

When repeating the above experiment in whole-cell configuration, we observed a fraction of unresponsive or less responsive CA3 PCs which was in stark contrast to the perforated patch results (Figure 3.2.2). Thus, the average data acquired in whole-cell configuration underestimates the observation of a long-lasting V_m hyperpolarisation and might be the reason why this form of plasticity has not been observed before. We defined a cut-off to be able to sort the whole-cell data into "reactive" and "unreactive" cells. We reasoned that this would give a better estimate of the true average ΔV_m and does not artificially reduce it by including washout failures in the analysis that have no biological meaning but constitute an experimental artefact. Because the whole-cell data showed a Gaussian distribution and no apparent two clusters were identifiable (see analysis below), we chose the threshold according to the mean (-1.8mV) plus the standard error of the mean (-0.3mV), yielding a cut-off of -2.1mV.

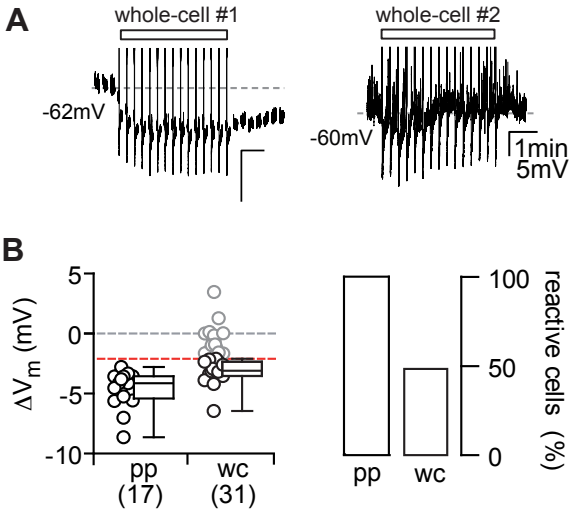

Figure 3.2.2 Whole-cell patch clamp recordings interfere with the V_m hyperpolarisation. (**A**) Whole-cell current-clamp recording of a reactive (whole-cell #1, left) and an unreactive CA3 PC (whole-cell #2, right) in response to the action potential train stimulus (rectangle). (**B**) Left panel: the ΔV_m of each recorded cell (open circles) and the median, 25th and 75th percentile of the average ΔV_m recorded in the different recording conditions are shown for perforated patch (pp, data as in Figure 1) and n(N)=31(14) whole-cell recordings (wc, with n=15 reactive cells: -3.1, -3.5 and -2.3mV). The dashed red line indicates the cut-off of -2mV by which cells were classified as reactive (black circles) or unreactive (grey circles). Right panel: the percentage of reactive cells is shown for perforated patch (100%) and whole-cell (48.4%) recordings respectively.

Correlation analyses of the different possible underlying factors, including series resistance, input resistance and the amount of direct current injection needed to keep the cells at -60mV (listed in Table 3.2.1), did not yield any significant correlations when compared to the change in membrane potential (Figure 3.2.3). The initial input resistance shows a (non-significant) tendency to inversely influence the change in membrane potential, which could indicate that it somehow facilitates the disturbance of the cell's intracellular milieu in whole-cell configuration. The reasons for this, however, are not clear. The AHP was similarly affected by the recording condition, and the maximal AHP amplitude was significantly bigger in perforated patch than in whole-cell recordings of CA3 PCs (-13.3±0.6mV in perforated patch vs. -9.8±0.5mV in whole-cell configuration, unpaired t-test: $p<0.05$). Yet, the maximal AHP amplitude and the action potential-induced membrane potential hyperpolarisation did not correlate (r=-0.16, P=0.41), indicating that the underlying reasons are unrelated and are dependent on different factors being disturbed by the recording condition. Also, an additional subset of whole-cell recordings was performed with potassium gluconate (KGluconate)-based intracellular solution or with 0.2% biocytin added to $KMeSO_3$-based intracellular solution, in both of which cases we observed a (near-complete) abolition of the hyperpolarisation (median with 25th and 75th percentile of the ΔV_m: 0.68, 0.26 and 2.49mV and 0.76, -2.39 and 2.78mV respectively). The disruption by KGluconate, a calcium chelator, indicates that the hyperpolarisation may be a calcium-sensitive mechanism. For a more detailed experimental analysis of this, the reader is referred to chapter 3.10 of this thesis. Taken together, our findings are complementary to previous studies that have reported that intracellular solutions used for whole-cell patch-clamp studies alter and interfere with membrane properties (172, 320, 326), and thus encourage a more frequent use of non-disruptive recording methods.

Table 3.2.1. Passive and active membrane properties of CA3 PCs recorded in whole-cell configuration.

	Resting V_m (mV)	R_{in} at rest (MΩ)	R_{in} at -60mV (MΩ)	AHP, max. ampl. (mV)	AHP, area (mV/s)	R_s (MΩ)
CA3 PCs (n=31)	-73.8±0.82	82.4±5.2	128.9±6.6	9.8±0.5	-34.1±3.3	8.6±0.32

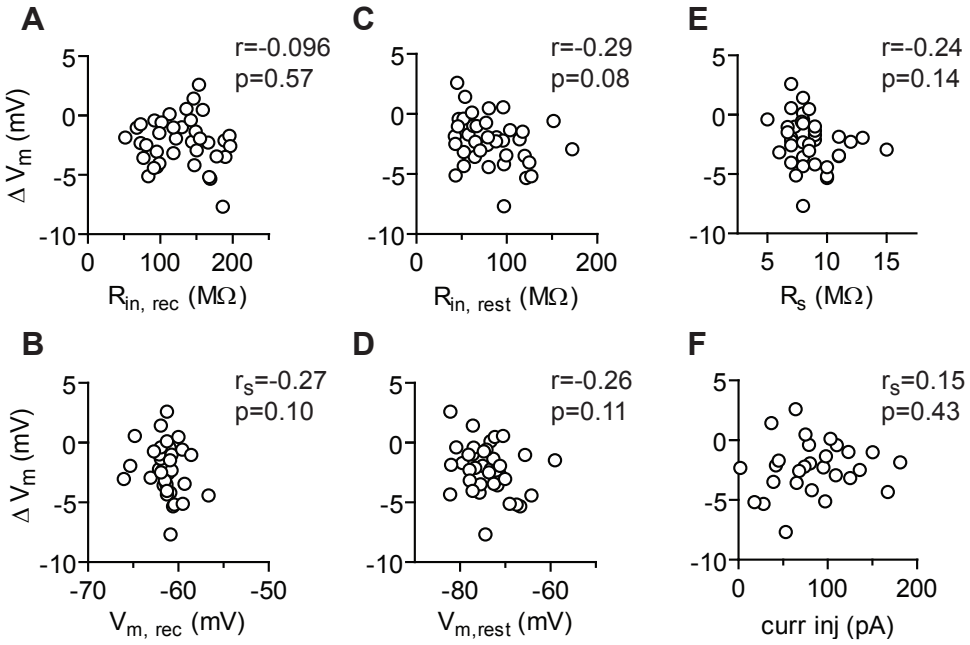

Figure 3.2.3 Correlation analysis of the average ΔV_m and recording variables. The average ΔV_m was not significantly correlated to any of the parameters tested that included the R_{in} and the V_m during the recording (**A, B**), the R_{in} and V_m at rest and without constant current injection (**C, D**), the R_s (**E**) and the current injection needed to keep the cell at a holding potential of -60mV (**F**). Both the correlation coefficient (r or r_s, depending on the distribution of the data) and the correlation's significance (p) are given for each correlation.

3.3 Cellular plasticity displays distinct cell-type specificity

To elucidate whether the hyperpolarisation is a mechanism common to all hippocampal principal cell types or displays cell-type specificity, we examined CA1 PCs and dentate gyrus GCs (recorded in perforated patch configuration, see Table 3.1.1 for membrane properties), as well as CA2 PCs. In contrast to CA3 PCs, that hyperpolarised independent of their location in CA3, neither CA1 PCs nor dentate gyrus GCs hyperpolarised persistently in response to action potential trains (Figure 3.3.1).

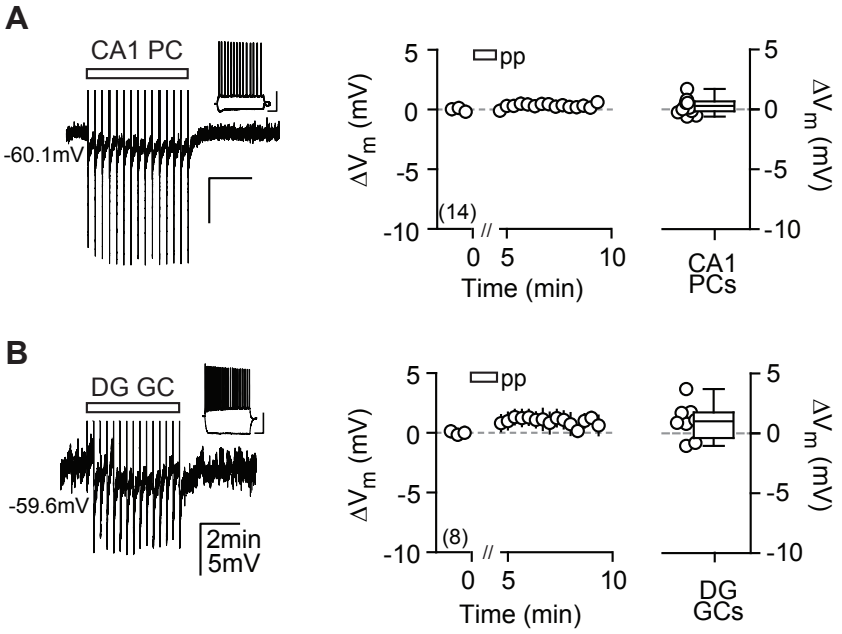

Figure 3.3.1 The V_m hyperpolarisation is absent in CA1 PCs and DG GCs. (**A, B**) Current injection-triggered action potential trains (black rectangle) fail to induce a long-lasting hyper-polarisation in CA1 PCs (A) and DG GCs (B). Left panels: exemplary pp recording of each principal cell population. Insets: firing patterns (scale bar: 40mV, 0.2s). Middle panels: summary time course of the ΔV_m average for CA1 PCs: n(N)=14(4) and DG GCs: n(N)=8(4). The x-axis is discontinued for the duration of the AP train. Right panels: median ΔV_m (including 25th and 75th percentile) calculated from min5-6 for CA1 PCs (0.30, -0.15 to 0.68mV) and DG GCs (1.04, -0.35 and 1.8mV).

Whole-cell recordings from post hoc morphologically identified CA2 PCs – that are very similar in their electrophysiological properties to CA3b PCs and can be distinguished from neighbouring CA3a PCs by their characteristic dendritic bifurcation close to the soma (95) – revealed that they also express this form of cellular plasticity. Indeed, they did not differ from CA3 PCs in the degree of hyperpolarisation (Student's t-test: P=0.69 in comparison to CA3 PC whole-cell recordings; Figure 3.3.2).

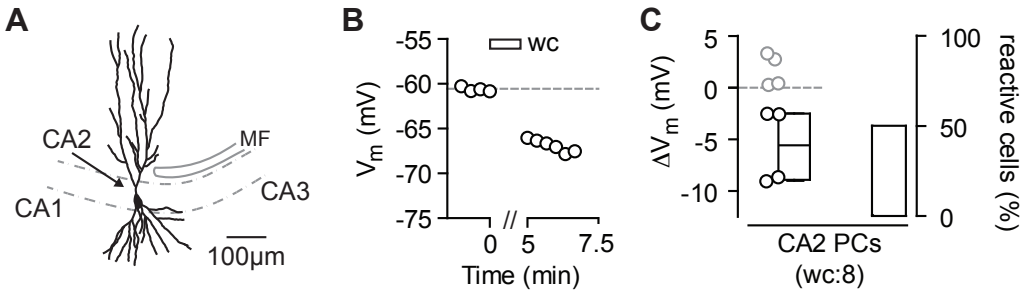

Figure 3.3.2. CA2 PCs display a hyperpolarisation that is similar to CA3 PCs. (**A**) Anatomical reconstruction of a CA2 PC filled with 30µM Alexa. Note the characteristic bifurcation of the proximal dendritic tree (indicated by black arrow). The pyramidal cell layer is indicated by the dashed lines and the dense axons from DG GCs, the mossy fibres (MF) that end at the border of CA3 to CA2 are shown in grey. (F) Time plot of the V_m of the same CA2 PC as in (A) in response to the action potential protocol (rectangle) recorded in whole-cell current clamp configuration. The dashed line indicates the average baseline V_m. (**C**) Left: The ΔV_m of each recorded cell (circles) and the median, 25th and 75th percentile of the average ΔV_m of all reactive cells is shown for n(N)=8(5) CA2 PCs: -5.8, -8.9 and -2.5mV. Right: The percentage of reactive CA2 PCs was 50%.

To conclude, we find a long-lasting hyperpolarisation in CA2/3 pyramidal neurons that can be induced in an activity-dependent manner and exhibits a phenomenological cell type specificity. The combined results of the three main hippocampal principal cell populations that were recorded in the perforated patch configuration are compared and illustrated below (Figure 3.3.3).

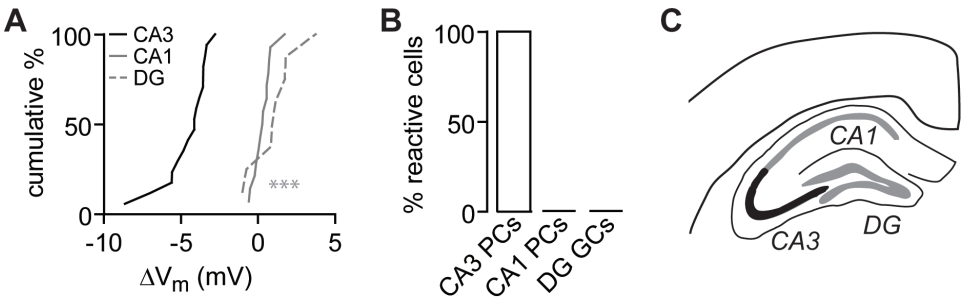

Figure 3.3.3 Comparison of the main principal cells of the hippocampus. (**A**) The ΔV_m averages of CA3 PCs (black line), CA1 PCs (grey line) and DG GCs (grey, dashed line) recorded in perforated patch configuration reveal a significant difference between the cell types as shown in the cumulative distribution with only CA3 PCs showing this type of plasticity (Kruskal-Wallis with Dunn's post-test: $p<0.05$ for CA3 PCs vs. CA1 PCs and DG GCs). (**B**) The percentage of reactive cells is shown for CA3 PCs: 100%, CA1 PCs: 0% and DG GCs: 0%. (**C**) Schematic depiction of the results (colour-coded as in (A); scheme modified from Paxinos).

3.4 Cannabinoid type 2 receptors mediate long-lasting hyperpolarisation

Next, we explored how backpropagating action potentials induce this form of cellular plasticity. Previously, a similar phenomenon has been reported to be dependent on a CB_1R-mediated activation of a potassium-conductance on subsets of cortical neurons (327, 328). To test this, we recorded CA3 PCs from $CB_1R^{-/-}$ mice, but found that the effect was fully intact in these animals (Figure 3.4.1A). We then recorded CA3 PCs from mice lacking the CB_2R – the other main cannabinoid receptor. Surprisingly, the effect was absent in these animals, suggesting that CB_2Rs mediate the long-lasting hyperpolarisation (Figure 3.4.1B). To verify this key finding, in addition to recording from homozygously bred $CB_2R^{-/-}$ mice, we performed n(N)=6(2) and 4(2) recordings from CB_2R KO and CB_2R WT littermates respectively with the experimenter blind to the genotype of the animals. The results for each genotype did not differ and were hence pooled (Mann-Whitney test: P=0.79 for ΔV_m in homo- vs. heterozygously bred $CB_2R^{-/-}$ and P=0.28 for B6N WT vs. $CB_2R^{+/+}$ mice).

The transient hyperpolarisation that can be observed during the induction protocol in CB_2R-lacking neurons (see Figure 3.4.1B) is due to the AHP that is induced by the action potential trains. The AHP lasts longer than the 20s interstimulus interval in perforated patch configuration, and thus only decays after the last AP train. As an additional control, because the CB_2R KO mouse we used still expresses a truncated residue of the receptor (8, 43), we furthermore confirmed that the transient hyperpolarisation is independent of cannabinoid-mediated signalling by recording from CB_2R KO slices preincubated with the CB_2R-specific antagonist SR144528. As expected, a similar transient hyperpolarisation was still present in these recordings (n(N)=6(3), data not shown). Further evidence for the lack of residual receptor activity in these KO mice by pharmacological means will be presented in Chapter 3.7.

It is known that CB_2Rs are expressed in macrophage lineage cells including microglia that have been shown to modulate neuronal transmission (329). Furthermore, as of yet, direct evidence for the neuronal expression of CB_2Rs is still missing given the lack of specific antibodies against CB_2Rs. Thus, in order to test for the neuronal expression of CB_2Rs we used a neuron-specific CB_2R knockout mouse in which the CB_2R protein is deleted under a synapsin promoter via the Cre/loxP system. We find that in these mice the hyperpolarisation was equally absent as in the constitutive KO (Figure 3.4.1C) thus strongly pointing towards a neuronal localisation of the CB_2Rs responsible for the hyperpolarising response.

In summary, all experiments performed in CB_1R KO and WT animals show a similar hyperpolarisation that is completely abolished in animals of both constitutive and neuron-specific CB_2R KO mouse strains (Figure 3.4.1D-E) strongly pointing towards the involvement of neuronal CB_2R in the activity-dependent hyperpolarisation[17].

In addition to the perforated patch experiments shown in Figure 3.4.1, we performed whole-cell recordings from both CB_1R- and CB_2R knockout mice. These confirmed the phenotypic findings of both the dependence of the hyperpolarising effect on CB_2Rs and the presence of a gradual washout in whole-cell recordings of neurons from CB_1R KOs that was similar to the one found in WT (Figure 3.4.2).

17 | None of the KO strains show differences in their basic physiological properties, including resting membrane potential, input resistance and AHP amplitude, in comparison to WT (data not shown).

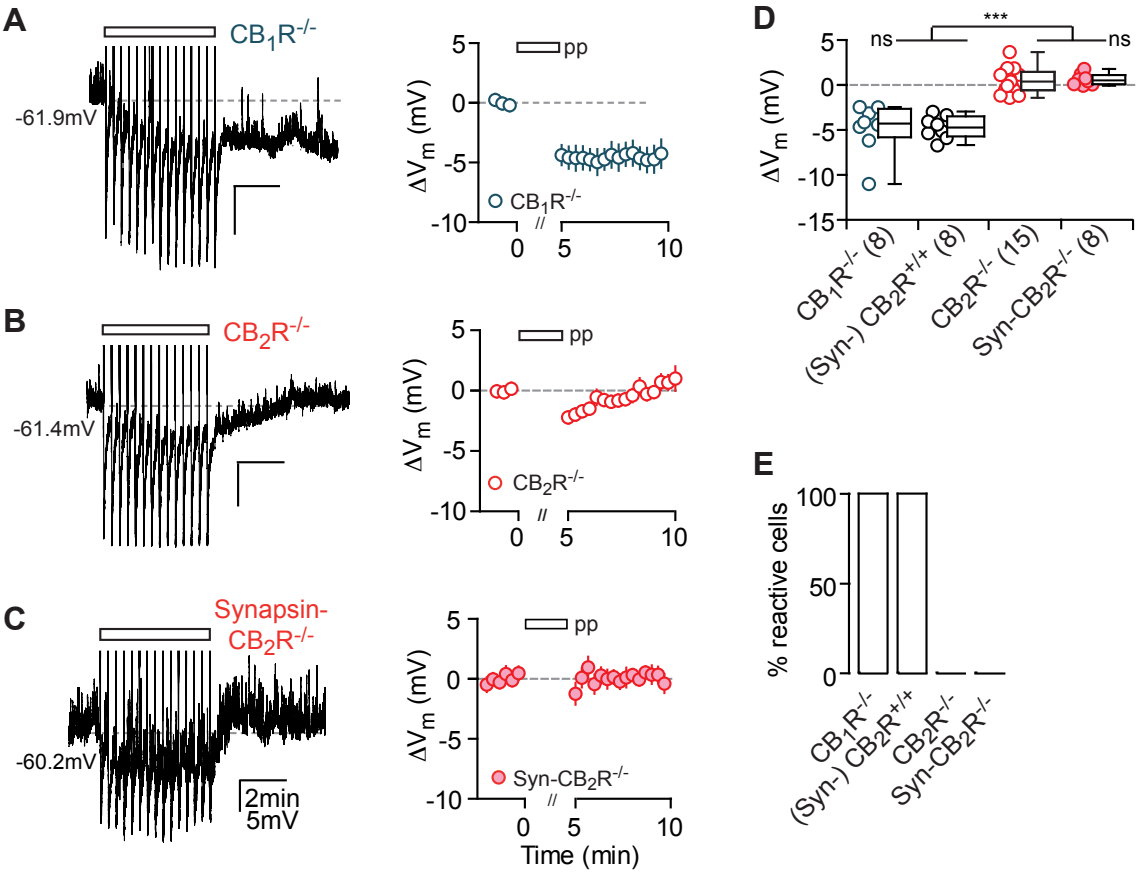

Figure 3.4.1 The long-lasting hyperpolarisation is absent in CB2R-deficient mice. (**A-C**) Action potential trains (rectangle) induce a long-lasting V_m hyperpolarisation in CB_1R-deficient CA3 PCs (A) but not in CA3 PCs of constitutive $CB_2R^{-/-}$ (B) or synapsin cre-dependent (Syn-) $CB_2R^{-/-}$ mice (C). Left: exemplary pp recordings of a CA3 PC in each respective KO animal. Right: summary time course of the average ΔV_m of CA3 PCs recorded from $CB_1R^{-/-}$: n(N)=8(6), $CB_2R^{-/-}$: n(N)=15(8) and Syn-$CB_2R^{-/-}$: n(N)=8(5). The x-axis is discontinued for the duration of the AP train. (**D**) The ΔV_m of each recorded cell (circles) and the median, 25th and 75th percentile of the average ΔV_m (min9-10) are shown for CA3 PCs recorded in $CB_1R^{-/-}$ (-4.3, -5.8 and -2.6mV), $CB_2R^{+/+}$ littermates (-4.7, -5.8 to -3.5mV, n=4 from each CB_2R KO strain), $CB_2R^{-/-}$ (0.16, -.87 to 1.1mV) and Syn-$CB_2R^{-/-}$ (0.53, 0.086 to 1.1mV). Kruskal-Wallis with Dunn's post test: P<0.0001 for WT and $CB_1R^{-/-}$ vs. $CB_2R^{-/-}$ and Syn-$CB_2R^{-/-}$. The average ΔV_m of WT vs. $CB_1R^{-/-}$ and $CB_2R^{-/-}$ vs. Syn-$CB_2R^{-/-}$ did not differ significantly. (**E**) The percentage of reactive CA3 PCs is shown for CB_1R KOs (100%), CB_2R WTs (100%), const. CB_2R KOs (0%) and Syn-CB_2R KOs (0%).

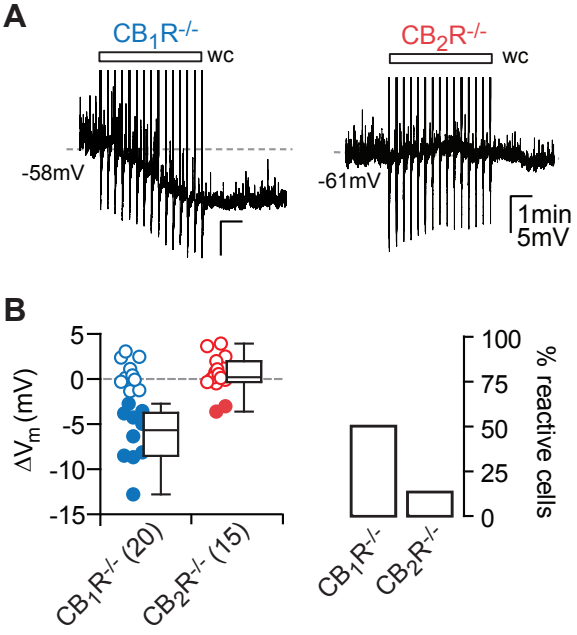

Figure 3.4.2 Whole-cell recordings of CA3 PCs in CB_1R- and CB_2R KO mice. Whole-cell current-clamp recordings from both knockout animal lines confirm the results obtained in pp configuration. (**A**) Exemplary V_m traces of a $CB_1R^{-/-}$ (left) and a $CB_2R^{-/-}$ CA3 PCs (right) recorded in whole-cell configuration. (**B**) Left: summary box plot of the median ΔV_m (with 25th and 75th percentile) for reactive $CB_1R^{-/-}$ CA3 PCs (n(N)=20(5): -5.6, -8.5 and -3.7mV) and all $CB_2R^{-/-}$ CA3 PCs (n(N)=15(3): 0.21, -0.31 and 2mV). Note that the filled circles indicate reactive cells. The V_m of $CB_2R^{-/-}$ CA3 PCs after the induction protocol did not differ significantly from baseline, whereas it did differ significantly for $CB_1R^{-/-}$ (paired t-test: P=0.45 and P=0.007 respectively). Right: the percentage of reactive cells for all recorded $CB_1R^{-/-}$ and $CB_2R^{-/-}$ CA3 PCs (50% vs 13.3%).

To further corroborate the CB_2R-dependency of the mechanism, we used a combined pharmacological and genetic approach. Firstly, we preincubated slices of WT and CB_1R-mutant mice with the cannabinoid inverse agonist AM-251 that prevented an action potential-induced hyperpolarisation in CA3 PCs of both genotypes (recorded in whole-cell configuration, Figure 3.4.3A, left panel). It is of note that in acute slice experiments such as these, AM-251 is commonly used as a CB_1R-specific drug at the concentrations used (2-5µM). However, our experiments in the CB_1R KO mice clearly show that it targets non-CB_1Rs as well. Secondly, we tested the CB_2R-specific inverse agonist SR144528. To circumvent possible issues regarding its specificity, we used slices from $CB_1R^{-/-}$ mice for this experiment in which preincubation with SR144528 successfully blocked the hyperpolarisation in all cells tested (Figure 3.4.3A, right panel).

In summary, the pharmacological blockage of CB_2Rs and the resulting lack of hyperpolarisation reproduced the results of the genetic ablation of CB_2Rs and thus supports these findings (Figure 3.4.3B-C). It is of note that in all whole-cell experiments in which the CBR-dependent hyperpolarisation was abolished (by pharmacological means as well as in the CB_2R KO), we did not observe a transient hyperpolarisation as we did in perforated patch configuration in the CB_2R KO (compare Figures 3.4.3A and 3.4.1B). This further corroborates the finding that the residual transient hyperpolarisation in perforated patch reflects the action-potential induced calcium-dependent AHP that is markedly reduced in the whole-cell configuration.

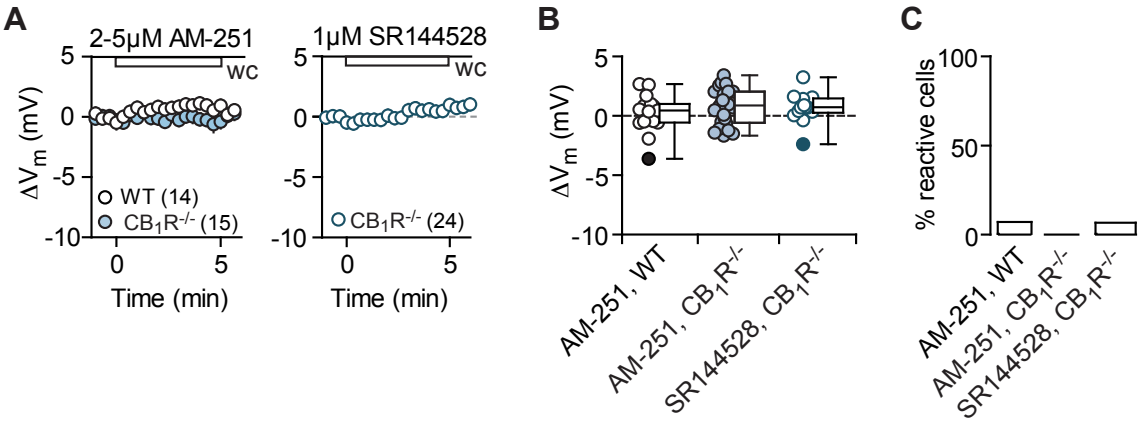

Figure 3.4.3. Cannabinoid receptor antagonists block the hyperpolarisation in WT and CB_1R KO animals. (**A**) Summary time course of the average ΔV_m in response to the action potential stimulus of whole-cell CA3 PCs recordings in slices of WT (n(N)=14(3)) and CB_1R KO mice (n(N)=15(3)) preincubated in 2-5µM AM-251 (left) and slices of CB_1R KO mice preincubated in 1µM SR144528 (right, n(N)=24(3)). (**B**) The ΔV_m of each recorded cell (circles) and the median, 25thand 75th percentile of the average ΔV_m are shown for WT in AM-251 (0.72, 0.27 and 1.5mV), CB_1R KO in AM-251 (0.45, -0.56 and 1mV) and CB_1R KO in SR144528 (0.88, -0.58 and 2.05mV). Note that the filled circles indicate reactive cells. (**C**) The percentage of reactive CA3 PCs is shown for WT in AM-251 (7.1%), $CB_1R^{-/-}$ in AM-251 (0%) and $CB_1R^{-/-}$ in SR144528 (6.7%).

3.5 The long-lasting hyperpolarisation is dependent on the production and release of endogenous 2-AG via the DAGLα pathway

CB_2Rs are activated by most (endogenous) cannabinoids. To assess whether the activity-dependent release of 2-AG – the most ubiquitous endocannabinoid in the CNS that is synthesised and released upon a sufficient rise in intracellular calcium (330) – mediates the plasticity, we recorded from mice lacking the 2-AG-synthesising enzyme DAGLα (in perforated patch configuration). We found that the long-lasting hyperpolarisation was absent in these animals (Figure 3.5.1), thereby establishing that this effect is dependent on action potential-driven 2-AG release. Similar to the perforated patch recordings in CB_2R KO mice (Figure 3.5.2B), a transient hyperpolarisation is present during the induction that slowly recovers after the last action potential train. We again confirmed its independence of cannabinoid receptor activation by preincubating slices from DAGLα-deficient mice with SR144528 where the maximal hyperpolarisation of CA3 PCs (pp, n(N)=5(2)) during the action potential train was the same as in untreated slices (SR155528 treated: 4.7±1.1mV vs. untreated: 5.7±1.1mV, Mann-Whitney test P=0.54). Additionally, to confirm the lack of 2-AG synthesis in the DAGLα KOs, we recorded DSI in CA3 PCs (Figure 3.5.1C-D) since 2-AG has been established as the main endocannabinoid involved in both DSI and DSE (331, 332). In contrast to WT controls, DSI was completely abolished in DAGLα$^{-/-}$ CA3 PCs as measured by the change in amplitude and frequency of spontaneous IPCSs.

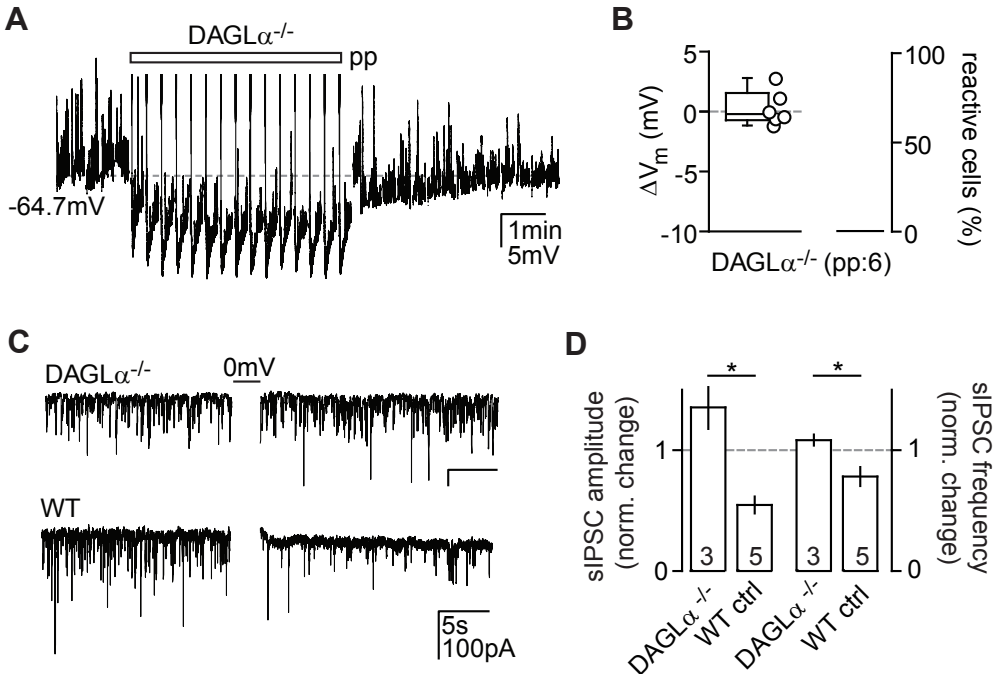

Figure 3.5.1 Lack of the 2-AG synthesising enzyme DAGLα leads to the abolition of the hyperpolarisation. (**A**) Example trace of the V_m response of a DAGLα$^{-/-}$ CA3 PC to the action potential stimulus (rectangle). (**B**) Left: The ΔV_m of each recorded cell (circles) and the median, 25th and 75th percentile of the average ΔV_m are shown for n(N)=6(3) experiments in pp configuration (-0.2, -0.7 and 1.5mV; Wilcoxon matched pairs test: P=0.84 in comparison to baseline). Right: no DAGLα$^{-/-}$ CA3 PC hyperpolarised long-lastingly >-2mV (reactive cells: 0%). (**C**) As a control, sIPSCs were recorded from DAGLα$^{-/-}$ CA3 PCs to test for the presence of DSI that is known to be absent in DAGLα KO mice. Depolarisation of a DAGLα$^{-/-}$ CA3 PC to 0mV for 3x1s fails to induce DSI in that cell (upper trace) in contrast to a DSI-positive WT CA3 PC (lower trace). (**D**) The normalised change in amplitude (left panel) and frequency (right panel) of sIPSCs in DAGLα$^{-/-}$ CA3 PCs (n(N)=3(1): 1.4±0.17 and 1.08±0.05) is significantly different from WT controls (n(N)=5(1)), 0.55±0.07 and 0.78±0.08, Mann-Whitney test: P=0.036 for both). Additionally, the absolute values of amplitude and frequency in the DAGLα KO after DSI induction do not differ from baseline values (Wilcoxon matched pairs test: P=0.25 for both).

3.6 Endocannabinoid release is not affected by the recording condition

Neither DSI nor DSE have been reported to be affected by the recording configuration. Thus, it is likely that the 'washout' we observe is not due to a failure in 2-AG release but due to an interference downstream of receptor binding. To corroborate this hypothesis, we analysed the reduction in frequency of spontaneous EPSPs (as a measure of DSE) in WT CA3 PCs before and after the action potential induction period to test for 2-AG release. We confirmed that the reduction in EPSP frequency was endocannabinoid-mediated by analysing a subset of neurons recorded in slices preincubated with 2µM AM-251. Those cells did not show a reduction in EPSP frequency after the AP train in contrast to CA3 PCs that were recorded without drugs and showed DSE (Figure 3.6.1). Furthermore and most importantly, the induction of DSE was not correlated to the membrane potential hyperpolarisation in whole-cell recordings thus confirming the initial hypothesis.

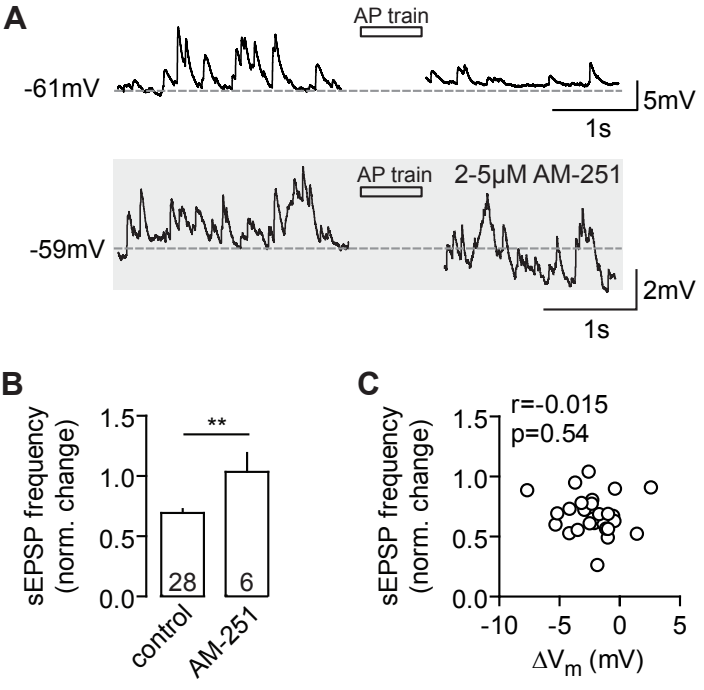

Figure 3.6.1 Whole-cell configuration does not interfere with 2-AG release. (**A**) V_m traces of CA3 PCs recordings from before (left) and after (right) the action potential induction stimulus (black rectangle) in a cell in which DSE was successfully induced (upper panel) and a cell in which DSE was blocked by preincubation of the slice with 2µM AM-251 (lower panel). (**B**) Summary graph of the change in normalised spEPSP frequency for n(N)=28(11) CA3 PCs recorded without drugs (0.68±0.03) and n(N)=7(2) CA3 PCs recorded in 2µM AM-251 (1.03±0.16) (**C**) The change in spEPSP frequency is not correlated to the ΔV_m (Pearson's r: -0.015, P=0.54).

3.7 The activity-induced hyperpolarisation can be mimicked and occluded by cannabinoid receptor agonists

As a further line of evidence supporting the presence of functional CB_2Rs, we tested whether cannabinoid receptor agonists could also directly activate CB_2Rs and thus mimic the action potential induced hyperpolarisation pharmacologically. The mixed cannabinoid receptor agonists 2-AG and WIN, as well as the CB_2R-specific agonist HU-308, all strongly hyperpolarised CA3 PCs in WT mice (Figure 3.7.1A-C/E-F). To confirm that the drug-induced hyperpolarisation is indeed due to CB_2R activation and as a control for the specificity of HU-308 for CB_2Rs at the concentration used, we tested 2-AG and HU-308 in slices of constitutive $CB_2R^{-/-}$ mice. Neither of the drugs led a hyperpolarisation in these animals, strongly arguing for a purely CB_2R-dependent mechanism (Figure 3.7.1D-F). These results also invalidate the concern of a residual action of a truncated CB_2R version still expressed in the Zimmer strain KO (43). In addition, we tested the CB_2R agonist HU-308 in the synapsin-Cre dependent, neuron-specific CB_2R KO and cre-negative (WT) littermates. As expected, we observe a hyperpolarisation in the WT, but not the knockout animals (Figure 3.7.1E).

As already suggested in the previous chapter, the percentage of reactive cells is similar between action potential (48.4% in WT CA3 PCs) and pharmacological induction (56% average of all agonists) of the hyperpolarisation (Figure 3.7.1F). This clearly indicates that the interference in whole-cell configuration occurs downstream of receptor binding.

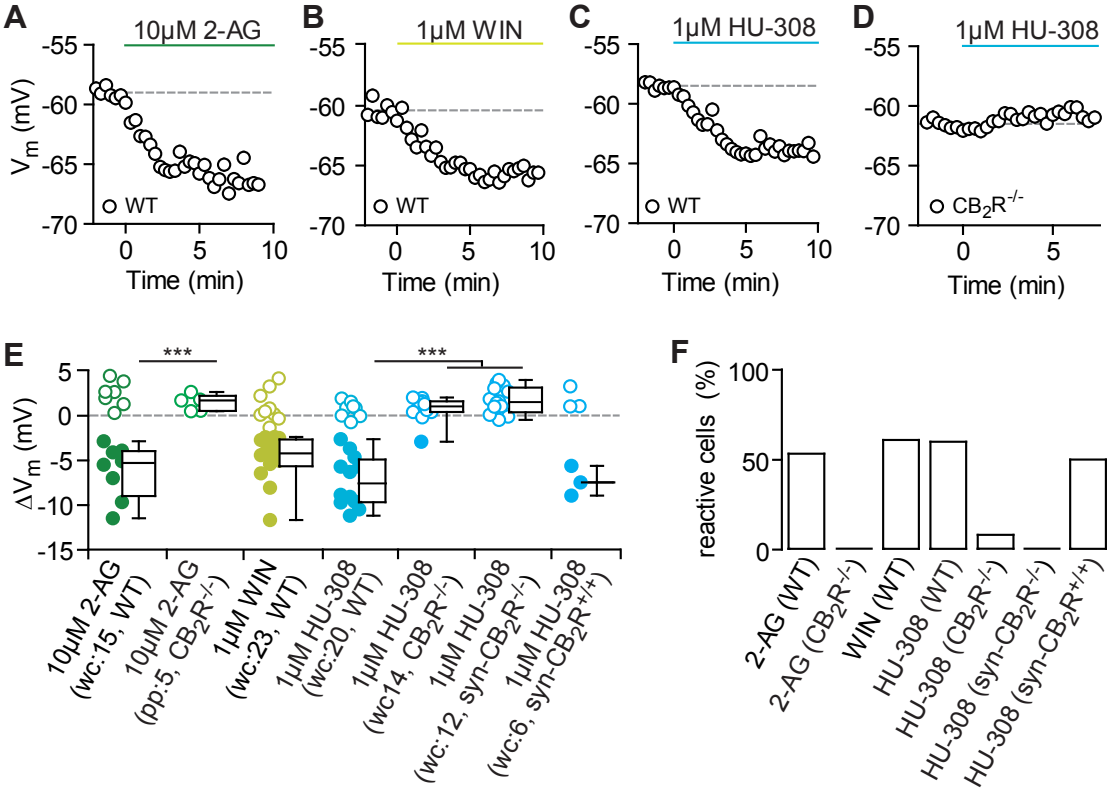

Figure 3.7.1 CB_2R agonists mimic action potential-driven V_m hyperpolarisation. (**A-D**) Exemplary V_m time courses of whole-cell CA3 PC recordings are shown for the application of 10µM 2-AG (A), 1µM WIN (B) and 1µM HU-308 (C) that hyperpolarise CA3 PCs. The hyperpolarising effect of HU-308 is gone in the $CB_2R^{-/-}$ (D). (**E-F**) The ΔV_m of each recorded cell (circles) and the median, 25thand 75th percentile of the average ΔV_m (E) as well as the percentage of reactive cells (F) are shown for the application of 10µM 2-AG in WT (wc, n(N)=15(5): -5.3, -9.0 to -3.9mV; 53.3%) and in $CB_2R^{-/-}$ (pp, n(N)=5(2): 1.6, 0.48 to 2.2mV; 0%), 1µM WIN in WT (wc, n(N)=23(15): -4.2, -5.6 to -2.7mV; 60.9%), 1µM HU in WT (wc, n(N)=20(10): -7.6, -9.7 to -4.9mV; 60%), 1µM HU in $CB_2R^{-/-}$ (wc, n(N)=12(3): 0.91, 0.30 to 1.5mV; 8.3%), 1µM HU in syn-$CB_2R^{-/-}$ (wc, n(N)=14(5): 1.4, 0.27 to 3mV, 0%) and 1µM HU in syn-$CB_2R^{+/+}$ (wc, n(N)=6(4): -7.5, -9 to -5.7mV; 50%). Note that the filled circles indicate reactive cells. Colour code: 2-AG/green, WIN/yellow and HU-308/blue. Kruskal-Wallis with Dunn's post-test: $p<0.05$ for 2-AG and HU-308 in $CB_2R^{-/-}$ vs. WT.

To further substantiate the assumption of a shared CB_2R-dependent mechanism between action potential-dependent release of endogenous 2-AG and exogenously applied cannabinoid receptor agonists, we performed occlusion experiments. To facilitate the analysis of these experiments, we only included cells that hyperpolarised by more than 2mV in response to the first stimulus. When the agonist HU-308 was applied before action potential trains, and also when these stimuli were applied in the reverse sequence, the maximal CB_2R activation via one process occluded the other, as the respective second stimulus failed to elicit an additional hyperpolarisation (Figure 3.7.2). Even though both processes occlude one another, the average hyperpolarisation induced pharmacologically was significantly bigger than the one inducible with action potential trains (Mann-Whitney test: $p<0.05$; compared to whole-cell recordings presented in Figure 3.2.2).

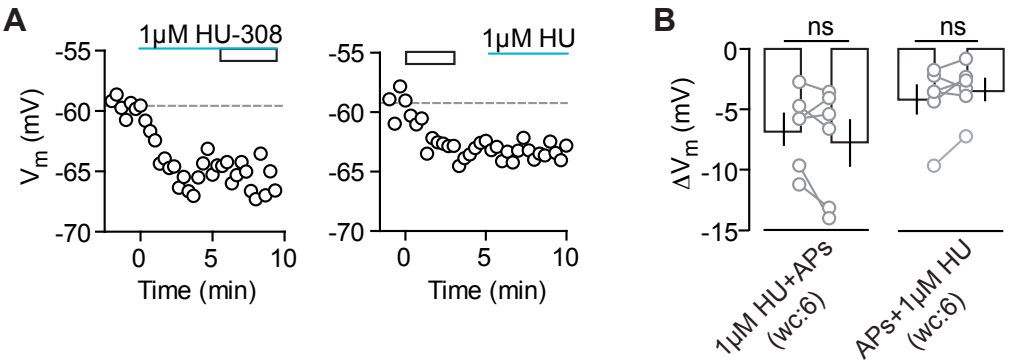

Figure 3.7.2 Occlusion of CB_2R activation. (**A**) Hyperpolarisation by HU-308 (blue line) occludes further hyperpolarisation of CA3 PCs in response to action potentials (black rectangle) and vice versa. Exemplary ΔV_m time course of CA3 PCs that hyperpolarise in response to HU-308 (left) and action potential trains (right). (**B**) Single occlusion experiments (grey circles) and mean±SEM (black) are shown for each condition. Average ΔV_m for HU-308 followed by APs (left, n(N)=6(4): -6.6±1.3 and -7.8±1.9mV, paired t-test: p=0.24) and APs followed by HU-308 (right, n(N)=6(6): -4.2±1.2 and -3.4±0.89mV, p=0.19).

3.8 Further analysis of cell type-specificity

Knowing that CB_2Rs can be activated pharmacologically, we explored the underlying cause of the cell-type specificity of the action potential induced hyperpolarisation in more depth. The latter could be due to a variety of reasons. Firstly, the physiological induction failure could be caused by a different induction threshold. This could, besides others, be due to a) differences in the distance between the site of 2-AG release and CB_2R location, b) differences in the extracellular matrix that may limit diffusion of the endocannabinoid or c) differences in cell morphology that lead to a reduced activation of 2-AG release in CA1 vs. CA3 PCs in response to action potentials. To test for this, we used a theta-frequency burst protocol consisting of four times as many action potentials as the standard protocol (see methods) that is known to trigger eCB-mediated LTD in these cells (333). However, this also failed to induce a persistent hyperpolarisation in CA1 PCs recorded in whole-cell configuration (Figure 3.8.1A-C). Secondly, a cell-type specific expression of CB_2R would explain the lack of effect. To test for this possibility, we bath applied the CB_2R-specific drug HU-308 and the mixed cannabinoid agonist WIN respectively, and recorded the membrane potential of CA1 PCs in whole-cell configuration. We found that both drugs readily hyperpolarise CA1 PCs (Figure 3.8.1D-F) indicating that functional CB_2Rs are present in CA1. In summary, we find that although the expression of CB_2Rs on CA1 PCs is suggested by their successful pharmacological activation, even very strong action-potential stimuli are insufficient to activate them via release of endogenous cannabinoids (Figure 3.8.1G)

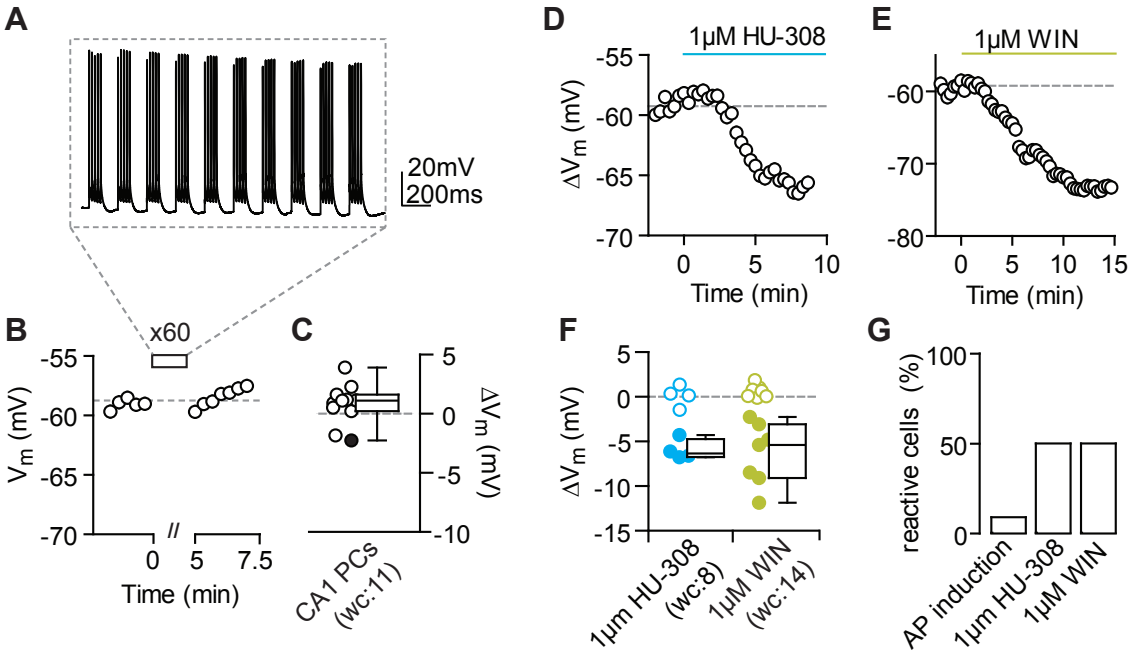

Figure 3.8.1 Stronger AP stimuli fail to hyperpolarise CA1 PCs, whereas pharmacological CB_2R activation induces a V_m hyperpolarisation similar to CA3. (**A-C**) A theta-frequency burst protocol was used to elicit a total of 3000 action potentials in CA1 PCs recorded in whole-cell current-clamp configuration. (A) The first ten bursts in a recorded CA1 PCs are shown that were repeated 60x over 5 min. (B) The complete induction protocol (rectangle) did not induce a long-lasting hyperpolarisation in the same CA1 PC as can be seen in the time plot of its V_m. The V_m during the induction protocol is not included for display purposes. (C) Summary plot of n(N)=11(2) CA1 PCs with a ΔV_m (median, 25th and 75th percentile) of 1.12, 0.22 and 1.63mV (Wilcoxon test: P=0.64 compared to baseline). (**D,E**) Example V_m responses over time of CA1 PCs recorded in whole-cell configuration that hyperpolarised in response to 1µM HU-308 (D) and 1µM WIN (E). (**F**) The ΔV_m of each recorded cell (circles) and the median, 25th and 75th percentile of the average ΔV_m of all reactive cells are shown for n(N)=8(3) CA1 PCs in HU-308 (-6.4, -6.7 and -4.7mV) and for n(N)=14(6) CA1 PCs in WIN (-5.4, -9. and -3.1mV). (**G**) The percentage of reactive CA1 PCs was 9.1% for the theta-burst induction protocol and 50% for both HU and WIN application.

3.9 Acute reversal of the hyperpolarisation by CB_2R inverse agonists

To test for the cause of the persistency of the hyperpolarising response, we acutely applied the CB_2R-specific inverse agonist SR144528 *after* eliciting the hyperpolarisation in CA3 PCs with the standard action potential protocol (in perforated patch configuration). It has been previously shown that antagonists can acutely reverse other forms of long-term plasticity such as mGluR-dependent LTD (334) which is likely to be due to a persistent receptor activation even in an agonist-unbound state (335). We found that late application of SR144528 repolarised the membrane potential back to its baseline levels in all cells tested (Figure 3.9.1C-E), suggesting that constitutive receptor activation is indeed the mechanism underlying the persistency of this particular form of cellular plasticity. As mentioned before in Chapter 3.4, we performed these experiments in CB_1R-lacking animals to eliminate possible off-target effects of the pharmacological agent. We furthermore applied the drug at different time points (5-10min after the induction) to be able to identify and rule out a spontaneous repolarisation of the membrane potential. To have an additional comparison for the longer time period recorded after the induction protocol, we did control recordings in n(N)=5(5) WT CA3 PCs for ›25min (Figure 3.9.1A-B, data also included in Figure 3.2.1).

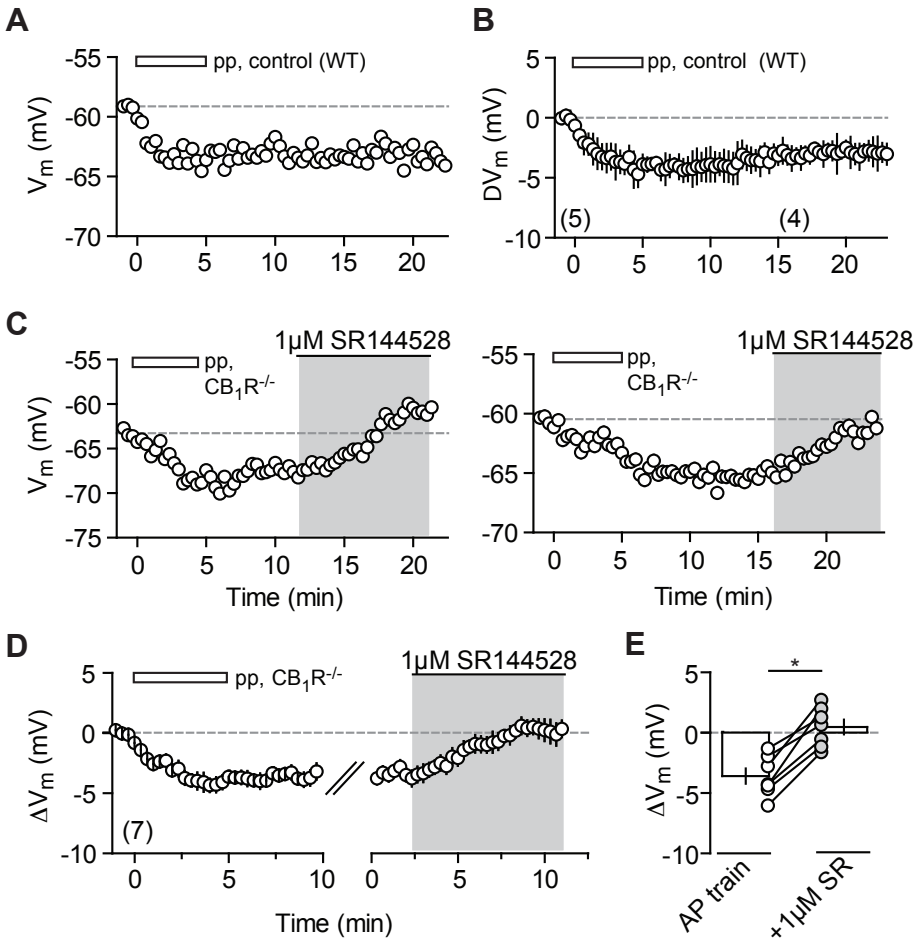

Figure 3.9.1. Wash-in of a CB_2R inverse agonist acutely reverses the action potential-induced V_m hyperpolarisation. Perforated patch recordings of CA3 PCs in CB_1R KO and WT mice show that the V_m hyperpolarisation can be acutely reversed by wash-in of the CB_2R inverse agonist 1µM SR144528. (**A**) Exemplary time plot of the V_m of a WT CA3 PC that was recorded for ›15min post induction (AP train: rectangle). (**B**) Summary time plot of the average ΔV_m from n(N)=5(5) WT CA3 PCs. At min15-20 the ΔV_m is still significantly different from baseline (-3.07±0.29mV; paired t-test: p‹0.05). Note that this data is also included in Figure 1. (**C**) Exemplary recordings of CB_1R-lacking CA3 PCs in which SR144528 (grey) was washed in at different time points after the induction. (**D**) Summary time plot of n(N)=7(6) experiments in CB_1R KOs. (**E**) Before-after plot of each experiment showing the maximal ΔV_m after the AP train and the average ΔV_m of 10-15min after wash-in of SR144528. The mean ΔV_m is -3.6±0.63mV after the AP train is significantly different from the mean ΔV_m after the SR144528 application (0.48±0.62mV; Wilcoxon matched pairs test: P=0.016). Furthermore, the V_m in SR144528 does not differ from the V_m baseline values (Wilcoxon matched pairs test: P=0.47).

3.10 Mechanism underlying the hyperpolarisation – a G Protein-dependent, calcium-sensitive and conductance-independent process

Given that with both action potential-driven and pharmacological induction ~50% of cells were observed to be reactive in whole-cell configuration, it seems feasible that intracellular/single-cell manipulations could be used to further investigate the underlying molecular mechanism. We performed control experiments with normal intracellular solution to ensure that a ≥5min baseline period after break-in, to allow sufficient perfusion of the intracellular solution would not lead to a complete washout of hyperpolarisation in these experiments per se. These controls with HU-308 bath application were not different from the other WT whole-cell recordings (Mann-Whitney test: P=0.5, 58% reactive cells, ΔV_m: -4.3, -13.7 and -3.3mV, this data is included in Figure 3.7.1). We thus conclude that the intracellular manipulations are indeed practicable.

To confirm and extend our finding that neuronal, G Protein-coupled CB_2Rs are responsible for the hyperpolarisation, we performed experiments with 0.5mM GDPßS in the intracellular solution. GDPßS is a non-hydrolysable GDP analog that blocks G protein-coupled activity. Its inclusion into the pipette abolished the pharmacologically induced hyperpolarisation within the manipulated neuron, supporting the idea of a cell-intrinsic, G Protein-dependent mechanism (Figure 3.10.1A,D-E).

As mentioned in Chapter 3.2, we noticed that KGluconate abolished the hyperpolarisation which hints towards an involvement of calcium. We thus explored the role of this second messenger by intracellular application of 30mM BAPTA to block calcium-dependent signalling cascades. Interestingly, not only the action potential-induced hyperpolarisation was absent but the also the hyperpolarisation following pharmacological activation of CB_2Rs by the agonist HU-308 (Figure 3.10.1B-E). Note that the two remaining reactive cells for the application of HU-308 with intracellular GDPßS and BAPTA respectively are most likely due to an insufficient perfusion of the cell given the short incubation of 5min. Usually, experiments requiring intracellular perfusion are allowed a baseline period of 30min, which we shortened to prevent washout.

In summary, these experiments indicate that the cascade downstream of receptor activation is a) a G Protein-dependent step as indicated by the GDPßS experiments and b) crucially dependent on calcium signalling as shown by the calcium-chelating experiments with BAPTA.

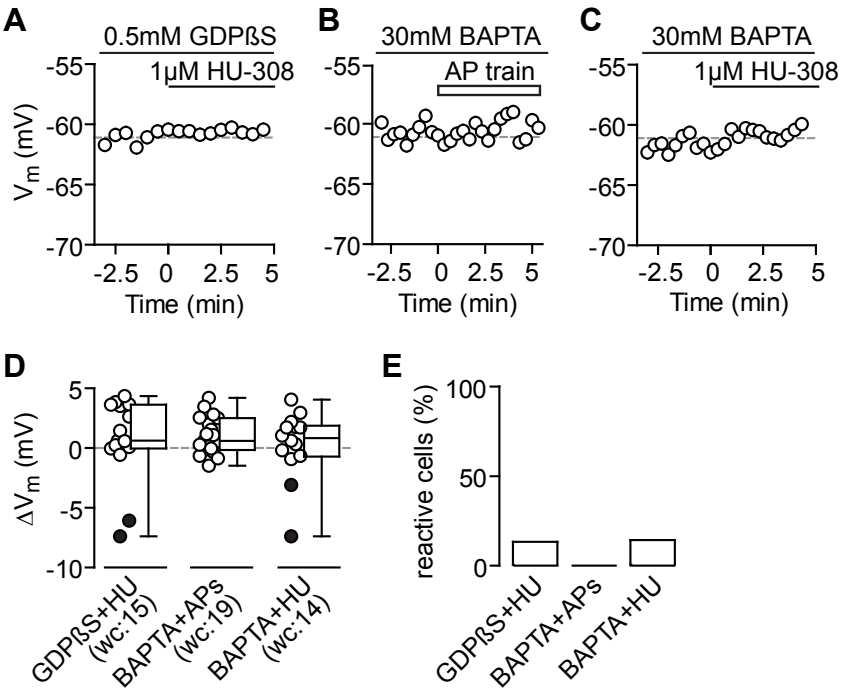

Figure 3.10.1 Intracellular manipulations support a G Protein-dependent and Ca^{2+}- sensitive mechanism under-lying the CB_2R-dependent plasticity. (**A-C**) Exemplary ΔV_m time courses of whole-cell CA3 PC recordings in which the respective cell was perfused with 0.5mM GDPßS (A) or 30mM BAPTA (B-C) via the intracellular solution for ≥5min. The subsequent application of 1µM HU-308 or the action potential stimulus (as indicated) fails to hyperpolarise the CA3 PCs. (**D-E**) The ΔV_m of each recorded cell (circles) and the median, 25th and 75th percentile of the average ΔV_m (D) as well as the percentage of reactive cells (E) are shown for GDPßS+HU-308 (n(N)=15(5): 0.62, -0.037 and 3.6mV; 13.3%), BAPTA+APs (n(N)=19(9): 0,6, -0.15 and 2.5mV; 0%) and BAPTA+HU-308 (n(N)=14(5):0.84, -0.71 and 1.9mV; 14.3%). Reactive cells are indicated by filled black circles.

Cannabinoid receptors, as many other neuronal GPCRs, couple to GIRK channels (254, 336) which at a first glance appear as a likely downstream target of CB_2R activation to mediate the hyperpolarisation via an extrusion of potassium from the cell. When analysing the input resistance of WT CA3 PCs (recorded in whole-cell configuration) after the action-potential stimulus we found that it was indeed persistently reduced (R_{in} normalised to baseline: 0.82±0.023). However, this was also the case when cannabinoid receptors were blocked with 2-5µM AM-251 and is thus unrelated to the hyperpolarisation (R_{in} normalised to baseline: 0.81±0.059, t-test: P=0.96 compared to WT CA3 PCs without drug preincubation). It is very likely that the action potential trains elicit an additional, conductance-based long-term plasticity that confounds the analysis of the input resistance in this set of experiments. We thus focused on the pharmacologically induced hyperpolarisation, for which we observed no change in input resistance simultaneous to the hyperpolarisation (Figure 3.10.2A-B). As a control for a GPCR-dependent activation of GIRK, we recorded from CA3 PCs and applied 1µM Adenosine that is known to act on adenosine receptors that in turn activate GIRK. As expected for a conductance-based mechanism, we find a significant reduction of the input resistance that is furthermore reversed the GIRK antagonist SCH23390 (Figure 3.10.2B). In contrast to this, the acute application of SCH23390 failed to repolarise the membrane potential of CA3 PCs after the successful induction of the hyperpolarisation by both action potential dependent release of 2-AG and pharmacological CB_2R activation (Figure 3.10.2C). To conclude, this set of experiments strongly argues against a conductance-based process and the involvement of GIRK channels in the hyperpolarisation.

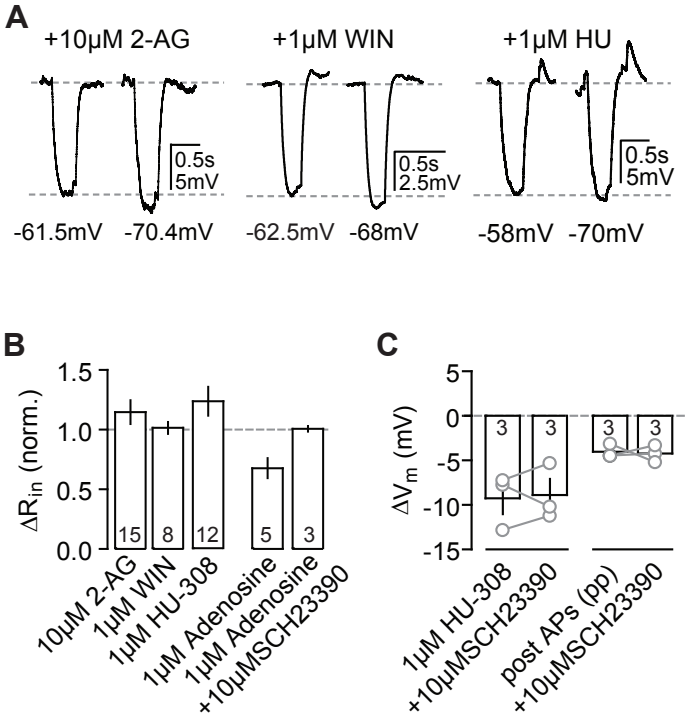

Figure 3.10.2 The hyperpolarisation is not accompanied by a change in R_{in} and is not mediated by a GIRK-conductance. (**A**) Exemplary V_m traces of CA3 PCs recorded in current-clamp/whole-cell configuration that hyperpolarised in response to 10µM 2-AG (left), 1µM WIN (middle) and 1µM HU-308 (right panel). The R_{in} was calculated from the steady-state response to a -80pA test pulse that was applied every 20s. In each panel, the left trace represents the baseline condition (1min before agonist application) and the right trace is taken from 5-10min after the drug was bath applied. The respective V_m values are indicated below each trace. (**B**) Summary bar graph of all reactive cells (›-2mV hyperpolarisation) showing the normalised ΔR_{in} (mean±SEM) after drug application for 10µM 2-AG (n=8: 1.1±0.1), 1µM WIN (n=14: 1.01±0.05) and 1µM HU-308 (n=12: 1.2±0.12) that do not differ significantly from baseline levels (paired t-test for 2-AG, WIN and HU-308: P=0.30, 0.99 and 0.12). Additionally, as a control, the relative change in R_{in} in response to 1µM Adenosine (n(N)=5(2): 0.67±0.08) is shown that was reversed by the application of 10µM SCH23390 (1.01±0.02). (**C**) Acute application of 10µM SCH-23390 does not reverse the agonist- or AP-induced hyperpolarisation and thus excludes the involvement of GIRK channels. Left: single experiments (grey circles) and mean±SEM of n(N)=3(2) whole-cell recordings showing the ΔV_m in HU and after SCH23390 application (-9.3±1.8/-8.9±1.8mV, paired t-test: P=0.82). Right: single experiments (grey circles) and mean±SEM of n(N)=3(2) pp recordings showing the ΔV_m after AP induction and with subsequent SCH-23390 application (-4±0.45/-4.2±0.54mV, paired t-test: P=0.83).

3.11 Comparison of CB_2R- vs presynaptic endocannabinoid-mediated effects

Do CB_2Rs also modulate known endocannabinoid-mediated alterations of presynaptic function and does the hyperpolarisation have similar characteristics? DSI has been shown to be a mechanism that acts in an auto- *and* paracrine manner (4). To test if the action potential-driven release of 2-AG by one neuron is sufficient to elicit a hyperpolarisation in neighbouring neurons, we performed dual perforated patch recordings of adjacent CA3 PCs (distance between pipette tips: 11±1.2µm) and found no evidence for a detectable 'spread' of the effect between principal cells (Figure 3.11.1). As a control in addition to recording the 'test' cell in perforated patch to ensure it ability to hyperpolarise, the initially unstimulated cell was brought to spiking after a second baseline period in three experiments and hyperpolarised in all cases (-4.4±0.51mV).

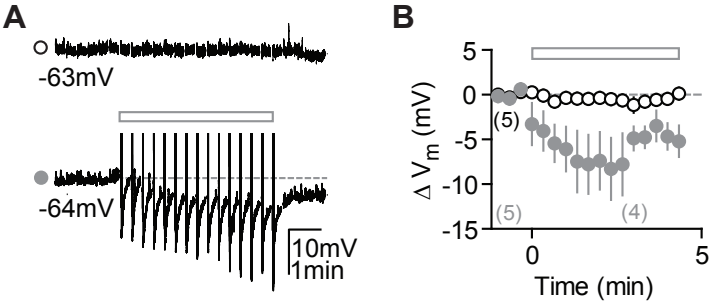

Figure 3.11.1. No detectable spread of hyperpolarisation between neighbouring CA3 PCs. Dual recordings indicate that endocannabinoid release triggered by one cell does not affect the membrane potential of adjacent cells. (**A**) exemplary simultaneous perforated patch recording of two CA3 PCs. Action potential firing in the control cell (lower trace) elicits a hyperpolarisation in the same, but not in the other cell (upper trace). (**B**) In 5 out of 5 recordings (N=5) the control cell hyperpolarised in response to the action potential trains (filled grey circles, ΔV_m: -6.0±1.5mV), whereas the unstimulated cell did not (open black circles, ΔV_m: 0.024±0.63mV).

Furthermore, contrary to DSI and DSE, the hyperpolarisation is independent of synaptic transmission (Figure 3.11.2). In addition to the block of GABAergic transmission as done in most experiments, we blocked glutamatergic synaptic transmission by blocking both AMPA- and NMDA receptors with 10µM NBQX and 25µM D-AP5 respectively. The hyperpolarisation was unchanged under these conditions.

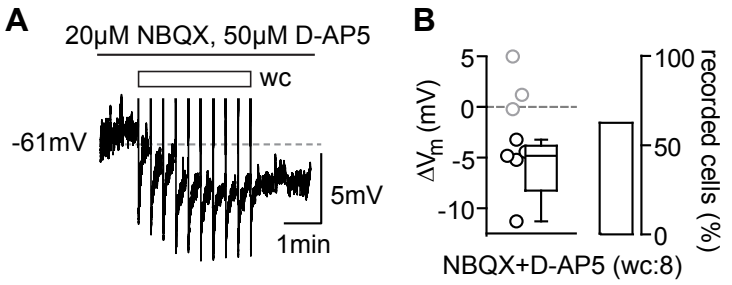

Figure 3.11.2. The hyperpolarisation is independent of synaptic transmission. The continuous block of glutamatergic (20µM NBQX, 50µM D-AP5) as well as GABAergic (1µM Gabazine, 1µM CGP) transmission does not abolish the AP-induced hyperpolarisation. (**A**) Example wc recording of a reactive CA3 PC in response to the AP train (rectangle). (**B**) The ΔV_m of each recorded cell (circles) and the median, 25th and 75th percentile of the average ΔV_m of all reactive cells is shown for n(N)=8(2) experiments (-4.8, -8.3 and -3.8mV; left panel). The percentage of reactive cells is 62.5% (right panel).

Finally, we did not find evidence for a participation of CB_2Rs in 'classic' presynaptic endocannabinoid-mediated effects. To test whether pharmacological CB_2R activation could mimic DSI, we recorded eIPSCs in CA3 PCs in whole-cell voltage-clamp mode and induced DSI by depolarisation of the recorded neuron. Cells were defined as DSI-positive when the reduction in eIPSC amplitude in response to the depolarisation exceeded 15%. Conversely, subsequent application of 1µM HU-308 did not alter the eIPSC amplitude of DSI-positive neurons (Fig. 3.11.3A). Additionally, the reduction of fEPSPs (recorded in CA3), observed upon application of the mixed endocannabinoid agonist WIN, which is ascribed a presynaptic mode of action (303, 337), could not be mimicked by HU-308 (Fig. 3.11.3B). To conclude this chapter, the hyperpolarisation appears to be a solely self-regulatory mechanism that acts complementary to presynaptic CBRs and independent of synaptic transmission.

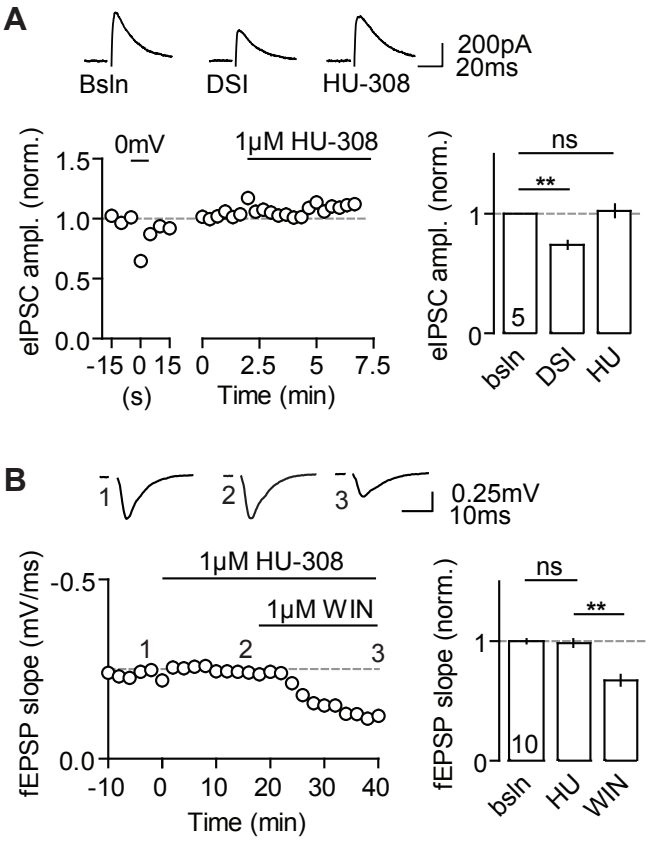

Figure 3.11.3. CB_2R agonists cannot mimic CB_1R-mediated depression of synaptic transmission. (**A**) HU-308 has no effect on DSI-positive eIPSCs. Left: example recording of a CA3 PC (whole-cell). Depolarisation of the neuron results in a transient reduction of eIPSC amplitude, whereas bath application of HU does not. Right: mean normalised eIPSC amplitudes of n(N)=5(4) experiments for DSI (0.74±0.034) and HU-308 application (1.02±0.054) in comparison to baseline (paired t-test: P=0.0016 and P=0.67). (**B**) WIN, but not HU-308, suppresses evoked field responses in CA3. Left panel: exemplary fEPSP recording with HU-308 and WIN bath application. Right panel: mean normalised fEPSP slopes for HU (0.98±0.033) and WIN (0.67±0.046) in comparison to baseline (paired t-test: P=0.33 and p<0.001).

3.12 Physiological stimulation and functional significance of CB_2R activation

In stark contrast to the so far employed induction stimulus which is an artificial, fixed-frequency action potential train, both the frequency and amount of neuronal spiking in vivo are irregular, highly variable and temporally complex (338). We thus considered whether physiologically relevant activity patterns are able to induce the hyperpolarisation, too and constructed a spike train based on in vivo place field recordings in rat (see methods). We applied the physiological spike train to rat CA3 PCs and found that it elicited a hyperpolarising change in the membrane potential that did not differ from the one induced by the standard protocol (unpaired Student's t-test: P=0.42; Figure 3.12.1A-D). As a control, we additionally confirmed that the standard induction protocol also induces a hyperpolarisation in rat CA3 PCs. As expected, tha protocol induces a hyperpolarisation that is comparable to the hyperpolarisation observed in mouse CA3 PCs (Figure 3.12.1C-D, unpaired Student's t-test; P=0.59 in comparison to the whole-cell data present in Figure 3.2.2).

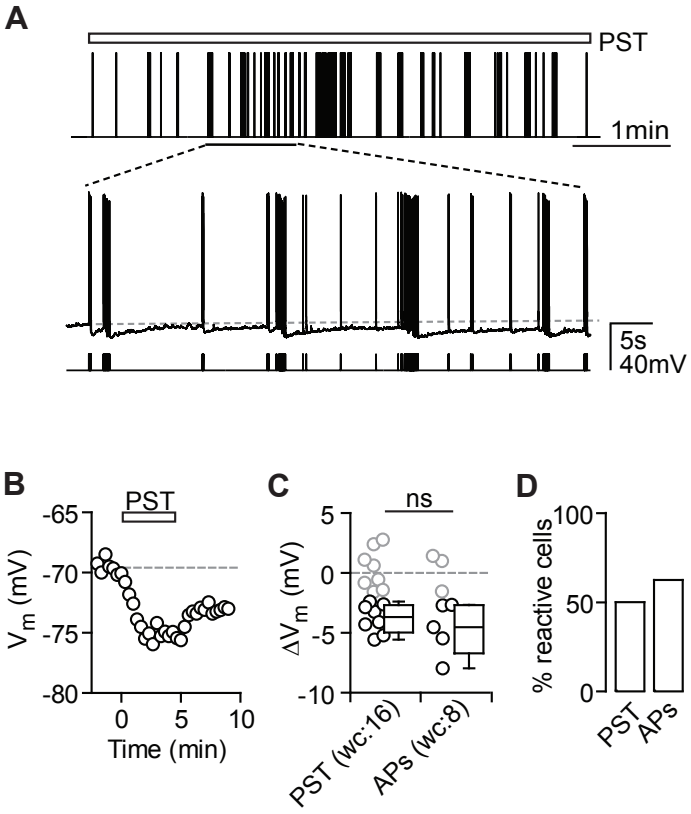

Figure 3.12.1 Physiological activity patterns induce hyperpolarisation in rat CA3 PCs. (**A**) Graphic illustration of the presented physiological spike train (PST, upper panel) as well as a segment of an exemplary V_m trace of a rat CA3 PC that fires in response to the respective stimuli (lower panel). (**B**) Time plot of the V_m of the same CA3 PC responding to the PST (rectangle) with a long-lasting V_m hyperpolarisation. (**C**) The ΔV_m of each recorded cell (circles) and the median, 25th and 75th percentile of the average ΔV_m of reactive rat CA3 PCs recorded in response to the PST (n(N)=16(6): -4.5, -6.7 and -2.7mV) and the standard action potential protocol (APs, n(N)=8(3): -3.7, -5 and -2.7mV) recorded in whole-cell configuration and at resting V_m. The average ΔV_m did not differ between PST and AP (Mann-Whitney test: P=0.52). (**D**) Percentage of reactive cells for PST (50%) and APs (62.5%).

Finally, we assessed the functional significance of CB_2R activation on both a single cell and (local) network level in vitro and in vivo. CA3 PCs are known to spike frequently when recorded in vivo, both as single spikes and in bursts (96), and we showed that physiological activity patterns are sufficient to induce the hyperpolarisation (see above). We thus investigated the change in spike probability of synaptically evoked action potential firing in CA3 PCs before and after the activation of CB_2Rs by the specific CB_2R agonist HU-308. In those cells that hyperpolarised (whole-cell: 5 out of 8 reactive cells) we find a simultaneous, robust reduction in spike probability by over 80% (Figure 3.13.2). To test whether this was causally linked to the membrane potential hyperpolarisation induced by the CB_2R agonist, we "clamped" the cells to their initial baseline membrane potential with constant current injection at the end of each experiment. As expected, this was sufficient to restore the initial spike probability in all neurons (0.93±0.04, normalised to 1). Conversely, when we manually hyperpolarised the unreactive cells with current injections (n=3, baseline V_m: -64.7±0.77mV, hyperpolarised V_m: -72.5±0.5mV, ΔV_m: -7.7±-0.26mV) we were able to mimic the reduction in spike probability induced by the CB_2R agonist-mediated hyperpolarisation (0.1±0.036, normalised to 1). In summary, these experiments indicate that the membrane potential hyperpolarisation following activation of CB_2Rs significantly shifts the spiking threshold of CA3 PCs to more negative values and thus profoundly reducing their input/output function.

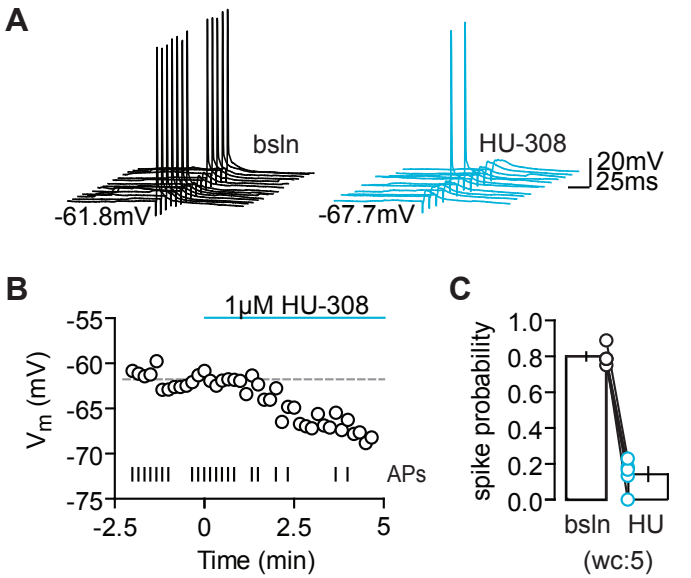

Figure 3.12.2 Activation of CB_2Rs reduces spike probability in CA3 PCs. (**A**) The spiking probability of a CA3 PC in response to the application of the CB_2R agonist HU-308. Example traces show spikes elicited by synaptic stimulation during baseline conditions (black) and 5min after agonist application (red). The V_m values are indicated below the traces. (**B**) Time plot the V_m (circles) of the same cell and its AP firing (lines) for each given V_m. (**C**) Summary graph of the spike probability for n(N)=5(3) reactive cells under baseline and agonist conditions (0.8±0.02 and 0.14±0.038 respectively, normalised to 1). The change in spike probability was accompanied by a mean V_m hyperpolarisation of -6.3±0.3mV. Recordings were performed in whole-cell configuration.

In a next step we thus asked whether CB_2R activation will have any effects on network function in vivo. To this end, we implanted mice with wire arrays that allow to extracellularly record the LFP and ongoing population (network) activity in the area of interest. We were interested in theta (5-10Hz) and gamma oscillations that occur during exploratory behaviour in area CA3, and recorded the local LFP in CA3 while the animals were exploring freely in an open arena, before/after the application of the CB_2R agonist HU-308. Gamma and theta power and frequency per se were not changed (data not shown). Instead, we found a selective change in the theta-dependent modulation of locally generated, slow (30-85Hz) gamma oscillations after the pharmacological activation of CB_2Rs with 10mg/kg HU-308 diluted in DMSO and injected i.p. (Figure 3.12.3). Intermediate gamma oscillations (60-120Hz) were not affected. As a control, we injected the same concentrations of the vehicle DMSO with which we did not observe any changes in either frequency band.

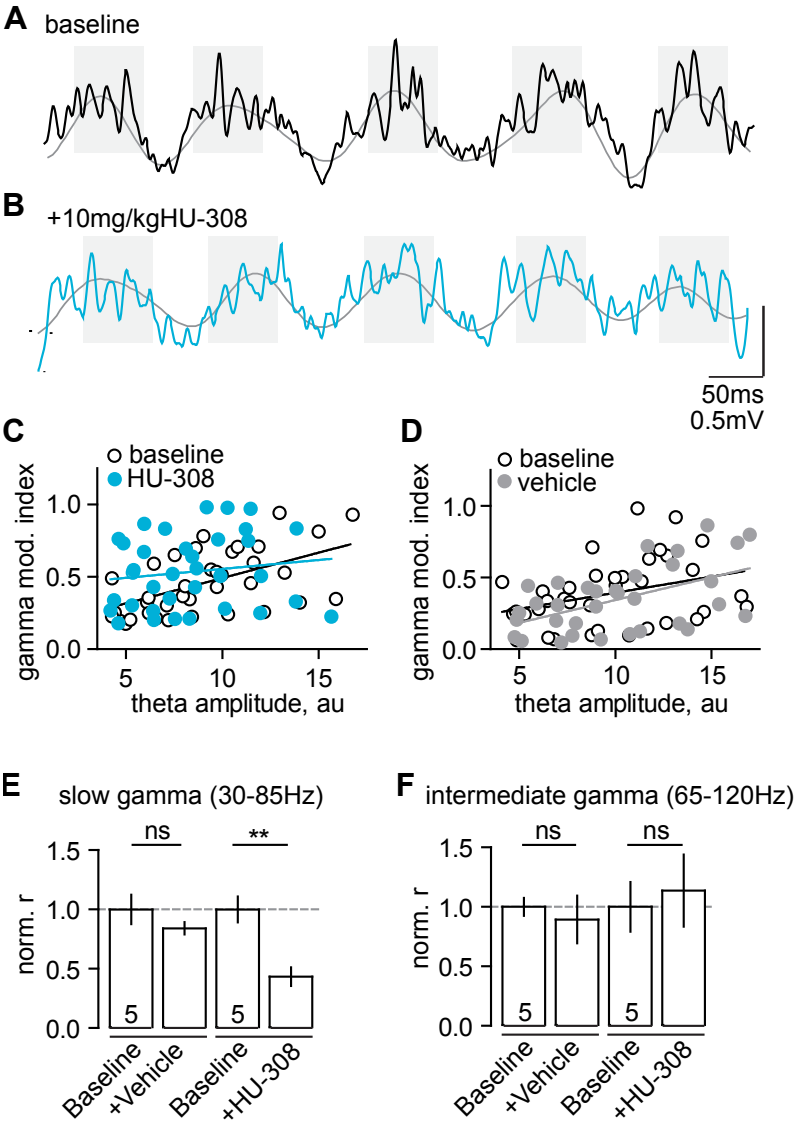

Figure 3.12.3. Altered coupling of slow gamma (30-85Hz) and theta (5-10Hz) oscillations after CB_2R agonist application. (**A-B**) Representative signal traces of the local field potential (1-150 Hz band-pass filtered) recorded in the stratum pyramidale of the CA3 area during exploratory behaviour before (A) and 30min after (B) the i.p. administration of the CB_2R agonist HU-308 (10mg/kg). (B) Note that the typical association of high amplitude gamma oscillations with theta oscillation peaks (grey shades) and low amplitude gamma oscillations with theta oscillation troughs is altered after the CB_2R agonist administration. (**C-D**) Changes of gamma amplitude - theta phase coupling index as a function of theta amplitude and the respective population linear regression lines are shown for slow gamma oscillations. (C) Baseline vs. post-vehicle administration (n(N)=5(5), p=0.0473 and p=0.0019 respectively), (D) baseline vs. post-agonist administration (n(N)=5(4), p=0.0004 and p=0.42 respectively). (**E-F**) Average z-transformed correlation coefficients (r, normalised to baseline) quantifying the association of the gamma amplitude - theta phase coupling index with theta oscillations amplitude. (E) Slow gamma: 0.84±0.05, post-vehicle; 0.43±0.08, post-agonist; p=0.34 and p=0.002 respectively (two-way repeated measures ANOVA (treatment x drug), interaction: $F(1,8)=6.29$, p=0.037, followed by Bonferroni post-hoc tests); (F) intermediate gamma (65-120 Hz): 0.89±0.2, post-vehicle; 1.14±0.3, post-agonist; $F(1,8)=1.216$, p=0.3. Data are presented as mean±SEM, **: p<0.01.

4 Discussion

Neuronal CB_2Rs have been reported to be modulated during a variety of complex neuropsychiatric disorders including depression, schizophrenia and autism spectrum disorders (14) and, due to their non-psychotropic mode of action, are considered promising therapeutic targets (339). Yet little is known about their role in basic neurotransmission. Our findings now reveal a novel role for CB_2Rs in the CNS that challenges the classic, CB_1R-focused view on endocannabinoid function. We provide a first description of CB_2Rs in area CA3 of the hippocampus which may serve as a basis for further studies regarding its role in physiological and pathophysiological network states.

In the following, I will discuss our findings in a bottom up approach. Firstly, I will discuss the cellular/molecular results presented in this thesis in order to elucidate the mechanistic details of the phenomenon in respect to single cell physiology. Secondly, I will then focus on the functional importance of our finding and, in an attempt to conceptually embed our results into a greater contextual framework, ask the following questions: How may CB_2Rs contribute to the fine-tuned, highly complex endocannabinoid neuromodulatory system that controls a single neuron's physiology and excitability from presynaptic transmitter release to spike output? In what way is this activity-dependent, cell-autonomous negative feedback signal suited to influence an active circuit of connected excitatory and inhibitory cells? What would its implications be for area CA3 that integrates a multitude of local, long-range and multiplexed signals and how could we test our predictions? In addition to their function in the healthy brain, CB_2R (dys-)function has been implicated in many complex neuropsychiatric diseases. Lastly, I will thus discuss the role of and evidence for CB_2R (dys-)function in pathophysiological brain states, and their potential as a pharmacological target before giving a general outlook of possible future studies exploring the role of CB_2Rs in the hippocampal formation.

4.1 Cellular analysis of CB_2 receptors in hippocampal principal cells

4.1.1 Characterisation of hippocampal cell types

Most neurons in the hippocampal formation display distinct characteristics that allow a classification based upon their electrophysiological properties, location, morphology and somatic/dendritic orientation. For this study, which focuses solely on principal cells of the hippocampal formation, it was necessary to identify and exclude INs from the analysis that constitute about 10% of cells in the hippocampal formation (340). For example, the most numerous inhibitory INs found in the hippocampus – fast-spiking PV+ BCs – can be distinguished very reliably based on their non-adapting high firing rate (≥400Hz) that is due to the expression of K_V3-like delayed-rectifier potassium channels and that CA3 PCs lack or only express at very low levels (341). Furthermore PV+ BCs have a distinctly low input resistance, lack (somatically detectable) I_h-current and have characteristically fast decaying spontaneous EPSPs. The latter results from the differential expression of AMPAR subunits: in contrast to CA3 PCs, BCs lack the GluR2 subunit which renders their AMPARs calcium permeable but express GluR4 which additionally endows them with fast decay kinetics (341–343). It is thus feasible to exclude these cells by electrophysiological characterisation based on somatic current injections and "online analysis" of their spontaneous inputs. Similarly, other classes of INs can be excluded based on spike shape/threshold/adaptation, resting membrane potential, input resistance, I_h and AHP. Thus, even though we have no morphological reconstructions of the neurons included for analysis in this thesis (except for CA2 PCs) we can be confident that the majority of recorded cells constitute the respective hippocampal principal cell population. Conversely though, it is important to acknowledge the fact that especially CA3 PCs are highly diverse and do not represent a homogenous cell population. For example, their firing patterns range from regular-spiking to bursting (127), and their input resistances and the frequency of spontaneous inputs can vary dramatically (own observations). Which of these characteristics, that depend on intrinsic parameters such as morphology and underlying ionic currents, are "hardwired" and which reflect differences in previous activity respectively is not clear and it is likely a mixture of both (96, 127, 344). In contrast to CA3 PCs, CA1 and DG principal cells exhibit a very homogenous firing pattern and are easily identified. Generally, the remarkable differences of both passive and active properties between the hippocampal principal cell populations hint towards their fundamentally different roles in information processing within the hippocampus. How this difference may be further augmented by the cell-type specificity of the here described plasticity mechanism will be discussed in chapter 4.1.6.

4.1.2 Basic features of the CA3-specific hyperpolarisation

The CB_2R-dependent membrane potential hyperpolarisation that we observe in CA3 and CA2 PCs can be triggered via the endogenous release of 2-AG or by direct pharmacological receptor activation. The hyperpolarisation is approximately 5-10mV in size (depending on its mode of activation, see chapter 4.1.3) and long-lasting (›20min). Because it is persistent in its nature and is additionally independent of excitatory and inhibitory synaptic transmission, it appears to be an intrinsic plasticity

process that negatively modulates the excitability of CA3 PCs. A potassium conductance as the effector suggests itself given that many types of K_V-mediated intrinsic plasticity have been described (see p18). Surprisingly though, the hyperpolarisation is *not* accompanied by a change in membrane resistance which rules out the involvement of a conductance-based mechanism and suggests the involvement of an ion pump or ion co-transporter. Experiments with intracellular application of GDPßS and the calcium chelator BAPTA indicate that the cascade downstream of receptor activation involves a G Protein- and calcium-triggered cascade. Yet, the final target causing the inhibitory plasticity remains to be identified. The cause of the persistency on the other hand could be identified: the acute application of a CB_2R antagonist reversed the action potential-triggered hyperpolarisation, arguing for a persistent receptor activation. The synapsin-Cre dependent CB_2R KO provides a unique tool to provide evidence of the neuronal localisation of CB_2R, which is strengthened by additional data sets (GDPßs, dual recordings of neighbouring cells). A comparison to classic, CB_1R-dependent actions of endocannabinoids suggests that postsynaptic CB_2Rs act complementary to presynaptic CB_1Rs. Finally, the in vivo and in vitro analysis of the functional significance of CB_2Rs shows that they significantly impact the output of CA3 PCs and alter locally generated network oscillations in vivo.

4.1.3 CB_2Rs are expressed in CA3 PCs: verification with multiple levels of controls

What are the controls we performed that allow us to formulate these statements? First, we provide extensive pharmacological and genetic evidence for the involvement of CB_2Rs and additionally validate all KOs with pharmacological controls[18]. For example, while mixed and specific CB_2R agonists were still effective in the CB_1R KO, they did not elicit a hyperpolarisation in the constitutive nor the synapsin-Cre CB_2R KOs which also strongly argues for a *neuronal* localisation of the receptor. Vice versa, even though CB_2R agonists were still fully functional in the CB_1R KO, we controlled for the absence of CB_1R-mediated effects to eliminate possible compensatory effects which is an important control given that CB_2Rs have been shown to be able to assume the presynaptic function of CB_1Rs if overexpressed in autaptic cultures of CB_1R KO (236). To test this, we recorded evoked fEPSPs and applied the CBR agonist WIN that has been shown to reduce the amplitude and slope of the fEPSP in a CB_1R-dependnet manner. While the effect was absent in the KO, it was fully intact in control WT animals (data not shown). The lack of residual 2-AG signalling in the DAGLα KO animals was confirmed by the absence of DSI in DAGLα-lacking CA3 PCs (see figures 3.5.1-3.8.1). 2-AG levels in the DAGLα KO have been reported to only be decreased by 80% (289) which is most likely due to the remaining activity of DAGLß whereas anandamide levels are increased in some brain areas. Because DSI has been shown to depend solely on 2-AG release (204, 331, 345), this was a crucial control to validate the KO. To test that the action potential-driven and pharmacological hyperpolarisation were mediated by the same downstream target receptor we performed occlusion experiments. Because the physiological activation of CB_2Rs occluded their pharmacological activation and vice versa, it seems highly likely that the same target receptor is activated in both stimulation paradigms. Furthermore we could block the action potential-induced hyperpolarisation with CB_2R-specific antagonists in both WT and CB_1R KO animals. To compare CB_2Rs to presynaptically expressed CBRs, we used CB_1R-dependent phenomenon as controls. Both DSI and the CB_1R-induced reduction in fEPSP amplitude could not be mimicked by CB_2R agonists and were always induced at the end of *each* experiment after the application of the CB_2R agonist as a positive control. The intracellular manipulations we employed were particularly vulnerable to artefacts, given the induction failure rate of approximately 40-50% in whole-cell experiments. We thus performed control experiments in which we applied the CB_2R agonists after a baseline period of >10min. The loss of effect was similar to shorter baseline periods and we thus concluded that intracellular manipulations were feasible. Finally, for the in vivo recordings, we used DMSO-only injections to control for its possible off-target effects. The desirable control however would be to use the neuron-specific CB_2R KO which would also uncover off-target effects of the i.p.-administered HU-308.

In addition to the combined genetic and pharmacological evidence of neuronal CB_2R mediating the hyperpolarisation, other potential downstream targets can be ruled out by (published) experimental evidence: GPR55 is not sensitive to WIN (222), TRPV1 is not sensitive to AM-251 (and would depolarise the cells) (223), activation of intracellular CaCCs would similarly depolarise the cell (17)[19], inhibition of N_V channels by endocannabinoids is not sensitive to AM-251 (258) and finally, the experiments in the CB_1R KO certainly rule out to the involvement of CB_1Rs. To summarise, our data very strongly hints towards a necessary role of CB_2Rs in this phenomenon because their functional presence is a critical requirement for the hyperpolarisation to occur.

18 | The CB_2R KO strain we used that was created by N. Buckley, A. Zimmer et al. has been questioned in regards to its 'completeness' because its promoter was found to be still active leading to the expression of a truncated version of the CB_2R (232). However, this concern can be refuted because ligand binding of both the endogenous agonist 2-AG and as well as HU-308 is completely abolished in these animals (see figure 3.7.1 and (8)).

19 | Of note, we have never observed a similar, delayed, 20-30mV big depolarisation in CA3 PCs which argues that they do not express intracellular CB_2Rs that are coupled to CaCCs. Of course they could still express both proteins but for other reason lack the necessary components for them to interact.

A side note on CBR pharmacology: we found that AM-251 targets non-CB_1 CBRs at concentrations of 2-5µM that are commonly used as CB_1R-specific in slice experiments. Even though its K_i values for CB_1 and CB_2 are very different (7.49 and 2290nM respectively), AM-251 is known to be an antagonist of both receptors (319). We confirmed this by using AM-251 in a CB_1R KO mouse in which the hyperpolarisation was effectively blocked by both AM-251 and the CB_2R-specific antagonist SR144528 (Figure 3.4.3). We thus postulate that, when bath applied at concentrations of 2-5µM, AM-251 also acts on CB_2Rs. This finding highlights the crucial need for a better understanding of CB_2R function in the CNS and underlines the necessity of combined pharmacogenetic controls to test for the specificity of drugs.

4.1.4 Expression pattern and localisation of CB_2Rs in the CNS

The logically following question that must be answered is: are CB_2Rs expressed in neurons? How can we exclude the involvement of microglia and astrocytes that are both well-known to influence neuronal signalling and express CBRs (208, 329)? As already hinted at in the introductory part of this thesis, CB_2Rs are classically viewed to be part of the immune system and their expression in the CNS has been subject to much debate. Initial studies were unable to detect CB_2R mRNA or ligand binding in brain preparation (8, 346). Then, with the generation of CB_2R antibodies, a plethora of papers was published that described CB_2R protein expression in the somatodendritic domains of neurons and in most brain areas. A paper published in 2005 by M.D. Van Sickle et al. did not only for the first time identify functional CB_2R in the CNS (located in the brainstem) but they reported their location in cerebellum, cortex and brain stem in rat, ferret and mouse, using antibody staining and CB_2R KO controls (15)[20]. Consequent studies used a variety of commercially available antibodies without appropriate controls and reported conflicting results (ranging from no expression to alleged very high expression of CB_2Rs in neurons), see for example (347). As a consequence, two recent studies investigated the reliability/specificity of commercially available antibodies and came to the devastating conclusion that none of them were specific to CB_2R (9, 10). Y. Marchalant and colleagues tested one particular polyclonal antibody to remind the scientific community that antibody sensitivity (that means the antibody detects the protein of interest when sufficiently abundant) must not be confused with antibody specificity (in which case the antibody only binds to the protein of interest and not, like in the case of the tested antibody, additionally cross-reacted with other proteins). This particular antibody was shown to be unreliable as it displayed avidity to - but lacked specificity for - CB_2Rs as shown by KO controls and mass spectrometry (9). Baek et al. come to a similar conclusion when testing the specificity of the most regularly used/published CB_2R antibodies: none of them were specific to CB_2R and failed the KO control (10). To conclude, using positive controls only is not sufficient for antibody validation and the use of KO tissue is the most important control to unequivocally identify CB_2R protein in native tissue. Curiously, they did not test the antibody from Alpha diagnostics (which also had not been used in any subsequent study on brain CB_2Rs). To conclude, except for the antibody used by M.D. Van Sickle et al. no antibody for CB_2R protein that has been validated properly has been published as of yet (to the best of my knowledge). Thus great caution needs to be exercised when assessing literature on CB_2R protein localisation and the use of CB_2R antibodies without the necessary controls must be questioned and criticised.

In contrast to CB_2R protein localisation, CB_2R mRNA expression was convincingly demonstrated by means of reverse transcription polymerase chain reaction (RT PCR) and in situ hybridisation assays (ISH). Including the appropriate KO controls, CB_2R mRNA expression was detected in most brain areas including prefrontal cortex, hippocampus[21], VTA, striatum, amygdala, nucleus accumbens and cerebellum (20, 234). A recent study on VTA dopamine neurons provided fluorescence double labelling for CB_2Rs (with ISH) and tyrosine hydroxylase (with immunohistochemistry) and demonstrated the expression of CB_2R mRNA in dopaminergic neurons (19). This study was the first to demonstrate the expression of CB_2Rs in neurons by complex double-labelling strategies and CB_2R KO controls. From the same experiments data is now available on the hippocampus and shows the presence of CB_2R mRNA in stratum pyramidale of CA1-3 that co-localises with neuronal nuclear antigen (NeuN), a neuronal marker[22].

4.1.5 Neuronal versus non-neuronal expression of CB_2Rs in area CA3

Cumulatively, the genetic and pharmacological manipulations provide strong evidence of a neuronal localisation of the G-Protein coupled CB_2R that mediates the hyperpolarisation and argue against a microglial and/or astrocytic localisation. The above mentioned ISH data indicates that CB_2R mRNA is located in stratum pyramidale of CA3, and to a lesser extent also in the CA1 PC and dentate gyrus GC layer. Currently, the best tool available to test for the neuronal location of CB_2Rs is the

20 | This study used an antibody generated by Alpha Diagnostic whose specificity was confirmed using KO controls in another study on CB_2R expression in the enteric nervous system (382).

21 | We have successfully confirmed CB_2R mRNA expression in isolated hippocampi as well as whole brain samples with CB_2R KO controls as well (data not shown).

22 | This data has not been published yet and our information is based on the personal communication with H.Y. Zhang and Z.X. Xi, NIDA, Baltimore, USA.

synapsin-Cre-dependent CB_2Rs KO. In the initial description of synapsin, co-localisation of synapsin with neuronal markers was shown as well as the lack of co-localisation with glial markers (312, 313). However, at least two studies report expression of synapsin I, albeit at very low level, in astrocytes as well and astrocytes, similarly to neurons, contain the protein machinery needed for vesicle release/fusion (348, 349). Thus, even though synapsin seems to be primarily expressed in neurons, it remains controversial whether it can be considered 'purely' neuronal. We thus performed complementary experiments where we used the GDP analogue GDPßS to block G Protein-dependent signalling in the recorded cell only. As expected, the intracellular application of GDPßS also efficiently blocked the hyperpolarisation and supports the hypothesis of a neuronal origin of the CB_2Rs. We cannot finally exclude the possibility of only a secondary GPCR being activated on the recorded neuron (for example through activity-triggered astrocyte stimulation of the neuronal GPCR). However, additional factors argue against this possibility: the hyperpolarising displays a great temporal sensitivity with an immediate onset after the action potential train and it does not spread between neighbouring neurons. Furthermore, a study investigating endocannabinoid-mediated neuron-astrocyte communication found that astrocytes express CB_1Rs and that their pharmacological activation via the mixed cannabinoid receptor agonist WIN leads to a PLC-dependent increase in astrocytic calcium levels (see p20 and (207)). Importantly, this agonist-stimulated increase of calcium was absent in the CB_1R KO which does not support an astrocytic localisation of CB_2Rs (207). Taken together, cumulative evidence argues against trans-cell secondary messenger processes, and especially against the involvement of astrocytes which impinge on many cells (160, 329). Vice versa, the data supports a neuronal location of CB_2Rs but ultimately, a specific antibody to test for the localisation of CB_2R on a protein level with high-resolution microscopy will be indispensible.

4.1.6 Cell type-specific expression of the CB_2R-mediated plasticity

The action-potential triggered hyperpolarisation can only be induced in CA3 and CA2 PCs but not in the other two main principal cell populations of the hippocampus, namely CA1 PCs and dentate gyrus GCs. This may be either due to a lack of protein or due to an induction failure. We tested this and found that we can readily induce a hyperpolarisation of CA1 PCs by pharmacological activation of CB_2Rs with both HU-308 and WIN (Figure 3.8.1). This supports the notion that functional CB_2Rs are present in CA1 but are not activated by physiological activity. Possible explanations of the physiological induction failure are manifold: differences in the protein distribution of the eCB machinery including the site of 2-AG release and CB_2R location; differences in the extracellular matrix that may limit diffusion of the endocannabinoid; differences in cell morphology that lead to a reduced or location-limited release or diffusion of 2-AG in CA1 versus CA3 PCs in response to action potentials; differences in location of degradation enzymes of 2-AG. Any of these reasons could potentially explain this discrepancy and why even strong, theta burst-like stimuli that are known to trigger eCB-mediated LTD at this synapse (333) still fails to induce the hyperpolarisation. An antibody against the CB_2R that can be used with the Zimmer-strain CB_2R KO mouse as a control would be infinitely helpful to be able to look at the (sub-)cellular protein distribution of the receptor (especially in comparison to the 2-AG synthesising and degrading enzymes DAGL and MAGL, and CB_1Rs). Currently however, we are only able to speculate upon the nature of this induction failure. The physiological relevance of this functional dichotomy will be discussed in the third part of this chapter.

4.1.7 Action potential-driven versus pharmacological stimulation

We find that the hyperpolarisation induced by activity-triggered endogenous 2-AG release is smaller compared to direct pharmacological activation (see for example the occlusion experiments in figure 3.8.2). Two immediately obvious possible reasons to explain this discrepancy are that 1) the concentration of endogenously released 2-AG is not sufficient to saturate receptor binding or that 2) the affinity of 2-AG for CB_2Rs is lower than that of synthesised agonists. Both reasons must be refuted however based on our experimental evidence: the above mentioned occlusion experiments show that the action potential-driven hyperpolarisation could not be additionally enhanced by subsequent pharmacological receptor activation. This result suggests that endogenous 2-AG levels are sufficiently high to saturate receptor binding. Furthermore, we observe a similar difference not only in comparison to synthetic ligands such as HU-308, but also with exogenously applied 2-AG (Figure 3.8.1). Even though the hyperpolarisation induced by HU-308 is slightly greater than that induced by bath applied 2-AG, the higher efficacy of HU-308 in comparison to 2-AG (350) cannot explain the difference between endogenous release and exogenous application of 2-AG (assuming that they are chemically identical). Taken together, these findings suggest pharmacological differences in the efficacy of the applied and endogenous ligands and not in their affinity or (too low) concentration. For example, since the drugs used are highly lipophilic, DMSO is being used as a solvent. Whether that could directly affect ligand efficacy needs to be tested but could explain the systematic difference between the ligands.

4.1.8 Persistent receptor activation

The persistency of the hyperpolarisation may be due to several reasons: the constitutive activation of the CB_2R in presence or absence of the agonist, or downstream alterations in the signalling cascade. Given that 2-AG is being degraded very quickly

after its release (as reflected by the fast decay time of DSI), this is unlikely to underlie the persistency of the response. To distinguish between constitutive receptor activation and alterations in the downstream signalling cascade, we acutely applied the CB_2R-specific inverse agonist SR144528 *after* eliciting the hyperpolarisation in CA3 PCs with the action potential protocol. It has been previously shown that antagonists can acutely reverse other forms of long-term plasticity such as mGluR-dependent LTD (334) which is likely to be due to a persistent receptor activation even in an agonist-unbound state (335). We found that the late application of SR144528 repolarised the membrane potential back to its baseline levels in all cells tested (Figure 3.9.1C-E), suggesting that constitutive receptor activation is indeed the mechanism underlying the persistency of this particular form of cellular plasticity. We performed these experiments in CB_1R-lacking animals to eliminate possible off-target effects of the pharmacological agent. We furthermore applied the drug at different time points (5-10min after the induction, see examples in Figure 3.9.1C,D) to be able identify and rule out a spontaneous repolarisation of the membrane potential. As an additional control, we recorded the membrane potential of WT CA3 PCs for a longer period of time and still observed the hyperpolarisation >15min after the AP induction protocol when the membrane potential is still significantly different from baseline values (figure 3.9.1A-B).

4.1.9 From CB_2R activation to hyperpolarisation – the molecular signalling pathway

We show in this study that activation of CB_2Rs leads to a G Protein-dependent and calcium-sensitive signalling cascade that changes the membrane potential in a conductance-*independent* manner. But it remains an open question which downstream target of CB_2Rs ultimately mediates the hyperpolarisation and via which mechanism it may be activated. Given the multitude of a) potential targets of calcium and b) ion transporters, pumps and channels expressed in various cellular compartments, it will be necessary to experimentally test for involved proteins/ions. Firstly, we need to determine where the activated receptors are located. For example, previous studies have described the mitochondrial expression of both CB_1- and CB_2Rs (17, 351). Secondly, CBRs are known to activate a diverse array of signalling cascades both via the α and βγ subunit of G Protein. Again, the plethora of possible targets renders the analysis of this phenomenon complex.

Based on the description of SSI (see p20) that is phenotypically very similar to the here observed hyperpolarisation, we first assessed whether a GIRK-mediated potassium conductance could really be excluded. We acutely applied the GIRK blocker SCH-23390 after successfully eliciting the long-lasting hyperpolarisation by action potentials and CB_2R agonists respectively. This failed to repolarise the V_m in both sets of experiments, thus strongly arguing against an involvement of GIRK. As a comparative control, we performed recordings of CA3 PCs and applied 1µM Adenosine that is known to activate a GIRK- type potassium channel via adenosine receptors. In these recordings, a clear reduction in the input resistance of CA3 pyramidal cells could be seen that was reversed by the application of SCH-23390 (see figure 3.7.2) and thus substantiate that GIRK is not mediating this effect. In a next step, we aimed to analyse the potential involvement of the Na^+/K^+-pump that has been previously described to hyperpolarise CA3 PCs upon tetanic stimulation (125). However, because the Na^+/K^+-pump is crucially important for the maintenance of the resting membrane potential, its pharmacological block renders the interpretation of results extremely difficult because the intracellular ion homeostasis is being perturbed and cells depolarise significantly (own, unpublished observations). Another possible target could involve calcium co-transporters that are located on mitochondria and set the extremely hyperpolarised potential of mitochondria in respect to the intracellular ion concentrations. A reduction in activity of this transporter that would lead to a reduced calcium-concentration in the intracellular milieu of the neuron would lead to a net hyperpolarisation of the cell in comparison to the extracellular space. As a first step however, calcium-imaging experiments should be performed to confirm the experiments with BAPTA and also to test whether CB_2R activation leads to a de- or increase in cytosolic calcium concentrations and whether these are localised to certain organelles (such as endoplasmic reticulum and/or mitochondria).

4.2 Implications for information processing in CA3 pyramidal cells

CA3 pyramidal cells are known to spike frequently when recorded in vivo and we show that physiological spike trains based on the place cell activity recorded in vivo can readily induce the hyperpolarisation (Figure 3.12.1). Additionally, we show that activation of CB_2R dramatically changes spike probability of synaptically evoked AP firing in CA3 PCs from 80% to below 15% (Figure 3.12.2). This indicates that the activation of CB_2R has profound effects on the spiking threshold of single CA3 PCs and may serve to counterbalance states of high network activity. The possible effects of the hyperpolarisation and the altered spike output will be discussed twice: first, in respect to the excitability of single cells and later in respect to CA3 network function.

4.2.1 Activity-dependent neuromodulation of (dendritic) excitability

In CA3 pyramidal cells, sodium spikes are initiated in the axon hillock or AIS and then propagate back to the dendrites, either passively or actively. The backpropagating action potential is especially relevant for information processing within a neuron due to two particular reasons: a) the number and frequency of backpropagating action potential determines dendritic calcium influx and b) the invasion of dendritic segments depends on the membrane potential. Thus an activity-dependent hyperpolarisation of the membrane of the entire cell and/or segments of the dendritic tree may selectively modulate the information processing within one neuron based upon its previous history of activity and may counteract periods of intense network activity. Given that cannabinoids have been shown to have beneficial effects in epileptic seizures in CA3 (352), it is tempting to speculate on the role of CB_2Rs as a 'safety break'. Furthermore, dependent on the location of CB_2Rs, dendritic calcium spikes may locally alter the weight of incoming inputs by activating CB_2Rs on specific branch segments only, thus providing a spatially and temporally confined signal. If however, CB_2Rs would only be located somatically and on proximal dendrites, they would be activated by all backprogagating action potentials and calcium waves, thus acting as a global signal, dampening all incoming/outgoing information rather than acting on a subcellular level. To answer these questions, it will again be necessary to have a specific antibody for CB_2Rs to look at their distribution on an electron-microscopic, subcellular compartmental level. We know from confocally targeted, improved subcellular patch-clamp recording techniques that spikes generated in the axon hillock of CA3 PCs propagate into the dendrites very efficiently with large amplitude and fast time course. It was shown that up to distances of 400µm into dendrite, the action potential amplitude was still ~40mV (129). Our experimental evidence certainly hints towards a global action of CB_2Rs since backpropagating action potentials were able to consistently activate them. This also argues for a somatic/promixal dendritic expression. Whether they could have additional dendrite-specific effects upon activation by dendritic spikes remains to be elucidated but seems highly likely given the presence of dendritic sodium and calcium spikes in CA3 PCs (129). To this purpose, local puff application of HU-308 in combination with dendritic calcium-imaging would give insights into the distribution and efficacy of CB_2Rs along the dendritic tree. As a general rule, high activity and consequent calcium-influx into the cell will lead to CB_2R activation which may serve to counterbalance states of high network and/or burst activity both on a global as well as branch-specific manner.

Many other neuromodulators have been shown control dendritic excitability, for example 5-HT receptors via the activation of GIRK channels (353). A self-regulatory modulation of CA3 PCs by activity-triggered endocannabinoid release would further add to the complexity of modulatory systems influencing excitability.

4.2.2 In vitro analyses of cellular phenomenon – a critical note

The analysis of cellular phenomenon in vitro has been crucial in the advancement of our understanding of neuronal physiology and synaptic transmission. The current state of knowledge in the field of basic neurotransmission was predominantly sourced from investigations in cell cultures, recombinant expression systems, simple model organisms and acute slices from mammalian brains. The use of electrodes to directly probe and record the electrical signals of neurons (next to advances in molecular biology) has propelled this field forward. The invention of the patch-clamp technique, that enables high-quality low-noise recordings of even single channels, justly led to the Nobel prize being awarded to B. Sakmann and E. Neher "for their discoveries concerning the function of single ion channels in cells" (354). Today, patch-clamp recordings are even possible in awake, behaving animals and have, in combination with population calcium imaging and classic LFP recordings, increased our already detailed understanding of neuronal function further yet. We must not forget however that all of these techniques come with a whole slew of potential errors, the latter being introduced into the system under investigation by means of external disturbance. The washout artefact we observe in whole-cell configuration is maybe the most stark error source that occurred in our study, but fortunately it was possible to bypass this by employing perforated-patch recordings. More subtle problems arise when 'errors' are not this obvious. For example, one reason for why this phenomenon has not been described before may be the frequent use of intracellular solutions based on KGluconate, a calcium chelator which abolishes the calcium-sensitive CB_2R-mediated hyperpolarisation. Because it enables stable recordings, KGluconate is being frequently used despite studies showing is rather drastic effects on other calcium-sensitive passive and active membrane properties (172). Furthermore, the acute brain slice itself is subject to preparation-induced changes, including a reorganisation of spines after slicing (355) and reduced neuromodulatory and synaptic input from other brain areas. The lack of synaptic input especially leads to very hyperpolarised resting membrane potentials and a comparably higher input resistance of cells. For example, reported values for CA3 PC input resistances from in vivo recordings range from 20-30MΩ (109), whereas in our in vitro preparation the average input resistance was ~80MΩ (see p32). The input resistance cannot be adapted in vitro, and will certainly increase the likelihood of a cell to spike. However, the resting membrane potential can be manipulated in vitro, and we recorded all cells at -60mV to mimic a more physiological, depolarised membrane potential and to also reduce variability between recordings. Especially in respect to a small hyperpolarisation of 5-10mV the resting membrane potential will be a very important factor

in determining the effect's impact on neuronal processing. If we consider a hypothetical CA3 PC with a resting membrane potential of -85mV (corrected for LJP, see p29), which is approximately 40mV away from its action potential threshold, the functional significance of a CB_2R receptor-dependent hyperpolarisation to their responses would be questionable (without knowing the level of in vivo synaptic activation). On the other hand, a CA3 PCs with a resting membrane potential around -60mV that is easily driven over threshold will most certainly be affected by a 10mV hyperpolarisation. This is also the reason why we refrained from analysing effects of CB_2R activation in vitro, but moved to in vivo approaches to analyse its modulation of network oscillations.

4.3 Physiological relevance of CB_2R activation in the hippocampus

4.3.1 Causal link between cellular activity and hippocampal memory

A first, general question regarding the correlation of cellular activity and hippocampal memory processing is: is there proof of a *causal* link between the activity/modulation of hippocampal cells and memory formation? Looking at a different type of learning in the hippocampus, namely contextual fear conditioning, recent studies from the group of S. Tonegawa could directly relate the activity of hippocampal principal cells of the dentate gyrus to behaviour. They used a combined transgenic and viral approach that allows 1) for the identification of single neurons that have been activated during learning and memory retrieval respectively by means of activity-induced fluorescent tagging (356) and 2) to specifically target the dentate gyrus. More specifically, they made use of the c-fos promoter, an immediate early gene whose transcription is up-regulated by neuronal spiking and is thus frequently used for the detection of recent activity. During contextual fear learning (as measured by amount of freezing), the promoter drives activity-induced expression of a light-activated cation channel (channelrhodopsin, ChR2) that is tagged with a fluorescent protein. Reactivation of the same cells by activating ChR2 with an implanted optical fibre, led to a freezing response in the animals (357, 358). Similarly, they were able to generate artificial, 'false' memories in mice by activating labelled CA1 or dentate gyrus neurons in a new context (358). Last but not least, they showed that the (re-)activated neurons had more dendritic spines and increased AMPA/NMDAR ratios, as well as a higher connectivity rate (359). Taken together, these studies provide a direct, causal proof that hippocampal memory engrams of a learned behaviour are 'stored' through the activity of cell ensembles, and that their specific reactivation causes the same behavioural output. Furthermore, they suggest that synaptic strength and connectivity are critical parameters underlying successful memory retrieval. Another study looked at learning-dependent changes at the CA3-CA1 synapse while a mouse performed an associative learning task (360). The authors recorded the population response (fEPSP) of CA1 PCs during stimulation of the SC-CA1 synapse and found that its slope increased across conditioning sessions and decreased during extinction of the task. LTP evoked by HFS prevented the acquisition, extinction, recall, or reconditioning (when administered time-locked to the respective experimental paradigm). The occlusion of the behavioural output by HFS is probably due to a saturation of the synapse and again, links NMDAR-dependent changes in synaptic strength to the ability to process information with the appropriate behavioural outcome (360). To conclude, these and other studies provide a causal link between cellular, activity-dependent changes to hippocampus-dependent learning and memory retrieval.

4.3.2 Complementary action of CB_1- and CB_2 receptors

Membrane-derived lipids including cannabinoids predominantly function by maintaining an excitation/inhibition balance through presynaptic inhibition of transmitter release and modulation of short- and long-term plasticity (200, 229, 256, 361, 362). Only few studies have demonstrated changes in neuronal excitability that solely depend on cell-intrinsic cannabinoid modulation (17, 327). An important observation is that CB_2- and CB_1Rs seem to have both overlapping and non-overlapping functions. As mentioned earlier (p15), CB_1Rs mediate most THC-related behavioural effects and their lack has been shown to improve memory function (288). However, their lack also renders certain brain areas prone to epilepsy (352) thus establishing them an important player in maintaining a balanced network function. Acute block of both CB_1- and CB_2Rs has been shown to induce anxiolytic behaviours in mice (295, 363) and similarly, the overexpression of CB_2Rs decreases the vulnerability to anxiety and leads to a depression-resistant phenotype in mice (294). Mounting evidence suggests that CB_1- and CB_2Rs may provide a complementary functionality with CB_1Rs being expressed mostly presynaptically and CB_2Rs on postsynaptic compartments of pyramidal cells (see (17, 21) and our own observations). A CBR subtype-specific regulation during pathophysiological brain states could thus provide an even more fine-tuned correction tool during imbalanced network states. If we consider the hippocampal-EC loop as a closed, simplistic network, adding features of post- and presynaptic modulation of excitability and synaptic transmission in a cell type and input-specific way provides a perfectly fine-tuned system to control excitability. If we furthermore consider that glial cells and microglia also express CB_1Rs and CB_2Rs respectively and release endocannabinoids, and that afferent information from subcortical regions is also under heavy influence of both presynaptically located CB_1Rs as well as postsynaptic CB_2Rs, then the possibilities to affect network function seem infinite and difficult to predict. To conclude,

a complementary modulation of the auto-associative CA3 network by 1) CB_1Rs that presynaptically modulate chemical transmission and alter synaptic weights of incoming inputs and 2) CB_2Rs that alter the cell's intrinsic properties in response to action potential firing provides a most powerful mechanism to fine-tune the network's functionality.

4.3.3 CA3 – a recurrently connected, highly active network prone to seizure

Area CA3 of the hippocampus is particularly susceptible to hyperexcitability due to its recurrent, associative connectivity (91) and the hypothesis of CB_2Rs providing a functional 'safety brake' suggests itself, considering that CB_2Rs activation has a robust, inhibitory effect on the spike probability of CA3 PCs. Furthermore, given the slow and long-lasting temporal dynamics of the hyperpolarisation, one might speculate that – especially during ongoing activity in vivo – CB_2Rs will provide a rather 'tonic' inhibitory tone. CA1 and the DG principal cells are, in stark contrast, not nearly as susceptible to pathophysiological hyperexcitability as they have no recurrent connections. Again, the subfield specific hyperpolarisation should be investigated further along these lines of research. Because CA1 PCs do express CB_2Rs, it may be the case that pathophysiological stimulation (and potentially morphological changes induced thereby) is needed to successfully activate CB_2Rs. This could be easily tested with in vitro and in vivo models for epilepsy (such as 4-AP and kainate respectively) (364, 365). Conversely, the potential protective effects of CB_2Rs activation in CA3 hyperexcitability should be investigated, preferentially in vivo *and* in vitro.

4.3.4 CB_2R modulation of place cells – a hypothesis

Hippocampal place cells fire at specific locations in a given environment, but anatomically neighbouring place cells do not necessarily fire at proximal locations in space. The mechanisms underlying place field firing are not well understood. It is thought that they 'inherit' some attributes from EC grid cells but whether for example hardwired connections are necessary for place cell formation is not known (366). In vivo recordings have shown that place field firing is accompanied by a small depolarisation of the membrane potential that is absent in spatially unturned, silent cells. Surprisingly, these silent cells can be converted into place cells by small somatic depolarisations (5-10mV) elicited by current injection that lead to the immediate and reversible emergence of place field spiking (367). Vice versa, place cells could be silenced by small hyperpolarising current injections. This study directly demonstrates that non-spatial, cellular factors influence the emergence of place fields and that de- and hyperpolarisation of ~5mV was enough convert cells into spatially-tuned and silent cells respectively. To conclude, place fields display characteristics that suggest a possibly potent modulation of their intrinsic characteristics by CB_2Rs. The CB_2R-dependent hyperpolarisation is directly related to the amount of action potentials a cell fires (before reaching a saturated steady-state after approximately 400 action potentials). It is intriguing to speculate that ongoing, irregular spiking of any given cell during exploration activates CB_2Rs that provides a tonic inhibitory tone to subserve network stability. The hyperpolarisation following strong CB_2R activation would fulfil the requirements necessary to silence cells in a cell-autonomous manner and depending on their activity-state. If a biochemical feedback signal existed that could reverse the persistency of the hyperpolarisation in a similarly activity-dependent manner, this system could provide flexible, but powerful control over a spiking-dependent network with high sensitivity to membrane potential alterations. Because place fields have been shown to exist without theta, it is still possible that CB_2R activation may influence place cell firing without having any obvious effects on theta oscillation power or frequency (see below).

4.3.5 Altered theta-modulation of locally generated gamma oscillations in CA3

As mentioned in the introduction (p3), the hippocampus exhibits several types of gamma oscillations including locally generated, slow oscillations and intermediate/fast oscillations that propagate to CA3 from the EC (69–71). It is thought that the coupling/interaction of hippocampal theta and gamma rhythms as observed during exploratory behaviours may serve as coding scheme for working memory and to provide the basis for simultaneously encoding multiple layers of information(66, 67, 368). To investigate the effects of CB_2R activation of on local CA3 network oscillations we recorded the LFP in stratum pyramidal of CA3 in freely moving animals before and after pharmacological CB_2R activation. We find that neither theta nor gamma amplitude and frequency are significantly altered, but that the theta-dependent modulation of gamma oscillations is selectively altered for slow, locally generated gamma oscillations (Figure 3.12.3).

What is the cause of this alteration? This question is difficult to answer since the activity of many types of neurons, including INs, underlies these oscillatory patterns and it is not clear how exactly the tightly locked coupling of theta and gamma is generated and maintained in the first place (66). Preliminary experiments suggest that at least some INs (presumptive CCK+ BCs), but not PV+ BCs, also display a long-lasting hyperpolarisation (data not shown)[23]. Thus, the disruption of

23 | It is thought that PV+ BCs drive theta oscillations (383) which would be in line with our observation that theta power and frequency are not modulated by CB_2R activation.

theta-modulation could be the result of a multifactorial change in local network activity dependent on both PCs and INs. A simultaneous hyperpolarisation of INs and PCs will lead to manifold changes including reduced feedback inhibition, but also reduced drive onto INs and pyramidal cells alike. Even in a very simplified local circuit, it is difficult to theoretically estimate the changes imposed on the network by the activation of CB_2Rs. One possibility to tackle this problem would be to record from multiple cells simultaneously, preferably from reciprocally connected pyramidal cell-IN pairs to directly experimentally test the change in thresholds of spike initiation and the resulting change in single propagation between pairs of cells. Unfortunately, it is not feasible to record from connected pyramidal cells because of their low connectivity rate that has been estimated to be 1% (369). To summarise, the selective disruption of the theta-modulation of slow gamma that is locally generated in CA3 by the activation of CB_2Rs argues for a local network effect and yields exciting possibilities for future experiments analysing their effect on spatial navigation, in particular place cell activity, and hippocampus-dependent memory tasks. Of course, these results need to be confirmed with the Synapsin-Cre dependent CB2R KO as a control.

As a general note, the spatiotemporally precise nature of physiological oscillations hints towards their role in spatial navigation and memory formation/retrieval, and they are thought to facilitate the transfer of memory between the hippocampus and the neocortex during consolidation. However there is no proof as of yet that they are indeed causal to information processing and not merely 'background hum" (78). Although experimental studies have so far failed to causally link oscillations to behavioural states, it is clear that they correlate. One of the studies to provide the most direct evidence for the involvement of SWR in memory consolidation was performed by G. Girardeau and colleagues who could show that suppression of SWR during post-training consolidation in a hippocampus-dependent, spatial-reference memory task led to a significant performance impairment (79). In a follow-up study, they could furthermore demonstrate that SWR incidence was altered in a learning-dependent manner supporting their role in consolidation during rest/sleep (75). Also, theta oscillations have been shown to be necessary for spatial learning by comparison of rodents performing a spatial task with and without septal lesioning that leads to a loss of theta rhythm (80, 81). Interestingly, even though theta oscillations are tightly correlated to the temporal pattern of place cell firing under normal conditions, their disruption (here: by pharmacological inhibition of the septum) was shown to *not* preclude the emergence of hippocampal place fields, arguing that theta is not a requirement for the generation of spatial representations (82). In line with this, rats with septal lesions that could not find their way directly to the trained goal were nevertheless able to recognise its location if they came across it by chance (81). It will be necessary to find a way to specifically disrupt place field firing (without interfering with theta oscillations) to tear apart their exact role and interplay with theta-frequency network activity in spatial memory.

4.4 Diurnal, circadian control of endocannabinoid release

It has been shown that anandamide and 2-AG concentrations in the brain exhibit dramatic diurnal variations (370). Interestingly, the two cannabinoids seem to have opposite day-night concentration profiles where, for example in the hippocampus, anandamide is upregulated during the light phase (4.3fold) while 2-AG concentrations are lower during the light but increased during the night/dark phase (2.7fold). Given that we perform our experiments with nocturnal rodents that are in their resting phase during the day, we expect high concentrations of 2-AG being present in our specimen. It would be very important to record from mice in their active phase, when 2-AG levels will be low, and test whether physiological cannabinoid receptor activation is visibly reduced by analysing the hyperpolarisation and DSI/DSE as a read-out for 2-AG release. This will be additionally informative in regards to whether the physiological release of 2-AG is saturating CBR binding sites in the concentrations present during both active and inactive states of the animal. It is well-known that cannabinoids have sedative effects and it has been suggested that reduced striatal 2-AG levels during the night could explain increased activity in rats at night (370). We are not aware of any study in which varying concentration of endocannabinoids in the brain could be directly linked to diurnal activity changes and thus this concept, even though intriguing, remains speculation. However, experiments in which the concentration of 2-AG could be determined in tissue used for experiments and then compared to the magnitude of 2-AG mediated effects could yield very interesting insights into the diurnal modulation of endocannabinoid signalling.

4.5 CB_2Rs as therapeutic targets in complex neuropsychiatric diseases

Neuronal CB_2Rs have been reported to be modulated during a variety of complex neuropsychiatric disorders including depression, schizophrenia and autism spectrum disorders (14) and, due to their non-psychotropic mode of action, are considered promising therapeutic targets (339).

Our findings may furthermore help to shed light on the complex mechanisms underlying endocannabinoid function in health and disease which is especially significant given the recent surge of interest in cannabinoids in the treatment of psychiatric

disorders, and the involvement of CB_2Rs in many complex neuropsychiatric diseases (371) in which they may provide the basis for non-psychoactive treatments (22). As detailed in the introduction, CBR expression is subject to activity-dependent plasticity especially in pathophysiological brain states such as schizophrenia (293). It would thus be worth to analyse the degree of hyperpolarisation in comparison to CB_2R number in respective mouse models, in which CB_2R mRNA and protein are downregulated. Furthermore, many ionic conductances are similarly regulated by (pathological) activity and it would be interesting to see whether the degree of hyperpolarisation that we observe correlates to the magnitude of any currents mediated by K_V, Na_V or HCN channels in healthy and for example epileptic conditions. Finally, it will be important to find therapeutic strategies in which the toxic and beneficial effects of cannabinoids can be selectively targeted and manipulated. The therapeutic use of CB_1R agonists cannot be refuted and it is very effective in treating for example pain, anxiety and certain eating disorders (193). However, a major limitation for their clinical use are unwanted psychotropic side effects. Simultaneously, the CB_2R has emerged as an important alternative target for certain illnesses with great therapeutic potential because it is not psychoactive in its mode of action (242, 372).

4.6 Experimental outlook

For future studies on CB_2R function we would like to follow up on and expand our research with a focus on five main questions:

1 | **Is there a unifying generality of CB_2R function in the brain?**
We would like to analyse the importance of CB_2Rs and of the novel plasticity mechanism they mediate in other brain areas to establish whether this effect is a localised phenomenon suited to the properties of the recurrent CA3 network or a global feedback mechanism.

2 | **What are the biochemical steps involved in the hyperpolarisation and what underlies the conductance-independent change in membrane potential?**
It will be important to identify the underlying, end-of-signalling-cascade effector and determine its properties including the ions transported and gradient established. A final mechanistic assessment of this phenomenon is not possible without.

3 | **How do CB_2Rs affect the information processing in contained, local microcircuits?**
We know that CB_2Rs very effectively modulate the input/output function of CA3 PCs. To investigate their effects on the local CA3 network further, we want to analyse the role of CB_2Rs in microcircuits of excitatory and inhibitory neurons. As detailed above, preliminary evidence suggests that at least one class of INs expresses CB_2Rs as well. It will be decisive to discern their function in order to come up with a detailed model of CB_2R function in a given network. To experimentally analyse the effects of the hyperpolarisation within a network, simultaneous recordings of connected PC-IN pairs will be useful to directly monitor possible changes in synaptic integration and the relative weights of excitatory and inhibitory in- and output before and after CB_2R activation. To this cause, computational models of principal cell-IN networks would be of great help to predict possible effects of CB_2R expression and consequently identify suitable, hypothesis-driven experimental approaches.

4 | **What is the function of CB_2Rs during in vivo network activity?**
We know from LFP recordings in vivo that CB_2R activation alters the theta-dependent modulation of gamma during exploratory behaviour. To complement these findings, we aim to record action potential firing of CA3 PCs, preferentially while the animal is performing a hippocampus-dependent task, with silicon probes that allow for isolation of single units. If we postulate that CB_2R activation is also long-lasting in the intact brain, it will be more likely that they provide a tonic inhibitory tone because CA3 PCs have been shown to frequently spike in vivo (96). Thus, in addition to the pharmacological, artificial activation of CB_2Rs, it will be important to see whether the local application of CB_2R antagonists will alter oscillatory network and single cell activity. This would provide information on whether CB_2R are indeed endogenously active during 'normal' behaviour. As mentioned above, we would also very much like to assess the role of CB_2R activation on place field formation and stability.

5 | **What is the role of CB_2Rs in pathophysiological network states and are they a suitable pharmacological target to protect networks from hyperexcitability?**
We would like to test whether CB_2R have a protective function during pathophysiological network states. As a first experiment, kainate-induced seizures with and without prior application of a CB_2R agonist would yield a reference point to whether further investigation into this line of research is valuable. Given that no major side effects of CB_2R agonist application have been reported, their therapeutic potential is immense.

4.7 Concluding remarks

In comparison to the vast literature on CB_1Rs function in the CNS, the current state concerning CB_2Rs is negligible. It is thus crucial to highlight, and increase the awareness towards, their importance in basic neuronal transmission. Our results provide a first in depth description of CB_2R function in the hippocampus and we hope that our study will provide a basis for further research into CB_2R function regarding its role in physiological and pathophysiological network states and hippocampal plasticity mechanisms.

5 References

1. Katona I, et al. (1999) Presynaptically located CB_1 cannabinoid receptors regulate GABA release from axon terminals of specific hippocampal interneurons. *J Neurosci* 19(11):4544–58.
2. Alger BE (2012) Endocannabinoids at the synapse a decade after the Dies Mirabilis (29 March 2001): what we still do not know. *J Physiol* 590(10):2203–12.
3. Katona I, Freund TF (2012) Multiple functions of endocannabinoid signaling in the brain. *Annu Rev Neurosci* 35:529–58.
4. Wilson RI, Nicoll RA (2001) Endogenous cannabinoids mediate retrograde signalling at hippocampal synapses. *Nature* 410(6828):588–92.
5. Kreitzer AC, Regehr WG (2001) Retrograde inhibition of presynaptic calcium influx by endogenous cannabinoids at excitatory synapses onto Purkinje cells. *Neuron* 29(3):717–27.
6. Ohno-Shosaku T, Maejima T, Kano M (2001) Endogenous cannabinoids mediate retrograde signals from depolarized postsynaptic neurons to presynaptic terminals. *Neuron* 29:729–38.
7. Munro S, Thomas KL, Abu-Shaar M (1993) Molecular characterization of a peripheral receptor for cannabinoids. *Nature* 365:61–5.
8. Buckley NE, et al. (2000) Immunomodulation by cannabinoids is absent in mice deficient for the cannabinoid CB_2 receptor. *Eur J Pharmacol* 396:141–9.
9. Marchalant Y, Brownjohn PW, Bonnet A, Kleffmann T, Ashton JC (2014) Validating antibodies to the cannabinoid CB_2 receptor: Antibody sensitivity is not evidence of antibody specificity. *J Histochem Cytochem* 62:395–404.
10. Baek J-H, Darlington CL, Smith PF, Ashton JC (2013) Antibody testing for brain immunohistochemistry: Brain immunolabeling for the cannabinoid CB_2 receptor. *J Neurosci Methods* 216(2):87–95.
11. Zimmer A, Zimmer AM, Hohmann AG, Herkenham M, Bonner TI (1999) Increased mortality, hypoactivity, and hypoalgesia in cannabinoid CB_1 receptor knockout mice. *Proc Natl Acad Sci U S A* 96(10):5780–5.
12. Howlett AC, et al. (2002) International Union of Pharmacology. XXVII. Classification of cannabinoid receptors. *Pharmacol Rev* 54(2):161–202.
13. Onaivi ES (2006) Neuropsychobiological evidence for the functional presence and expression of cannabinoid CB_2 receptors in the brain. *Neuropsychobiology* 54(4):231–46.
14. Onaivi ES (2011) Commentary: Functional neuronal CB_2 cannabinoid receptors in the CNS. *Curr Neuropharmacol* 9(1):205–8.
15. Van Sickle MD, et al. (2005) Identification and functional characterization of brainstem cannabinoid CB_2 receptors. *Science* 310(5746):329–32.
16. Morgan NH, Stanford IM, Woodhall GL (2009) Functional CB_2 type cannabinoid receptors at CNS synapses. *Neuropharmacology* 57(4):356–68.
17. Den Boon FS, et al. (2012) Excitability of prefrontal cortical pyramidal neurons is modulated by activation of intracellular type-2 cannabinoid receptors. *Proc Natl Acad Sci U S A* 109(9):3534–39.
18. Páldy E, et al. (2008) CB_2 cannabinoid receptor antagonist SR144528 decreases mu-opioid receptor expression and activation in mouse brainstem: Role of CB_2 receptor in pain. *Neurochem Int* 53(6-8):309–16.
19. Zhang H-Y, et al. (2014) Cannabinoid CB_2 receptors modulate midbrain dopamine neuronal activity and dopamine-related behavior in mice. *Proc Natl Acad Sci U S A* 111(46):E5007–15.
20. Zhang H-Y, et al. (2014) Species differences in cannabinoid receptor 2 and receptor responses to cocaine self-administration in mice and rats. *Neuropsychopharmacology*:1–15.
21. Kim J, Li Y (2015) Chronic activation of CB_2 cannabinoid receptors in the hippocampus increases excitatory synaptic transmission. *J Physiol* 593(4):871-86.
22. Micale V, Di Marzo V, Sulcova A, Wotjak CT, Drago F (2013) Endocannabinoid system and mood disorders: priming a target for new therapies. *Pharmacol Ther* 138(1):18–37.
23. Howlett AC, et al. (2004) Cannabinoid physiology and pharmacology: 30 years of progress. *Neuropharmacology* 47:345–58.
24. Castillo PE, Younts TJ, Chávez AE, Hashimotodani Y (2012) Endocannabinoid signaling and synaptic function. *Neuron* 76(1):70–81.
25. Hájos N, Freund F (2002) Distinct cannabinoid sensitive receptors regulate hippocampal excitation and inhibition. *Chem Phys Lipids* 121:73-82
26. Zhang Y, Lu H, Bargmann CI (2005) Pathogenic bacteria induce aversive olfactory learning in Caenorhabditis elegans. *Nature* 438:179–84.
27. Quinn WG, Harris W a, Benzer S (1974) Conditioned behavior in Drosophila melanogaster. *Proc Natl Acad Sci U S A* 71(3):708–12.
28. Aceves-Piña E, Quinn W (1979) Learning in normal and mutant Drosophila larvae. *Science* 206:93–6.

29. Beugnon G (1986) Learned orientation in landward swimming in the cricket Pteronemobius Lineolatus. *Behav Processes* 12(3):215–26.
30. Pawlow IP (1902) *The work of the digestive glands* (C. Griffin, London).
31. Waston J, Rayner R (1920) Conditioned emotional reactions. *J Exp Psychol* 3:1–14.
32. Shepherd GM (2004) *The synaptic organization of the brain* (Oxford University Press, New York). 5th Ed.
33. Fain G (1999) *Molecular and cellular physiology of neurons* (Harvard University Press, London). 1st Ed.
34. Glanzman DL (2010) Common mechanisms of synaptic plasticity in vertebrates and invertebrates. *Curr Biol* 20(1):R31–R36.
35. Frost WN, Castellucci VF, Hawkins RD, Kandel ER (1985) Monosynaptic connections made by the sensory neurons of the gill- and siphon-withdrawal reflex in Aplysia participate in the storage of long-term memory for sensitization. *Proc Natl Acad Sci U S A* 82(23):8266–8269.
36. Brunelli M, Castellucci V, Kandel ER (1976) Synaptic facilitation and behavioral sensitization in Aplysia: possible role of serotonin and cyclic AMP. *Science* 194(4270):1178–1181.
37. Schacher S, Castellucci V, Kandel E (1988) cAMP evokes long-term facilitation in Aplysia sensory neurons that requires new protein synthesis. *Science (80-)* 240:1667–9.
38. Azevedo F a C, et al. (2009) Equal numbers of neuronal and nonneuronal cells make the human brain an isometrically scaled-up primate brain. *J Comp Neurol* 513(5):532–541.
39. Scoville WB, Milner B (1957) Loss of recent memory after bilateral hippocampal lesions. *J Neurol Neurosurg Psychiatry* 20:11–21.
40. O'Keefe J, Nadel L (1978) *The hippocampus as a cognitive map* (Oxford University Press).
41. Kandel ER, Schwarzer J, Jessel T (2000) *Principles of neural sciences* (McGraw-Hill Medical).
42. Wang DV, et al. (2015) Mesopontine median raphe regulates hippocampal ripple oscillation and memory consolidation. *Nat Neurosci* 18(5): 728-735.
43. Liu QR, et al. (2009) Species differences in cannabinoid receptor 2 (CNR2 gene): identification of novel human and rodent CB2 isoforms, differential tissue expression and regulation by cannabinoid receptor ligands. *Genes Brain Behav* 8(5):519–30.
44. Duvernoy HM (2005) *The human hippocampus* (Springer Verlag, Heidelberg Berlin New York).
45. Squire LR, Stark CEL, Clark RE (2004) The medial temporal lobe. *Annu Rev Neurosci* 27:279–306.
46. Marr D (1971) Simple memory : a theory for archicortex. *Philos Trans R Soc Lond B Biol Sci* 262:23–81.
47. Buzsáki G (1989) Two-stage model of memory trace formation: A role for "noisy" brain states. *Neuroscience* 31(3):551–70.
48. Mashour G a., Walker EE, Martuza RL (2005) Psychosurgery: Past, present, and future. *Brain Res Rev* 48(3):409–19.
49. Corkin S, Milner B, Rasmussen T (1964) Effects of different cortical excisions on sensory thresholds in man. *Trans Am Neurol Assoc* 89:112–16.
50. Corkin S (2002) What's new with the amnesic patient H.M.? *Nat Rev Neurosci* 3(2):153–60.
51. Milner B, Corkin S, Teuber H (1968) Further analysis of the hippocampal amnesic syndrome: 14-year follow-up study of H.M. *Neuropsychologia* 6:215–34.
52. Zola-Morgan S, Squire LR (1986) Memory impairment in monkeys following lesions limited to the hippocampus. *Behav Neurosci* 100:155–60.
53. Zola-Morgan S, Squire LR, Amaral DG (1986) Human amnesia and the medial temporal region: enduring memory impairment following a bilateral lesion limited to field CA1 of the hippocampus. *J Neurosci* 6(10):2950–67.
54. Squire LR, Wixted JT (2011) *The cognitive neuroscience of human memory since H.M.*
55. Squire LR, Knowlton B (1995) Memory, hippocampus, and brain systems. *The Cognitive Neurosciences* (The MIT Press).
56. Muñoz-López M (2015) Past, present, and future in hippocampal formation and memory research. *Hippocampus*.
57. Bunsey M, Eichenbaum HB (1996) Conservation of hippocampal memory function in rats and humans. *Nature* 379:255–257.
58. Bakker A, Kirwan CB, Miller M, Stark CEL (2008) Pattern separation in the human hippocampal CA3 and dentate gyrus. *Science* 319(5870):1640–2.
59. O'Keefe J, Dostrovsky J (1971) The hippocampus as a spatial map. Preliminary evidence from unit activity in the freely-moving rat. *Brain Res* 34(1):171–5.
60. Morris RGM (1981) Spatial localization does not require the presence of local cues. *Learn Motiv* 12:239–60.
61. Morris RG, Garrud P, Rawlins JN, O'Keefe J (1982) Place navigation impaired in rats with hippocampal lesions. *Nature* 297(5868):681–3.
62. Taube JS, Muller RU, Ranck JBJ (1990) Head-direction cells recorded from the postsubiculum in freely moving rats. I. Description and quantitative analysis. *J Neurosci* 10(2):420–35.
63. Witter MP, Moser EI (2006) Spatial representation and the architecture of the entorhinal cortex. *Trends Neurosci* 29(12):671–678.
64. Knierim J (2014) From the GPS to HM: Place cells, grid cells, and memory. *Hippocampus*:2–31.

65. Valerio S, Taube JS (2012) Path integration: how the head direction signal maintains and corrects spatial orientation. *Nat Neurosci* 15(10):1445–53.
66. Canolty RT, et al. (2006) High gamma power is phase-locked to theta oscillations in human neocortex. *Science* 313:1626–1628.
67. Wulff P, et al. (2009) Hippocampal theta rhythm and its coupling with gamma oscillations require fast inhibition onto parvalbumin-positive interneurons. *Proc Natl Acad Sci U S A* 106:3561–6.
68. Lisman JE, Jensen O (2013) The Theta-Gamma Neural Code. *Neuron* 77(6):1002–1016.
69. Colgin LL, et al. (2009) Frequency of gamma oscillations routes flow of information in the hippocampus. *Nature* 462(7271):353–7.
70. Schomburg EW, et al. (2014) Theta Phase Segregation of Input-Specific Gamma Patterns in Entorhinal-Hippocampal Networks. *Neuron* (84):470–85.
71. Zheng C, Bieri KW, Trettel SG, Colgin LL (2015) The relationship between gamma frequency and running speed differs for slow and fast gamma rhythms in freely behaving rats. *Hippocampus* 14:1–14.
72. Bragin A, et al. (1995) Gamma (40-100Hz) oscillation in the hippocampus of the behaving rat. *J Neurosci* 15:47–60.
73. Chrobak JJ, Buzsa G (1998) Gamma Oscillations in the Entorhinal Cortex of the Freely Behaving Rat. 18(1):388–98.
74. Fell J, et al. (2001) Human memory formation is accompanied by rhinal-hippocampal coupling and decoupling. *Nat Neurosci* 4(12):1259–64.
75. Girardeau G, Cei A, Zugaro M (2014) Learning-Induced Plasticity Regulates Hippocampal Sharp Wave-Ripple Drive. *J Neurosci* 34(15):5176–83.
76. Schmidt R, et al. (2009) Single-trial phase precession in the hippocampus. *J Neurosci* 29(42):13232–41.
77. Nádasdy Z, Hirase H, Czurkó A, Csicsvari J, Buzsáki G (1999) Replay and time compression of recurring spike sequences in the hippocampus. *J Neurosci* 19:9497–507.
78. Kullmann DM (2011) Interneuron networks in the hippocampus. *Curr Opin Neurobiol* 21(5):709–16.
79. Girardeau G, Benchenane K, Wiener SI, Buzsáki G, Zugaro MB (2009) Selective suppression of hippocampal ripples impairs spatial memory. *Nat Neurosci* 12(10):1222–3.
80. Olton DS, Walker JA, Gage FH (1978) Hippocampal connections and spatial discrimination. *Brain Res* 139(2):295–308.
81. Winson J (1978) Loss of hippocampal theta rhythm results in spatial memory deficit in the rat. *Science* 201:160–63.
82. Brandon M, Koenig J, Leutgeb J, Leutgeb S (2014) New and Distinct Hippocampal Place Codes Are Generated in a New Environment during Septal Inactivation. *Neuron* 82(4):789–796.
83. Larriva-Sahd JA. (2014) Some predictions of Rafael Lorente de Nó 80 years later. *Front Neuroanat* 8:1–8.
84. Zhao X, et al. (2001) Transcriptional Profiling Reveals Hippocampal Subregions. 196:187–96.
85. McNaughton B (1980) Evidence for two physiologically distinct perforant pathways to the fascia dentata. *Brain Cogn* 199:1–19.
86. Amaral DG, Scharfman HE, Lavenex P (2007) The dentate gyrus: fundamental neuroanatomical organization (dentate gyrus for dummies). *Prog Brain Res* 163:3–22.
87. Amaral DG (1978) A Golgi study of cell types in the hilar region of the hippocampus in the rat. *J Comp Neurol* 182(4 Pt 2):851–914.
88. Neves G, Cooke S, Bliss T (2008) Synaptic plasticity, memory and the hippocampus : a neural network approach to causality. *Nat Rev Neurosci* 9:65–75.
89. Agster KL, Burwell RD (2013) Hippocampal and subicular efferents and afferents of the perirhinal, postrhinal, and entorhinal cortices of the rat. *Behav Brain Res* 254:50–64.
90. Witter MP (2007) Intrinsic and extrinsic wiring of CA3: indications for connectional heterogeneity. *Learn Mem* 14(11):705–13.
91. Amaral DG (1993) Emerging principles of intrinsic hippocampal organization. *Curr Opin Neurobiol* 3:225–9.
92. Szabadics J, Varga C, Brunner J, Chen K, Soltesz I (2010) Granule cells in the CA3 area. *J Neurosci* 30(24):8296–307.
93. Chevaleyre V, Siegelbaum SA (2010) Strong CA2 pyramidal neuron synapses define a powerful disynaptic cortico-hippocampal loop. *Neuron* 66(4):560–72.
94. Kohara K, et al. (2014) Cell type-specific genetic and optogenetic tools reveal hippocampal CA2 circuits. *Nat Neurosci* 17(2):269–79.
95. Wittner L, Miles R (2007) Factors defining a pacemaker region for synchrony in the hippocampus. *J Physiol* 584:867–83.
96. Tropp Sneider J, Chrobak JJ, Quirk MC, Oler JA, Markus EJ (2006) Differential behavioral state-dependence in the burst properties of CA3 and CA1 neurons. *Neuroscience* 141(4):1665–1677.
97. Graves AR, et al. (2012) Hippocampal pyramidal neurons comprise two distinct cell types that are countermodulated by metabotropic receptors. *Neuron* 76(4):776–89.
98. Lee SH, et al. (2014) Parvalbumin-positive basket cells differentiate among hippocampal pyramidal cells. *Neuron* 82(5):1129–44.

99. Schmitz D, et al. (2001) Axo-axonal coupling. a novel mechanism for ultrafast neuronal communication. *Neuron* 31(5):831–40.
100. Halasy K, Miettinen R, Szabat E, Freund TF (1992) GABAergic interneurons are the major postsynaptic targets of median raphe afferents in the rat dentate gyrus. *Eur J Neurosci* 4(2):144–53.
101. Mosko S, Lynch G, Cotman CW (1973) The distribution of septal projections to the hippocampus of the rat. *J Comp Neurol* 152(2):163–74.
102. Vertes RP, Hoover WB, Do Valle AC, Sherman A, Rodriguez JJ (2006) Efferent projections of reuniens and rhomboid nuclei of the thalamus in the rat. *J Comp Neurol* 499(5):768–96.
103. Strange BA, Witter MP, Lein ES, Moser EI (2014) Functional organization of the hippocampal longitudinal axis. *Nat Rev Mol Cell Biol* 15(10):655–69.
104. Soetanto A, et al. (2010) Association of anxiety and depression with microtubule- associated protein 2– and synaptopodin-immunolabeled dendrite and spine densities in hippocampal CA3 of older humans. *Arch Gen Psychiatry* 67(5):448–57.
105. Jönsson S, Luts A, Guldberg-Kjaer N, Ohman R (1999) Pyramidal neuron size in the hippocampus of schizophrenics correlates with total cell count and degree of cell disarray. *Eur Arch Psychiatry Clin Neurosci* 249:167–73.
106. Haas KZ, Sperber EF, Opanashuk L a., Stanton PK, Moshé SL (2001) Resistance of immature hippocampus to morphologic and physiologic alterations following status epilepticus or kindling. *Hippocampus* 11(6):615–25.
107. Tsamis IK, et al. (2010) Properties of CA3 dendritic excrescences in Alzheimer's disease. *Curr Alzheimer Res* 7(1):84–90.
108. Gould E, Allan MD, McEwen BS (1990) Dendritic spine density of adult hippocampal pyramidal cells is sensitive to thyroid hormone. *Brain Res* 525(2):327–329.
109. Turner DA, Li X, Pyapali GK, Ylinen A, Buzsáki G (1995) Morphometric and electrical properties of reconstructed hippocampal CA3 neurons recorded in vivo. *J Comp Neurol* 594:580–94.
110. Spruston N (2008) Pyramidal neurons: dendritic structure and synaptic integration. *Nat Rev Neurosci* 9(3):206–21.
111. Blackstedt T (1956) Commissural connections of the hippocampal region in the rat, with special reference to their mode of termination. *J Comp Neurol* 105:417–537.
112. McBain CJ, Fisahn A (2001) Interneurons unbound. *Nat Rev Neurosci* 2(1):11–23.
113. Pouille F, Scanziani M (2004) Routing of spike series by dynamic circuits in the hippocampus. *Nature* 429(6993):717–23.
114. Pouille F, Scanziani M (2001) Enforcement of temporal fidelity in pyramidal cells by somatic feed-forward inhibition. *Science* 293(5532):1159–63.
115. Andersen P, Eccles JC, Loyning Y (1964) Location of postsynaptic inhibitory synapses on hippocampal pyramids. *J Neurophysiol* 27:592–607.
116. Klausberger T, Somogyi P (2008) Neuronal diversity and temporal dynamics: the unity of hippocampal circuit operations. *Science* 321(5885):53–7.
117. Li X, Somogyi P, Ylinen A, Buzsáki G (1994) The hippocampal CA3 network: an in vivo intracellularly labeling study. *J Comp Neurol* 339:181–208.
118. Le Duigou C, Simonnet J, Teleñczuk MT, Fricker D, Miles R (2014) Recurrent synapses and circuits in the CA3 region of the hippocampus: an associative network. *Front Cell Neurosci* 7:262.
119. Ishizuka N, Weber J, Amaral DG (1990) Organization of intrahippocampal projections originating from CA3 pyramidal cells in the rat. *J Comp Neurol* 295(4):580–623.
120. Shinohara Y, et al. (2012) Hippocampal CA3 and CA2 have distinct bilateral innervation patterns to CA1 in rodents. *Eur J Neurosci* 35(5):702–10.
121. Deguchi Y, Donato F, Galimberti I, Cabuy E, Caroni P (2011) Temporally matched subpopulations of selectively interconnected principal neurons in the hippocampus. *Nat Neurosci* 14(4):495–504.
122. Sloviter RS (1991) Permanently altered hippocampal structure, excitability, and inhibition after experimental status epilepticus in the rat: the "dormant basket cell" hypothesis and its possible relevance to temporal lobe epilepsy. *Hippocampus* 1(1):41–66.
123. Sloviter RS (1987) Decreased hippocampal inhibition and a selective loss of interneurons in experimental epilepsy. *Science* 235(4784):73–6.
124. Wright SH (2004) Generation of resting membrane potential. *Adv Physiol Educ* 28:139–42.
125. Gustafsson B, Wigström H (1983) Hyperpolarization following long-lasting tetanic activation of hippocampal pyramidal cells. *Brain Res* 275(1):159–63.
126. Fukuda A, Prince DA (1992) Postnatal development of electrogenic sodium pump activity in rat hippocampal pyramidal neurons. *Brain Res Dev Brain Res* 65(1):101–14.
127. Hemond P, et al. (2008) Distinct classes of pyramidal cells exhibit mutually exclusive firing patterns in hippocampal area CA3b. *Hippocampus* 18(4):411–24.

128. Núñez a, García-Austt E, Buño W (1987) Intracellular theta-rhythm generation in identified hippocampal pyramids. *Brain Res* 416(2):289–300.
129. Kim S, Guzman SJ, Hu H, Jonas P (2012) Active dendrites support efficient initiation of dendritic spikes in hippocampal CA3 pyramidal neurons. *Nat Neurosci* 15(4):600–6.
130. Kiss T (2008) Persistent sodium channels: origin and function. *Acta Biol Hung* 59:1–12.
131. Sipilä ST, Huttu K, Voipio J, Kaila K (2006) Intrinsic bursting of immature CA3 pyramidal neurons and consequent giant depolarizing potentials are driven by a persistent Na^+ current and terminated by a slow Ca^{2+}-activated K^+ current. *Eur J Neurosci* 23(9):2330–8.
132. Storm J (1987) Action potential repolarization and a fast after-hyperpolarization in rat hippocampal pyramidal cells. *J Physiol* 385(August):733–59.
133. Sah P (1996) Ca^{2+}-activated K^+ currents in neurones: types, physiological roles and modulation. *Trends Neurosci* 19(4):150–4.
134. Stocker M (2004) Ca^{2+}-activated K^+ channels: molecular determinants and function of the SK family. *Nat Rev Neurosci* 5:758–770.
135. Faber ES, Sah P (2003) Calcium-Activated Potassium Channels : Multiple Contributions to Neuronal Function. *Neuroscientist* 9(3):181-94.
136. Sah P, Bekkers JM (1996) Apical dendritic location of slow afterhyperpolarization current in hippocampal pyramidal neurons: implications for the integration of long-term potentiation. *J Neurosci* 16(15):4537–42.
137. Stackman RW, et al. (2002) Small conductance Ca^{2+}-activated K^+ channels modulate synaptic plasticity and memory encoding. *J Neurosci* 22(23):10163–71.
138. Alger BE, Nicoll RA (1980) Epileptiform burst afterhyperpolarization: calcium-dependent potassium potential in hippocampal CA1 pyramidal cells. *Science* 210:1122–1124.
139. Verma-Ahuja S, Evans MS, Pencek TL (1995) Evidence for decreased calcium dependent potassium conductance in hippocampal CA3 neurons of genetically epilepsy-prone rats. *Epilepsy Res* 22(2):137–44.
140. Schmitz D, Gloveli T, Empson RM, Heinemann U (1998) Comparison of the effects of serotonin in the hippocampus and the entorhinal cortex. *Mol Neurobiol* 17(1-3):59–72.
141. Malenka RC, Nicoll RA (1986) Dopamine decreases the calcium-activated afterhyperpolarization in hippocampal CA1 pyramidal cells. *Brain research* 379:210–15.
142. Shah MM (2014) Cortical HCN channels: function, trafficking and plasticity. *J Physiol* 592(13):2711–9.
143. Mokeichev A, et al. (2007) Stochastic emergence of repeating cortical motifs in spontaneous membrane potential fluctuations in vivo. *Neuron* 53(3):413–25.
144. Bender RA, et al. (2005) Synchronized network activity in developing rat hippocampus involves regional hyperpolarization-activated cyclic nucleotide-gated (HCN) channel function. *Eur J Neurosci* 22(10):2669–74.
145. Nolan M, et al. (2005) A behavioral role for dendritic integration: HCN1 channels constrain spatial memory and plasticity at inputs to dendrites of CA1 pyramidal neurons. *Cell* 120(1):151–2.
146. Giocomo LM, et al. (2011) Grid Cells Use HCN1 Channels for Spatial Scaling. *Cell* 147(5):1159–70.
147. Griesemer D, Zawar C, Neumcke B (2002) Cell-type specific depression of neuronal excitability in rat hippocampus by activation of ATP-sensitive potassium channels. *Eur Biophys J* 31(6):467–77.
148. Dale N, Frenguelli BG (2009) Release of adenosine and ATP during ischemia and epilepsy. *Curr Neuropharmacol* 7(3):160–79.
149. Storm JF (1988) Temporal integration by a slowly inactivating K^+ current in hippocampal neurons. *Nature* 336(6197):379–81.
150. Hyun JH, Eom K, Lee K, Ho W, Lee S (2013) Activity-dependent downregulation of D-type K^+ channel channel subunit $K_{v1.2}$ in rat hippocampal CA3 pyramidal neurons. *J Physiol* 15:5525–40.
151. Metz AE, Spruston N, Martina M (2007) Dendritic D-type potassium currents inhibit the spike afterdepolarization in rat hippocampal CA1 pyramidal neurons. *J Physiol* 581(1):175–87.
152. Hoffman DA, Johnston D (1998) Downregulation of transient K^+ channels in dendrites of hippocampal CA1 pyramidal neurons by activation of PKA and PKC. *J Neurosci* 18(10):3521–8.
153. Martin SJ, Grimwood PD, Morris RGM (2000) Synaptic plasticity and memory : an evaluation of the hypothesis. *Annu Rev Neurosci* 23:649–711.
154. Hydén H, Lange PW (1968) Protein synthesis in the hippocampal pyramidal cells of rats during a behavioral test. *Science* 159(821):1370–3.
155. Malenka RC, Bear MF (2004) LTP and LTD : An Embarrassment of Riches. *Neuron* 44:5-21.
156. Hebb D (1949) *The Organization of Behavior: A Neuropsychological Theory* (Wiley).
157. Bi G, Poo M (2001) Synaptic modification by correlated activity: Hebb's postulate revisited. *Annu Rev Neurosci* 29: 139-66.
158. Sjöström PJ, Turrigiano GG, Nelson SB (2003) Neocortical LTD via coincident activation of presynaptic NMDA and cannabinoid receptors. *Neuron* 39(4):641–54.

159. Debanne D, Gähwiler BH, Thompson SM (1998) Long-term synaptic plasticity between pairs of individual CA3 pyramidal cells in rat hippocampal slice cultures. *J Physiol* 507 (1):237–47.
160. Min R, Nevian T (2012) Astrocyte signaling controls spike timing–dependent depression at neocortical synapses. *Nat Neurosci* 15(5):746–53.
161. Cull-Candy S, Kelly L, Farrant M (2006) Regulation of Ca^{2+}-permeable AMPA receptors: synaptic plasticity and beyond. *Curr Opin Neurobiol* 16(3):288–97.
162. Nicoll RA, Schmitz D (2005) Synaptic plasticity at hippocampal mossy fibre synapses. *Nat Rev Neurosci* 6(11):863–76.
163. Turrigiano GG, Leslie KR, Desai NS, Rutherford LC, Nelson SB (1998) Activity-dependent scaling of quantal amplitude in neocortical neurons. *Nature* 391(6670):892–6.
164. Desai NS (2003) Homeostatic plasticity in the CNS: Synaptic and intrinsic forms. *J Physiol Paris* 97(4-6):391–402.
165. Misonou H, et al. (2004) Regulation of ion channel localization and phosphorylation by neuronal activity. *Nat Neurosci* 7(7):711–8.
166. Kourrich S, Calu DJ, Bonci A (2015) Intrinsic plasticity: an emerging player in addiction. *Nat Rev Neurosci* 16(3):173–84.
167. Sjöström PJ, Rancz EA, Roth A, Häusser M (2008) Dendritic excitability and synaptic plasticity. *Physiol Rev* 88:769–840.
168. Turrigiano GG (1999) Homeostatic plasticity in neuronal networks: the more things change, the more they stay the same. *Trends Neurosci* 22(5):221–7.
169. Cudmore RH, Fronzaroli-Molinieres L, Giraud P, Debanne D (2010) Spike-time precision and network synchrony are controlled by the homeostatic regulation of the D-type potassium current. *J Neurosci* 30(38):12885–95.
170. D'Angelo E (2010) Homeostasis of intrinsic excitability: making the point. *J Physiol* 588:901–2.
171. Hanse E (2008) Associating synaptic and intrinsic plasticity. *J Physiol* 586(3):691–2.
172. Kaczorowski CC, Disterhoft J, Spruston N (2007) Stability and plasticity of intrinsic membrane properties in hippocampal CA1 pyramidal neurons: effects of internal anions. *J Physiol* 578(Pt 3):799–818.
173. Lee KY, Chung HJ (2014) NMDA receptors and L-type voltage-gated Ca^{2+} channels mediate the expression of bidirectional homeostatic intrinsic plasticity in cultured hippocampal neurons. *Neuroscience* 277:610–623.
174. Robbins C a., Tempel BL (2012) $K_{v1.1}$ and $K_{v1.2}$: Similar channels, different seizure models. *Epilepsia* 53:134–41.
175. Gähwiler BH, Capogna M, Debanne D, McKinney RA, Thompson SM (1997) Organotypic slice sultures: a technique has come of age. 471–7.
176. Echegoyen J, Neu A, Graber KD, Soltesz I (2007) Homeostatic plasticity studies using in vivo hippocampal activity-blockade: Synaptic scaling, intrinsic plasticity and age-dependence. *PLoS One* 2(8):e700.
177. Powell KL, et al. (2008) Decreases in HCN mRNA expression in the hippocampus after kindling and status epilepticus in adult rats. *Epilepsia* 49(10):1686–95.
178. Fan Y, et al. (2005) Activity-dependent decrease of excitability in rat hippocampal neurons through increases in I_h. *Nat Neurosci* 8(11):1542–51.
179. Van Welie I, van Hooft JA, Wadman WJ (2004) Homeostatic scaling of neuronal excitability by synaptic modulation of somatic hyperpolarization-activated Ih channels. *Proc Natl Acad Sci U S A* 101(14):5123–8.
180. Campanac E, Daoudal G, Ankri N, Debanne D (2008) Downregulation of dendritic I_h in CA1 pyramidal neurons after LTP. *J Neurosci* 28(34):8635–43.
181. Blumenfeld H, et al. (2009) Role of hippocampal sodium channel $Na_{v1.6}$ in kindling epileptogenesis. *Epilepsia* 50(1):44–55.
182. Bennet C (2010) *Cannabis and the soma solution* (Trine Day, Walterville).
183. Clarke R, Watson D (2007) Cannabis and natural cannabis medicines. *Marijuana and the Cannabinoids* (Humana Press, Totowa).
184. Gaoni Y, Mechoulam R (1964) Isolation, structure and partial synthesis of an active constituent of hashish. *J Am Chem Soc* 86(8):1646–7.
185. Devane W, Dysarz F, Johnsont MR, Melvin LS, Howlett AC (1988) Determination and characterization of a cannabinoid receptor in rat brain. *Mol Pharmacol* 34:605–13.
186. Matsuda LA, Lolait SJ, Brownstein MJ, Young AC, Bonner TI (1990) Structure of a cannabinoid receptor and functional expression of the cloned cDNA. *Nature* 346(6284):561–4.
187. Devane WA, et al. (1992) Isolation and structure of a brain constituent that binds to the cannabinoid receptor. *Science* 258:1946–9.
188. Mechoulam R, et al. (1995) Identification of an endogenous 2-monoglyceride, present in canine gut, that binds to cannabinoid receptors. 50(1):83–90.
189. Kogan N, Mechoulam R (2006) The chemistry of endocannabinoids. *J Endocrinol Invest* 28:3–10.
190. Fukaya T, et al. (2007) Arachidonic acid preserves hippocampal neuron membrane fluidity in senescent rats. *Neurobiol Aging* 28(8):1179–86.
191. Piomelli D (2000) Arachidonic Acid - a tale of two roles. *Psychopharmacology - 4th Generation of Progress* (Lippincott Williams & Wilkins).

192. Basavarajappa BS (2007) Critical enzymes involved in endocannabinoid metabolism. *Protein Pept Lett* 14(3):237–46.
193. Piomelli D (2003) The molecular logic of endocannabinoid signalling. *Nat Rev Neurosci* 4(11):873–84.
194. Di Marzo V (2011) Endocannabinoid signaling in the brain: biosynthetic mechanisms in the limelight. *Nat Neurosci* 14(1):9–15.
195. Oudin MJ, Hobbs C, Doherty P (2011) DAGL-dependent endocannabinoid signalling: roles in axonal pathfinding, synaptic plasticity and adult neurogenesis. *Eur J Neurosci* 34(10):1634–46.
196. Di Marzo V, Melck D, Bisogno T, De Petrocellis L (1998) Endocannabinoids: endogenous cannabinoid receptor ligands with neuromodulatory action. *Trends Neurosci* 21(12):521–8.
197. Tanimura A, et al. (2010) The endocannabinoid 2-arachidonoylglycerol produced by diacylglycerol lipase alpha mediates retrograde suppression of synaptic transmission. *Neuron* 65(3):320–7.
198. Gao Y, et al. (2010) Loss of retrograde endocannabinoid signaling and reduced adult neurogenesis in diacylglycerol lipase knock-out mice. *J Neurosci* 30(6):2017–24.
199. Maejima T, et al. (2005) Synaptically driven endocannabinoid release requires Ca^{2+}-assisted metabotropic glutamate receptor subtype 1 to phospholipase C β4 signaling cascade in the cerebellum. *J Neurosci* 25(29):6826–35.
200. Stella N, Schweitzer P, Piomelli D (1997) A second endogenous cannabinoid that modulates long-term potentiation. *Nature* 388(6644):773–8.
201. Fukudome Y, et al. (2004) Two distinct classes of muscarinic action on hippocampal inhibitory synapses : M_2-mediated direct suppression and M_1/M_3 -mediated indirect suppression through endocannabinoid signalling. 19:2682–92.
202. Kim J, Isokawa M, Ledent C, Alger BE (2002) Activation of muscarinic acetylcholine receptors enhances the release of endogenous cannabinoids in the hippocampus. *J Neurosci* 22(23):10182–91.
203. Mechoulam R, Fride E, Di Marzo V (1998) Endocannabinoids. *Eur J Pharmacol* 359(1):1–18.
204. Hashimotodani Y, et al. (2013) Acute inhibition of diacylglycerol lipase blocks endocannabinoid-mediated retrograde signalling: evidence for on-demand biosynthesis of 2-arachidonoylglycerol. *J Physiol* 591:4765–76.
205. Barnett-Norris J, Lynch D, Reggio P (2005) Lipids, lipid rafts and caveolae: their importance for GPCR signaling and their centrality to the endocannabinoid system. *Life Sci* 77:1625–39.
206. Song Z, Bonner T (1996) A lysine residue of the cannabinoid receptor is critical for receptor recognition by several agonists but not WIN55212-2. *Mol Pharmacol* 49(5):891–6.
207. Navarrete M, Araque A (2008) Endocannabinoids mediate neuron-astrocyte communication. *Neuron* 57(6):883–93.
208. Walter L, Franklin A, Witting A, Möller T, Stella N (2002) Astrocytes in culture produce anandamide and other acylethanolamides. *J Biol Chem* 277(23):20869–76.
209. Katona I, et al. (2006) Molecular composition of the endocannabinoid system at glutamatergic synapses. *J Neurosci* 26(21):5628–37.
210. Yoshino H, et al. (2011) Postsynaptic diacylglycerol lipase mediates retrograde endocannabinoid suppression of inhibition in mouse prefrontal cortex. *J Physiol* 589(20):4857–84.
211. Ludányi A, et al. (2011) Complementary synaptic distribution of enzymes responsible for synthesis and inactivation of the endocannabinoid 2-arachidonoylglycerol in the human hippocampus. *Neuroscience* 174:50–63.
212. Kallendrusch S, et al. (2012) Intrinsic up-regulation of 2-AG favors an area specific neuronal survival in different in vitro models of neuronal damage. *PLoS One* 7(12):1–11.
213. Gomez O, et al. (2010) The constitutive production of the endocannabinoid 2-arachidonoylglycerol participates in oligodendrocyte differentiation. *Glia* 58(16):1913–27.
214. Gulyas AI, et al. (2004) Segregation of two endocannabinoid-hydrolyzing enzymes into pre- and postsynaptic compartments in the rat hippocampus, cerebellum and amygdala. *Eur J Neurosci* 20(2):441–58.
215. Blankman JL, Simon GM, Cravatt BF (2007) A comprehensive profile of brain enzymes that hydrolyze the endocannabinoid 2-Arachidonoylglycerol. *Chem Biol* 14(12):1347–56.
216. Tanimura A, et al. (2012) Synapse type-independent degradation of the endocannabinoid 2-arachidonoylglycerol after retrograde synaptic suppression. *Proc Natl Acad Sci U S A* 109(30):12195–200.
217. Marrs WR, et al. (2010) The serine hydrolase ABHD6 controls the accumulation and efficacy of 2-AG at cannabinoid receptors. *Nat Neurosci* 13(8):951–7.
218. Herkenham M, et al. (1990) Cannabinoid receptor localization in brain. 87:1932–6.
219. Matsuda LA, Bonner TI, Lolait SJ (1993) Localization of cannabinoid receptor mRNA in rat brain. *J Comp Neurol* 327(4):535–550.
220. Gérard CM, Mollereau C, Vassart G, Parmentier M, Gerard CM (1991) Molecular cloning of a human cannabinoid receptor which is also expressed in testis. *Biochem J* 279 (1):129–34.
221. Johns DG, et al. (2007) The novel endocannabinoid receptor GPR55 is activated by atypical cannabinoids but does not mediate their vasodilator effects. *Br J Pharmacol* 152(5):825–31.
222. Ryberg E, et al. (2007) The orphan receptor GPR55 is a novel cannabinoid receptor. *Br J Pharmacol* 152(7):1092–1101.

223. De Petrocellis L, Di Marzo V (2010) Non-CB1, non-CB_2 receptors for endocannabinoids, plant cannabinoids, and synthetic cannabimimetics: focus on G-protein-coupled receptors and transient receptor potential channels. *J neuroimmune Pharmacol* 5(1):103–21.
224. McPartland JM, Glass M, Pertwee RG (2007) Meta-analysis of cannabinoid ligand binding affinity and receptor distribution: interspecies differences. *Br J Pharmacol* 152(5):583–93.
225. Marsicano G, Kuner R (2008) Anatomical distribution of receptors, ligands and enzymes in the brain and in the spinal cord: circuitries and neurochemistry. *Cannabinoids and the Brain* (Springer Science & Business Media).
226. Köfalvi A, et al. (2005) Involvement of cannabinoid receptors in the regulation of neurotransmitter release in the rodent striatum: a combined immunochemical and pharmacological analysis. *J Neurosci* 25(11):2874–84.
227. Dudok B, et al. (2014) Cell-specific STORM super-resolution imaging reveals nanoscale organization of cannabinoid signaling. *Nat Neurosci* 18(1):75–86.
228. Monory K, et al. (2007) Genetic dissection of behavioural and autonomic effects of Delta(9)-tetrahydrocannabinol in mice. *PLoS Biol* 5(10):e269.
229. Monory K, et al. (2006) The endocannabinoid system controls key epileptogenic circuits in the hippocampus. *Neuron* 51(4):455–46.
230. Steindel F, et al. (2013) Neuron-type specific cannabinoid-mediated G protein signalling in mouse hippocampus. *J Neurochem* 124(6):795–807.
231. Kano M, Ohno-Shosaku T, Hashimotodani Y, Uchigashima M, Watanabe M (2009) Endocannabinoid-mediated control of synaptic transmission. *Physiol Rev* 89(1):309–80.
232. Onaivi ES, Ishiguro H, Gu S, Liu Q-R (2012) CNS effects of CB_2 cannabinoid receptors: beyond neuro-immuno-cannabinoid activity. *J Psychopharmacol* 26:92–103.
233. Boon FS Den, et al. (2012) Excitability of prefrontal cortical pyramidal neurons is modulated by activation of intracellular type-2 cannabinoid receptors. 109(9):1–6.
234. Zhang H-Y, et al. (2014) Cannabinoid CB_2 receptors modulate midbrain dopamine neuronal activity and dopamine-related behavior in mice. *Proc Natl Acad Sci* 111:E5007–E5015.
235. Felder CC, et al. (1995) Comparison of the pharmacology and signal transduction of the human cannabinoid CB_1 and CB_2 receptors. (48):443–50.
236. Atwood BK, Straiker A, Mackie K (2012) CB_2 cannabinoid receptors inhibit synaptic transmission when expressed in cultured autaptic neurons. *Neuropharmacology* 63(4):514–523.
237. Ritter SL, Hall R a (2009) Fine-tuning of GPCR activity by receptor-interacting proteins. *Nat Rev Mol Cell Biol* 10(12):819–830.
238. Neubig RR, Siderovski DP (2002) Regulators of G-protein signalling as new central nervous system drug targets. *Nat Rev Drug Discov* 1(3):187–197.
239. Filmore D (2004) It's a GPCR world. *Mod drug Discov* 7(11):24–27.
240. Turu G, Hunyady L (2010) Signal transduction of the CB_1 cannabinoid receptor. *J Mol Endocrinol* 44(2):75–85.
241. Callén L, et al. (2012) Cannabinoid receptors CB_1 and CB_2 form functional heteromers in brain. *J Biol Chem* 287(25):20851–65.
242. Dhopeshwarkar A, Mackie K (2014) CB_2 cannabinoid receptors as a therapeutic target - what does the future hold? *Mol Pharmacol Fast Forw*. doi:10.1124/mol.114.094649
243. Derkinderen P, et al. (2003) Regulation of extracellular signal-regulated kinase by cannabinoids in hippocampus. *J Neurosci* 23(6):2371–82.
244. Prather P (2008) CB_2 receptors: molecular, signaling and trafficking properties. *Cannabinoids and the Brain* (Springer Science & Business Media).
245. Twitchell W, et al. (2012) Cannabinoids inhibit N- and P/Q-type calcium channels in cultured rat hippocampal neurons. *J Neurophysiol* 78:43–50.
246. Mackie K, Hille B (1992) Cannabinoids inhibit N-type calcium channels in neuroblastoma-glioma cells. *Proc Natl Acad Sci* 89:3825–389.
247. Den Boon FS, et al. (2014) Endocannabinoids produced upon action potential firing evoke a Cl^- current via type-2 cannabinoid receptors in the medial prefrontal cortex. *Eur J Physiol*. doi 10.1007/s00424-014-1502-6.
248. Mu J, Zhuang SY, Kirby MT, Hampson RE, Deadwyler S a (1999) Cannabinoid receptors differentially modulate potassium A and D currents in hippocampal neurons in culture. *J Pharmacol Exp Ther* 291(2):893–902.
249. Deadwyler S, Hampson RE, Mu J, Whyte A, Childers SR (1995) Cannabinoids modulate voltage sensitive potassium A-current in hippocampal neurons via a cAMP-dependent process. *J Pharmacol Exp Ther* 273: 734-743.
250. Childers SR, Deadwyler SA (1996) Role of cyclic AMP in the actions of cannabinoid receptors.*Biochem Pharmacol* 52(6):819–27.
251. Kirby MT, Hampson RE, Deadwyler SA (2000) Cannabinoid receptor activation in CA1 pyramidal cells in adult rat hippocampus. *Brain Res* 863(1-2):120–31.

252. Schweitzer P (2000) Cannabinoids decrease the K^+ M-current in hippocampal CA1 neurons. *J Neurosci* 20(1):51–8.
253. Henry DJ, Chavkin C (1995) Activation of inwardly rectifying potassium channels (GIRK1) by co-expressed rat brain cannabinoid receptors in Xenopus oocytes. *Neurosci Biobehav Rev* 186:91–4.
254. Ho B, Uezono Y, Takada S, Takase I, Izumi F (1999) Coupling of the expressed cannabinoid CB_1 and CB_2 receptors to phospholipase C and G Protein-coupled inwardly rectifying K^+ channels. *Recept Channels* 6:363–74.
255. Marinelli S, Pacioni S, Cannich A, Marsicano G, Bacci A (2009) Self-modulation of neocortical pyramidal neurons by endocannabinoids. *Nat Neurosci* 12(12):1488–90.
256. Carta M, et al. (2014) Membrane lipids tune synaptic transmission by direct modulation of presynaptic potassium channels. *Neuron* 81:787–99.
257. Chávez AE, Chiu CQ, Castillo PE (2010) TRPV1 activation by endogenous anandamide triggers postsynaptic long-term depression in dentate gyrus. *Nat Neurosci* 13(12):1511–8.
258. Liao C, Zheng J, David LS, Nicholson RA (2004) Inhibition of voltage-sensitive sodium channels by the cannabinoid 1 receptor antagonist AM-251 in mammalian brain. *Basic Clin Pharmacol Toxicol* 94(2):73–8.
259. Shen M, Piser TM, Seybold VS, Thayer S a (1996) Cannabinoid receptor agonists inhibit glutamatergic synaptic transmission in rat hippocampal cultures. *J Neurosci* 16(14):4322–34.
260. Llano I, Leresche N, Marty A (1991) Calcium entry increases the sensitivity of cerebellar Purkinje cells to applied GABA and decreases inhibitory synaptic currents. *Neuron* 6(4):565–74.
261. Alger BE, Pitler TA, Williamson A (1990) A prolonged post-tetanic hyperpolarization in rat hippocampal pyramidal cells in vitro. *Brain Res*.521:118-24.
262. Pitler TA, Alger B (1992) Postsynaptic spike firing reduces synaptic $GABA_A$ responses in hippocampal pyramidal cells. *J Neurosci* 12(10):4122–32.
263. Pitler TA, Alger BE (1994) Depolarization-induced suppression of GABAergic inhibition in rat hippocampal pyramidal cells: G protein involvement in a presynaptic mechanism. *Neuron* 13(6):1447–55.
264. Alger BE, et al. (1996) Retrograde signalling in depolarization-induced suppression of inhibition in rat hippocampal CA1 cells. *J Physiol* 496 (1):197–209.
265. Bisogno T, et al. (1997) Biosynthesis, release and degradation of the novel endogenous cannabimimetic metabolite 2-arachidonoylglycerol in mouse neuroblastoma cells. *Biochem J* 322:671–7.
266. Földy C, Neu A, Jones M V, Soltesz I (2006) Presynaptic, activity-dependent modulation of cannabinoid type 1 receptor-mediated inhibition of GABA release. *J Neurosci* 26(5):1465–9.
267. Bénard G, et al. (2012) Mitochondrial CB_1 receptors regulate neuronal energy metabolism. *Nat Neurosci* 15:558–64.
268. Pan B, et al. (2009) Blockade of 2-arachidonoylglycerol hydrolysis by selective monoacylglycerol lipase inhibitor 4-nitrophenyl 4-(dibenzo[d][1,3]dioxol-5-yl(hydroxy)methyl)piperidine-1-carboxylate (JZL184) enhances retrograde endocannabinoid signaling. *J Pharmacol Exp Ther* 331(2):591–7.
269. Ohno-Shosaku T, et al. (2007) Endocannabinoid signalling triggered by NMDA receptor-mediated calcium entry into rat hippocampal neurons. *J Physiol* 584(2):407–18.
270. Varma N, et al. (2002) Presynaptic factors in the regulation of DSI expression in hippocampus. *Neuropharmacology* 43(4):550–62.
271. Földy C, Lee SY, Szabadics J, Neu A, Soltesz I (2007) Cell type-specific gating of perisomatic inhibition by cholecystokinin. *Nat Neurosci* 10(9):1128–30.
272. Hampson RE, Zhuang S-Y, Weiner JL, Deadwyler SA (2003) Functional significance of cannabinoid-mediated, depolarization-induced suppression of inhibition (DSI) in the hippocampus. *J Neurophysiol* 90(1):55–64.
273. Maejima T, Hashimoto K, Yoshida T, Aiba A, Kano M (2001) Presynaptic inhibition caused by retrograde signal from metabotropic glutamate to cannabinoid receptors. *Neuron* 31(3):463–475.
274. Yin HH, Lovinger DM (2006) Frequency-specific and D_2 receptor-mediated inhibition of glutamate release by retrograde endocannabinoid signaling. *Proc Natl Acad Sci U S A* 103(21):8251–6.
275. Gerdeman GL, Ronesi J, Lovinger DM (2002) Postsynaptic endocannabinoid release is critical to long-term depression in the striatum. *Nat Neurosci* 5(5):446–51.
276. Robbe D, Kopf M, Remaury A, Bockaert J, Manzoni OJ (2002) Endogenous cannabinoids mediate long-term synaptic depression in the nucleus accumbens. *Proc Natl Acad Sci U S A* 99(12):8384–8.
277. Tzounopoulos T, Rubio ME, Keen JE, Trussell LO (2007) Coactivation of pre- and postsynaptic signaling mechanisms determines cell-specific spike timing-dependent plasticity. *Neuron* 54(2):291–301.
278. Chevaleyre V, et al. (2007) Endocannabinoid-mediated long-term plasticity requires cAMP/PKA signaling and RIM1alpha. *Neuron* 54(5):801–12.
279. Yasuda H, Huang Y, Tsumoto T (2008) Regulation of excitability and plasticity by endocannabinoids and PKA in developing hippocampus. *Proc Natl Acad Sci U S A* 105(8):3106–11.
280. Kim J, Alger BE (2010) Reduction in endocannabinoid tone is a homeostatic mechanism for specific inhibitory synapses. *Nat Neurosci* 13(5):592–600.

281. Suárez J, et al. (2009) Early maternal deprivation induces gender-dependent changes on the expression of hippocampal CB_1 and CB_2 cannabinoid receptors of neonatal rats. *Hippocampus* 19(7):623–32.
282. Karlócai MR, et al. (2011) Redistribution of CB_1 cannabinoid receptors in the acute and chronic phases of pilocarpine-induced epilepsy. *PLoS One* 6(11):e27196.
283. Schoeler T, Bhattacharyya S (2013) The effect of cannabis use on memory function: an update. *Subst Abuse Rehabil* 4:11–27.
284. Meier MH, et al. (2012) Persistent cannabis users show neuropsychological decline from childhood to midlife. *Proc Natl Acad Sci* 109(40):E2657–E2664.
285. Riba J, et al. (2015) Telling true from false: cannabis users show increased susceptibility to false memories. *Mol Psychiatry* (20):772–77.
286. Smith MJ, et al. (2014) Cannabis-related working memory deficits and associated subcortical morphological differences in healthy individuals and schizophrenia subjects. *Schizophr Bull* 40(2):287–99.
287. García-Gutiérrez MS, et al. (2013) Synaptic plasticity alterations associated with memory impairment induced by deletion of CB_2 cannabinoid receptors. *Neuropharmacology* 73: 388-96.
288. Reibaud M, et al. (1999) Enhancement of memory in cannabinoid CB_1 receptor knock-out mice. *Eur J Pharmacol* 379(1):1–2.
289. Jenniches I, et al. (2015) Anxiety, stress, and fear response in mice with reduced endocannabinoid levels. *Biol Psychiatry* doi: 10.1016/j.biopsych.2015.03.033..
290. Fride E, et al. (2001) Critical role of the endogenous cannabinoid system in mouse pup suckling and growth. *Eur J Pharmacol* 419(2-3):207–14.
291. Di Marzo V, et al. (2001) Leptin-regulated endocannabinoids are involved in maintaining food intake. *Nature* 410(6830):822–25.
292. Sternson SM, Nicholas Betley J, Cao ZFH (2013) Neural circuits and motivational processes for hunger. *Curr Opin Neurobiol* 23(3):353–60.
293. Ishiguro H, et al. (2010) Brain Cannabinoid CB_2 Receptor in Schizophrenia. *Biol Psychiatry* 67(10):974–82.
294. García-Gutiérrez MS, Manzanares J (2011) Overexpression of CB_2 cannabinoid receptors decreased vulnerability to anxiety and impaired anxiolytic action of alprazolam in mice. *J Psychopharmacol* 25(1):111–20.
295. García-Gutiérrez MS, García-Bueno B, Zoppi S, Leza JC, Manzanares J (2012) Chronic blockade of cannabinoid CB_2 receptors induces anxiolytic-like actions associated with alterations in $GABA_A$ receptors. *Br J Pharmacol* 165(4):951–64.
296. García-Gutiérrez MS, Pérez-Ortiz JM, Gutiérrez-Adán A, Manzanares J (2010) Depression-resistant endophenotype in mice overexpressing cannabinoid CB_2 receptors. *Br J Pharmacol* 160(7):1773–1784.
297. Ortega-Alvaro A, Aracil-Fernández A, García-Gutiérrez MS, Navarrete F, Manzanares J (2011) Deletion of CB_2 cannabinoid receptor induces schizophrenia-related behaviors in mice. *Neuropsychopharmacology* 36(7):1489–504.
298. Khella R, Short JL, Malone DT (2014) CB_2 receptor agonism reverses MK-801-induced disruptions of prepulse inhibition in mice. *Psychopharmacology* doi 10.1007/s00213-014-3481-x.
299. Xi ZX, et al. (2011) Brain Cannabinoid CB_2 Receptors Modulate Cocaine's Actions in Mice. *Nat Neurosci* 14(9):1160–66.
300. Comings DE, et al. (1997) Cannabinoid receptor gene (CNR1): association with i.v. drug use. *Mol Psychiatry* 2(2):161–8.
301. Li T, et al. (2000) No association between (AAT)n repeats in the cannabinoid receptor gene (CNR1) and heroin abuse in a Chinese population. *Mol Psychiatry* 5(2):128–30.
302. Holderith N, et al. (2011) Cannabinoids attenuate hippocampal γ oscillations by suppressing excitatory synaptic input onto CA3 pyramidal neurons and fast spiking basket cells. *J Physiol* 589(Pt 20):4921–34.
303. Maier N, et al. (2012) Cannabinoids disrupt hippocampal sharp wave-ripples via inhibition of glutamate release. *Hippocampus* 22(6):1350–1262.
304. Robbe D, Buzsáki G (2009) Alteration of theta timescale dynamics of hippocampal place cells by a cannabinoid is associated with memory impairment. *J Neurosci* 29(40):12597–605.
305. Tukker JJ, Fuentealba P, Hartwich K, Somogyi P, Klausberger T (2007) Cell type-specific tuning of hippocampal interneuron firing during gamma oscillations in vivo. *J Neurosci* 27(31):8184–9.
306. Stark E, et al. (2013) Inhibition-induced theta resonance in cortical circuits. *Neuron* 80(5):1263–76.
307. Klausberger T, et al. (2003) Brain-state- and cell-type-specific firing of hippocampal interneurons in vivo. *Nature* 421:844–8.
308. Maier N, et al. (2011) Coherent phasic excitation during hippocampal ripples. *Neuron* 72(1):137–52.
309. Bartos M, Vida I, Jonas P (2007) Synaptic mechanisms of synchronized gamma oscillations in inhibitory interneuron networks. *Nat Rev Neurosci* 8(1):45–56.
310. Heyser CJ, Hampson RE, Deadwyler SA (1993) Effects of delta-9-tetrahydrocannabinol on delayed match to sample performance in rats: alterations in short-term memory associated with changes in task specific firing of hippocampal cells. *J Pharmacol Exp Ther* 264(1):294–307.

311. Sauer B, Henderson N (1988) Site-specific DNA recombination in mammalian cells by the Cre recombinase of bacteriophage P1. *Proc Natl Acad Sci U S A* 85(14):5166–70.
312. Hoesche C, Sauerwald A, Veh RW, Krippl B, Kilimann MW (1993) The 5'-flanking region of the rat synapsin I gene directs neuron-specific and developmentally regulated reporter gene expression in transgenic mice. *J Biol Chem* 268(35):26494–502.
313. Zhu Y, et al. (2001) Ablation of NF1 function in neurons induces abnormal development of cerebral cortex and reactive gliosis in the brain. *Genes Dev* 15(7):859–76.
314. Sambrook J, Russell D (2001) *Molecular cloning: A laboratory manual* (Cold Spring Harbor Laboratory Press, New York).
315. Haas HL, Schaerer B, Vosmansky M (1979) A simple perfusion chamber for the study of nervous tissue slices in vitro. *J Neurosci Methods* 1(4):323–5.
316. Iwamura H, Suzuki H, Ueda Y, Kaya T, Inaba T (2001) In vitro and in vivo pharmacological characterization of JTE-907, a novel selective ligand for cannabinoid CB_2 receptor. *J Pharmacol Exp Ther* 296(2):420–5.
317. Hanus L, et al. (1999) HU-308: a specific agonist for CB_2, a peripheral cannabinoid receptor. *Proc Natl Acad Sci U S A* 96(25):14228–33.
318. Rinaldi-Carmona M, et al. (1998) SR144528, the first potent and selective antagonist of the CB_2 cannabinoid receptor. *J Pharmacol Exp Ther* 284(2):644–50.
319. Lan R, et al. (1999) Structure-activity relationships of pyrazole derivatives as cannabinoid receptor antagonists. (42):769–776.
320. Kyrozis A, Reichling DB (1995) Perforated-patch recording with gramicidin avoids artifactual changes in intracellular chloride concentration. *J Neurosci Methods* 57:27–35.
321. Diba K, Buzsáki G (2008) Hippocampal network dynamics constrain the time lag between pyramidal cells across modified environments. *J Neurosci* 28(50):13448–56.
322. Barry PH (1994) JPCalc, a software package for calculating liquid junction potential corrections in patch-clamp, intracellular, epithelial and bilayer measurements and for correcting junction potential measurements. *J Neurosci Methods* 51(1):107–16.
323. Barry PH, Lynch JW (1991) Liquid junction potentials and small cell effects in patch-clamp analysis. *J Membr Biol* 121:101–17.
324. Zemankovics R, Káli S, Paulsen O, Freund TF, Hájos N (2010) Differences in subthreshold resonance of hippocampal pyramidal cells and interneurons: the role of h-current and passive membrane characteristics. *J Physiol* 588:2109–32.
325. Lancaster B, Adams PR, Brook S (1986) Calcium-dependent current generating the afterhyperpolarization of hippocampal neurons. 55(6): 1268-82.
326. Eckert WA, Willcockson HH, Light AR (2001) Interference of biocytin with opioid-evoked hyperpolarization and membrane properties of rat spinal substantia gelatinosa neurons. *Neurosci Lett* 297:117–20.
327. Bacci A, Huguenard JR, Prince DA (2004) Long-lasting self-inhibition of neocortical interneurons mediated by endocannabinoids. *Nature* 431:313–6.
328. Marinelli S, Pacioni S, Cannich A, Marsicano G, Bacci A (2009) Self-modulation of neocortical pyramidal neurons by endocannabinoids. *Nat Neurosci* 12(12):1488–90.
329. Salter MW, Beggs S (2014) Sublime microglia: Expanding roles for the guardians of the CNS. *Cell* 158(1):15–24.
330. Sugiura T, Kobayashi Y, Oka S, Waku K (2002) Biosynthesis and degradation of anandamide and 2-arachidonoylglycerol and their possible physiological significance. *Prostaglandins Leukot Essent Fatty Acids* 66(2-3):173–92.
331. Hashimotodani Y, Ohno-Shosaku T, Maejima T, Fukami K, Kano M (2008) Pharmacological evidence for the involvement of diacylglycerol lipase in depolarization-induced endocanabinoid release. *Neuropharmacology* 54(1):58–67.
332. Straiker A, Mackie K (2005) Depolarization-induced suppression of excitation in murine autaptic hippocampal neurones. *J Physiol* 569:501–17.
333. Younts TJ, Chevaleyre V, Castillo PE (2013) CA1 pyramidal cell theta-burst firing triggers endocannabinoid-mediated long-term depression at both somatic and dendritic inhibitory synapses. *J Neurosci* 33(34):13743–57.
334. Palmer MJ, Irving AJ, Seabrook GR, Jane DE, Collingridge GL (1998) The group I mGlu receptor agonist DHPG induces a novel form of LTD in the CA1 region of the hippocampus. *Neuropharmacology* 36(11-12):1517–32.
335. Lodge D, et al. (2013) Antagonists reversibly reverse chemical LTD induced by group I, group II and group III metabotropic glutamate receptors. *Neuropharmacology* 74:135–46.
336. Mackie K, Lai Y, Westenbroek R, Mitchell R (1995) Cannabinoids activate an inwardly rectifying potassium conductance and inhibit Q-type calcium currents in AtT20 cells transfected with rat brain cannabinoid receptor. *J Neurosci* 15(10):6552–61.
337. Takahashi KA, Castillo PE (2006) The CB_1 cannabinoid receptor mediates glutamatergic synaptic suppression in the hippocampus. *Neuroscience* 139(3):795–802.
338. Frerking M, Schulte J, Wiebe SP, Stäubli U (2005) Spike timing in CA3 pyramidal cells during behavior: implications for synaptic transmission. *J Neurophysiol* 94(2):1528–40.

339. Walter L, et al. (2003) Nonpsychotropic cannabinoid receptors regulate microglial cell migration. *J Neurosci* 23(4):1398–1405.
340. Olbrich HG, Braak H (1985) Ratio of pyramidal cells versus non-pyramidal cells in sector CA1 of the human Ammon's horn. *Anat Embryol (Berl)* 173(1):105–10.
341. Jonas P, Bischofberger J, Fricker D, Miles R (2004) Interneuron Diversity series: Fast in, fast out--temporal and spatial signal processing in hippocampal interneurons. *Trends Neurosci* 27(1):30–40.
342. Geiger JR, Lübke J, Roth a, Frotscher M, Jonas P (1997) Submillisecond AMPA receptor-mediated signaling at a principal neuron-interneuron synapse. *Neuron* 18(6):1009–23.
343. Geiger JRP, et al. (1995) Relative abundance of subunit mRNAs determines gating and calcium permeability of AMPA receptors in principal neurons and interneurons in rat CNS. *Neuron* 15:193–204.
344. Krichmar JL, Nasuto SJ, Scorcioni R, Washington SD, Ascoli GA (2002) Effects of dendritic morphology on CA3 pyramidal cell electrophysiology: A simulation study. *Brain Res* 941(1-2):11–28.
345. Min R, Di Marzo V, Mansvelder HD (2010) DAG lipase involvement in depolarization-induced suppression of inhibition: does endocannabinoid biosynthesis always meet the demand? *Neuroscientist* 16(6):608–13.
346. Galiègue S, et al. (1995) Expression of central and peripheral cannabinoid receptors in human immune tissues and leukocyte subpopulations. *Eur J Biochem* 232(1):54–61.
347. Gong J-P, et al. (2006) Cannabinoid CB_2 receptors: immunohistochemical localization in rat brain. *Brain Res* 1071(1):10–23.
348. Maienschein V, Marxen M, Volknandt W, Zemmermann H (1999) A plethora of presynaptic proteins associated with ATP-storing organelles in cultured astrocytes. *Glia* 26(3):233–44.
349. Monaghan PL, et al. (1986) Immunocytochemical characterization of neuron-rich primary cultures of embryonic rat brain cells by established neuronal and glial markers and by monospecific antisera against cyclic nucleotide-dependent protein kinases and the synaptic vesicle protein sy. *Brain Res* 363(2):205–21.
350. Pertwee RG, et al. (2010) International union of basic and clinical pharmacology. LXXIX. Cannabinoid receptors and their ligands : beyond CB_1 and CB_2. *Pharmacol Rev* 62(4):588–631.
351. Bénard G, et al. (2012) Mitochondrial CB_1 receptors regulate neuronal energy metabolism. *Nat Neurosci* 15(4):558–64.
352. Marsicano G, et al. (2003) CB_1 cannabinoid receptors and on-demand defense against excitotoxicity. *Science* 302(5642):84–8.
353. Sjöström PJ, Rancz EA, Roth A, Häusser M (2008) Dendritic excitability and synaptic plasticity. *Physiol Rev* 88:769–840.
354. Sakmann B, Neher E (1984) Patch clamp techniques for studying ionic channels in excitable membranes. *Annu Rev Physiol* 46:455-72.
355. Kirov SA, Petrak LJ, Fiala JC, Harris KM (2004) Dendritic spines disappear with chilling but proliferate excessively upon rewarming of mature hippocampus. *Neuroscience* 127(1):69–80.
356. Reijmers LG, Perkins BL, Matsuo N, Mayford M (2007) Localization of a stable neural correlate of associative memory. *Science* 317(5842):1230–3.
357. Liu X, et al. (2012) Optogenetic stimulation of a hippocampal engram activates fear memory recall. *Nature* 484(7394):381–385.
358. Ramirez S, et al. (2013) Creating a false memory in the hippocampus. *Science* 341:387–92.
359. Ryan T, Roy D, Pignatelli M, Arons A, Tonegawa S (2015) Engram cells retain memory under retrograde amnesia. *Science (80-)* 348:1007–13.
360. Gruart A, Muñoz MD, Delgado-García JM (2006) Involvement of the CA3-CA1 synapse in the acquisition of associative learning in behaving mice. *J Neurosci* 26(4):1077–87.
361. Chevaleyre V, Castillo PE (2004) Endocannabinoid-mediated metaplasticity in the hippocampus. *Neuron* 43(6):871–81.
362. Brenowitz SD, Regehr WG (2005) Associative short-term synaptic plasticity mediated by endocannabinoids. *Neuron* 45(3):419–31.
363. Navarro M, et al. (1997) Acute administration of the CB_1 cannabinoid receptor antagonist SR 141716A induces anxiety-like responses in the rat. *Neuroreport* 8(2):491–96.
364. Perreault P, Avoli M (1991) Physiology and pharmacology of epileptiform activity induced by 4-aminopyridine in rat hippocampal slices. *J Neurophysiol* 65(4):771–85.
365. Contractor A, Traub RD, Buhl EH, Heinemann SF, Mcbain CJ (2004) Distinct Roles for the Kainate Receptor Subunits GluR5 and GluR6 in Kainate-Induced Hippocampal Gamma Oscillations. *J Neurosci* 24(43):9658–68.
366. Moser EI, Kropff E, Moser M-B (2008) Place cells, grid cells, and the brain's spatial representation system. *Annu Rev Neurosci* 31:69–89.
367. Lee D, Lin B-J, Lee AK (2012) Hippocampal place fields emerge upon single-cell manipulation of excitability during behavior. *Science* 337(6096):849–53.
368. Lisman J, Buzsáki G (2008) A neural coding scheme formed by the combined function of gamma and theta oscillations. *Schizophr Bull* 34(5):974–80.

369. Guzman SJ, Frotscher M, Jonas P (2014) Properties of CA3-CA3 synapses optimize storage capacity in the CA3 microcircuit. *Neuroscience Meeting Planner. Society for Neuroscience.* (Washington DC).
370. Valenti M, et al. (2004) Differential diurnal variations of anandamide and 2-arachidonoyl-glycerol levels in rat brain. *Cell Mol Life Sci* 61:945–50.
371. Benke D, et al. (2004) Analysis of the presence and abundance of GABAA receptors containing two different types of alpha subunits in murine brain using point-mutated alpha subunits. *J Biol Chem* 279(42):43654–60.
372. Benito C, et al. (2008) Cannabinoid CB_2 receptors in human brain inflammation. *Br J Pharmacol* 153(2):277–85.
373. Dombeck DA, Harvey CD, Tian L, Looger LL, Tank DW (2010) Functional imaging of hippocampal place cells at cellular resolution during virtual navigation. *Nat Neurosci* 13(11):1433–40.
374. Martin SJ, Morris RGM (2002) New Life in an Old Idea : The Synaptic Plasticity and Memory Hypothesis Revisited. *Hippocampus* 12:609–36.
375. Soderling TR, Derkach V a (2000) Postsynaptic protein phosphorylation and LTP. *Trends Neurosci* 23(2):75–80.
376. Malinow R, Malenka RC (2002) AMPA receptor trafficking and synaptic plasticity. *Annu Rev Neurosci* 25:103–26.
377. Malinow R (2003) AMPA receptor trafficking and long-term potentiation. *Philos Trans R Soc Lond B Biol Sci* 358:707–14.
378. Losonczy A, Biró AA, Nusser Z (2004) Persistently active cannabinoid receptors mute a subpopulation of hippocampal interneurons. *Proc Natl Acad Sci U S A* 101(5):1362–67.
379. Halassa MM, Fellin T, Takano H, Dong J-H, Haydon PG (2007) Synaptic islands defined by the territory of a single astrocyte. *J Neurosci* 27(24):6473–7.
380. Wang X, et al. (2006) Astrocytic Ca^{2+} signaling evoked by sensory stimulation in vivo. *Nat Neurosci* 9(6):816–23.
381. Hoffman AF, Riegel AC, Lupica CR (2003) Functional localization of cannabinoid receptors and endogenous cannabinoid production in distinct neuron populations of the hippocampus. *Eur J Neurosci* 18(3):524–34.
382. Duncan M, et al. (2008) Cannabinoid CB_2 receptors in the enteric nervous system modulate gastrointestinal contractility in lipopolysaccharide-treated rats. *Am J Physiol Gastrointest Liver Physiol* 295(1):G78–G87.
383. Amilhon B, et al. (2015) Parvalbumin interneurons of hippocampus tune population activity at theta frequency. *Neuron* 86(5):1277–89.
384. Köhler H, et al. (1887) *Köhler's Medizinal-Pflanzen: Atlas zur Pharmacopoea germanica* (Gera-Untermhaus).
385. Wilson RI, Nicoll RA (2002) Endocannabinoid signaling in the brain. *Science* 296:678–82.

6 Appendix

6.1 Glossary

2-AG: 2-Arachidonoylglycerol
AC fibres: associational-commissural fibres
aCSF: artificial cerebrospinal fluid
AHP: afterhyperpolarisation
AIS: axon initial segment
AMPA: α-amino-3-hydroxy-5-methyl-4-isoxazolepropionic acid
Anandamide: N-arachidonoylethanolamide
AP: action potential
BC: basket cell
CA: Cornu ammonis
CaCC: calcium-activated chloride channel
CaMKII: calcium/calmodulin-dependent protein kinase II
cAMP: cyclic adenosine monophosphate
Ca_V: voltage-gated calcium channel
CB_1R: cannabinoid type 1 receptor
CB_2R: cannabinoid type 2 receptor
CBR: cannabinoid receptor
CCK+: Cholecystokinin-positive
CGP55845: (2S)-3-[[(1S)-1-(3,4-Dichlorophenyl)ethyl]amino-2-hydroxypropyl](phenylmethyl) phosphinic acid hydrochloride
CNS: central nervous system
COX-2: cyclo-oxygenase-2
DAG: diacylglycerol
DAGL: 1,2,-diacylglycerol lipase
D-AP5: D-(-)-2-Amino-5-phosphonopentanoic acid
DG: dentate gyrus
DMSO: dimethyl sulfoxide
DSE: depolarisation-induced suppression of excitation
DSI: depolarisation-induced suppression of inhibition
EC: entorhinal cortex
eCB-LTD: endocannabinoid-mediated long-term depression
eCB-STD: eCB-mediated short-term depression
ECS: endocannabinoid system
EEG: electroencephalogram
EPSP: excitatory postsynaptic potential
FAAH: fatty acid amide hydrolase
GABA: gamma-aminobutyric acid
GABA: γ-Aminobutyric acid
GC: granule cell
GDP: guanosine diphosphate
GDPβS: Guanosine 5′-[β-thio]diphosphate trilithium salt
GEF: guanine nucleotide exchange factors
GIRK: G Protein-coupled inwardly rectifying potassium channel
GPCR: G Protein-coupled receptor
GPR55: G Protein-coupled receptor 55
HCN: hyperpolarisation-activated cyclic nucleotide-gated
HFS: high-frequency stimulation
HU-308: 4-[4-(1,1-Dimethylheptyl)-2,6-dimethoxyphenyl]-6,6-dimethylbicyclo[3.1.1]hept-2-ene-2-methanol
IN: inhibitory interneuron
IP3: inositol 1,4,5-trisphosphate
IPSC: inhibitory postsynaptic current
K_A: A-type K_V channels

K_{ATP}: ATP-sensitive potassium channel
K_D: D-type K_V channel
KO: knockout
K_V: voltage-gated potassium channel
lEC: lateral EC
LFP: local field potential
lPP: lateral perforant path
LTP: long-term potentiation
LTP-IE: long-term potentiation of intrinsic excitability
lyso-PLC: lysophospholipase C
mAChR: muscarinic acetycholine receptor
MAGL: monoacylglycerol lipase
MAPK: mitogen-activated protein kinase
mEC: medial EC
Mf: mossy fibres
mGluR: metabotropic glutamate receptor
ML: molecular layer
mPP: medial perforant path
mtCBR: mitochondrial cannabinoid receptor
Na^+/K^+-pump: sodium-potassium pump
NAPE-PLD: N-acylphosphatidylethanolamine-specific phospholipase D
N-arachidonoyl-PE: N-arachidonoylphosphatidylethanolamine
Na_V: voltage-gated sodium channel
NBQX: 2,3-Dioxo-6-nitro-1,2,3,4-tetrahydrobenzo[f]quinoxaline-7-sulfonamide
NMDA: N-Methyl-D-aspartic acid
PC: pyramidal cell
PI: phosphoinositides
PKA: protein kinase A
PLA1: phospholipase A1
PLCβ: phospholipase C β
pp: perforated patch
PST: physiological spike train
PV+: parvalbumin-positive
R_{in}: input resistance
SC: Schaffer collateral
SR144528: 2-[[[5-(2,6-Dimethoxyphenyl)-1-[4-[[[3-(dimethylamino)propyl]methylamino]carbonyl]-2-(1-methylethyl)phenyl]-1H-pyrazol-3-yl]carbonyl]amino]-
SSI: slow self-inhibition
STDP: spike-timing-dependent plasticity
SWR: sharp wave ripple complexes
TA pathway: temporo-ammonic pathway
THC: delta-9-tetrahydrocannabinol
tLTD: spike timing-dependent LTD
tLTP: spike timing-dependent LTP
TRPV1: transient receptor potential vanilloid subfamily, member 1
VGCC: voltage-activated calcium channel
V_m: membrane potential
VTA: ventral tegmental area
wc: whole-cell
WIN55,212-2: (R)-(+)-[2,3-Dihydro-5-methyl-3-(4-morpholinylmethyl)pyrrolo[1,2,3-de]-1,4-benzoxazin-6-yl]-1-naphthalenylmethanone mesylate
WT: wildtype

6.2 Statement of contributions

All experiments in this thesis were conceived and designed by my PhD supervisor, Prof. Dietmar Schmitz and me. Some of the data presented was acquired with the kind help of other people. All data analysis, with exception of the data presented in figure 3.12.3, was performed by me.

In the following I state the contribution of other people to the data presented:

Tugba Özdoğan (AG Schmitz, Neuroscience Research Centre, Charité Berlin) performed and analysed the in vivo wire arrays presented in chapter 3.12.3 with the help of **Dr. Alexey Ponomarenko**. T. Özdoğan also contributed the corresponding methods part and figure legend with the help of A. Ponomarenko and has consented to publishing her data as part of this thesis.

Anne-Kathrin Theis (AG Schmitz, Neuroscience Research Centre, Charité Berlin), who was under my supervision as a Master student from January to August 2012, contributed 81/369 whole-cell and 8/94 perforated patch recordings.

Alexander Stumpf (AG Schmitz, Neuroscience Research Centre, Charité Berlin), who was under my supervision as a PhD student from October 2014 to May 2015, contributed 46/369 whole-cell recordings.

Dr. Ulrike Pannasch (AG Schmitz, Neuroscience Research Centre, Charité Berlin), a postdoctoral researcher in the laboratory, contributed 11/369 whole-cell recordings between October and December 2013 in addition to helping to set up and perform experiments for this project that are not shown in this thesis.

Susanne Rieckmann and **Anke Schönherr** (AG, Schmitz, Neuroscience Research Centre, Charité Berlin), technical assistants in the laboratory, performed all genotyping of transgenic animals (S.R.) and provided help with molecular biology (A.S.) such as with single-cell RT PCR (not shown in this thesis).

In addition to the data that is presented here, I conducted many pilot and control experiments that are not shown in this thesis. Furthermore, I participated in other studies that are listed in 'Publications' (chapter 6.4)

6.5 Erklärung an Eides statt

Ich, Anna Vanessa Stempel, versichere an Eides statt durch meine eigenhändige Unterschrift, dass ich die vorgelegte Dissertation mit dem Thema: „Cannabinoid type 2 receptors mediate a cell type-specific plasticity in the hippocampus“ selbstständig und ohne nicht offengelegte Hilfe Dritter verfasst und keine anderen als die angegebenen Quellen und Hilfsmittel genutzt habe.

Die Bedeutung dieser eidesstattlichen Versicherung und die strafrechtlichen Folgen einer unwahren eidesstattlichen Versicherung (§156,161 des Strafgesetzbuches) sind mir bekannt und bewusst.

Berlin, den 05. Juli 2015